
# UNIVERSTITY OF PARMA

Ph.D. in Biotechnology and Biosciences

XXX COURSE

## Proteomics of model organisms (*A. thaliana* and *S. cerevisiae*) exposed to nanoparticles.

Coordinator:
Prof. **Simone Ottonello**

Supervisor:
Prof. **Nelson Marmiroli**

Tutor:
Prof. **Marta Marmiroli**

Candidate: **Valentina Gallo**

2014-2017

# Summary

## Abstract

Engineered nanomaterials (ENMs) are structures with size in the range of 1-100 nm, and characterized by properties due to their small size and surface reactivity that make them suitable for many industrial applications. Nanotechnology is a rapidly growing industry producing tons of ENMs each year. Therefore, due to the wide diffusion of ENMs and of the lack of information about their mechanisms of their interaction with living organisms, it is crucial to assess the risks linked to their diffusion in the environment. In particular, Cadmium sulfide quantum dots (CdS QDs) are widely used in the electronic industry to produce semiconductors, LED, optical devices, solar energy cells, and medical devices.

The aim of the research carried out during the Ph.D. thesis was to evaluate the response of model systems to CdS QDs, exploiting proteomics approaches.

The first part of this work was performed on the model plant *Arabidopsis thaliana* L. (Heynh). In a previous study a collection of 398 mutants of *A. thalian*a were utilized for selection of resistant mutants to normally toxic concentrations of CdS QDs. Two of the selected mutants (*atnp01* and *atnp02*) were characterized phenotypically and the genotypically, demonstrating that the mechanism of resistance to CdS QDs was minimally overlapped with resistance to Cd ions, supporting the possibility that nanoparticles have specific toxicity mechanisms.

In this work, the proteomic analysis was performed on crude protein extracts, obtained from whole seedlings of *atnp01, atnp02*, and wild type, grown on agarized MS, treated with 80 mg/L CdS QDs and non-treated. Total protein were separated by 2D gel electrophoresis, analyzed utilizing PDQuest software, and proteins differentially abundant between wild-type and each of the mutants were marked. Nighty-eight (98) proteins, whose abundance was statistically (Student's t test $p<0,05$) different in response to the experimental conditions, were identified by MALDI-TOF/MS and searched within MASCOT and UNIPROT database to infer their possible role in the plant response to nanoparticles, in particular in the resistance to CdS QDs. Gene Ontology analysis of the identified proteins revealed that the main categories modulated by CdS QDs treatment were: oxidative stress response, protein ubiquitination and degradation, energy and sugar metabolism.

The aim of the second part of the work was to assess the response of the model system *Saccharomyces cerevisiae* to CdS QDs, developing and comparing two different protein isolation methods, set respectively on gel-based and gel-free proteomics. A comparative study on the two quantitative methods frequently used in proteomics, 2-DE (dimensional gel electrophoresis) and iTRAQ (isobaric

tags for relative and absolute quantification), was carried out. The first method is a familiar techniques used in gel based quantitative proteomics, the second method is an LC (liquid chromatography) -based technique which is gradually gaining scientific consent. The iTRAQ method allows for simultaneous protein identification and quantification in a complex mixture. iTRAQ is conceptually smart, since peptides are labelled at the N terminus and at the ε side chain of lysines. Thus, every peptide ion selected for fragmentation generates a sequence with abundant data for proteins up to eight samples, thanks to multiplex reagents design.

The proteomic analysis was performed in yeast cells collected in the exponential phases of growth in liquid YPD (yeast extract peptone dextrose), without any supplementation, or with a supplementation of: 0.25 mg $L^{-1}$ nystatin, 100 mg $L^{-1}$ CdS QDs and 0.25 mg $L^{-1}$ nystatin plus 100 mg $L^{-1}$ CdS QDS. This comparative analysis was used to identify differences in proteins abundance in the controls with respect to the treated. The data were analyzed through different bioinformatics tools to identify the proteins and the main pathways of response to CdS QDs. Pathway analysis of the identified proteins revealed that the main classes modulated by CdS QDs treatment were: glycolysis and gluconeogenesis, ribosome, protein processing in endoplasmic reticulum (ER), biosynthesis of secondary metabolism and biosynthesis of amino acids. The results obtained could provide information regarding mechanisms, biological process, and genes involved in response to nanomaterials in yeast, which could be extended to superior eukaryotes.

# Introduction

# I PART

## 1.1 Nanotechnologies

The European Union (EU) adopted a definition of a nanomaterial (NM) in 2011 (2011/696/EU). According to the EU recommendation a "Nanomaterial" means: "*A natural, incidental or manufactured material containing particles, in an unbound state or as an aggregate or as an agglomerate and where, for 50 % or more of the particles in the number size distribution, one or more external dimensions is in the size range 1 nm - 100 nm".*

NMs showed peculiar physico-chemical properties (optical, magnetic, dielectric, of density and mechanic resistance) and are currently used in different areas such as electronics, biomedicine, pharmaceuticals, cosmetics, environmental analysis and remediation, catalysis and material sciences. For these reasons, the global nanocomposite market, in value terms, should reach $5.3 billion by 2021 from $1.6 billion in 2016 at a compound annual growth rate (CAGR) of 26.7%, from 2016 to 2021 (BCC Research, 2017).

Nanoparticles are broadly classified in to three groups: (Hett A. 2004*)* (Figure 1)

• One dimension nanoparticles: One dimensional system (thin film or manufactured surfaces) has been used for decades. Thin films (sizes 1–100 nm) or monolayer is now common place in the field of solar cells offering, different technological applications, such as chemical and biological sensors, information storage systems, magneto-optic and optical device, fiber-optic systems;

• Two dimension nanoparticles: Carbon nanotubes;

• Three dimension nanoparticles: Dendrimers, Quantum Dots (QDs), Fullerenes (Carbon 60).

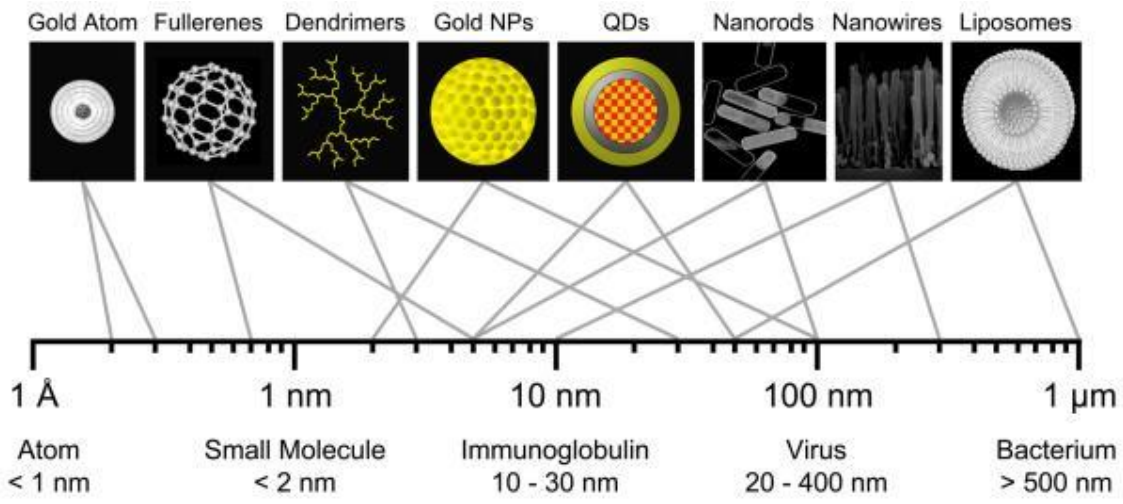


**Figure 1.** Relative Sizes of Nanoparticles: Hydrodynamic diameter (HD) ranges for nano-scale materials and naturally-occurring materials.

## 1.2 Nanotoxicology, risk assessment and legislation

Engineered Nano Materials (ENMs) behavior is strongly influenced by their small size, high surface/volume ratio, chemical stability and composition (Wani *et al*. 2017). They are rapidly becoming a part of our daily life in the form of cosmetics, food packaging, drug delivery systems, therapeutics, electronic components, biosensors, and many other every-day used gadgets and facilities. Thus, the exposed population to nanomaterials continues to increase as their application expands. Since many types of engineered nanoparticles are suspected to be toxic to living organisms and to have a negative impact on the environment, the process of designing new and safe nanoparticles must be accompanied by a thorough risk analysis (Silva *et al.* 2016*).* In the last years, ENMs hazards have been evaluated using both *in vitro*, *in vivo* and *in silico* techniques. The *in vitro* testes include the use of single cells type cultures, co-cultures, three-dimensional models of tissues and cell- free assays (Stone *et al.* 2016)*;* the abundance of tests allows the analysis of the validation on *in vivo* model and the use of a set of standards to compare different datasets. *In silico* models can be used to predict a variety of properties, including the toxicity of newly designed nanoparticles. Computational techniques, especially (Quantitative) Structure-Activity Relationship ([Q]SAR) modelling, provide hazard estimates which are fundamental for risk assessment. The concept underpinning (Q)SAR (Cherkasov *et al.* 2014*;* Dearden *et*

*al*. 2017*)* is that, when the structural characteristics (called "descriptors") are known for a group of compounds, and the experimental activity data are available only for a few of them, it is possible to predict the unknown activities for the remaining compounds directly from the descriptors and a suitable mathematical model derived from algorithmic analysis of the available data. Developed models can be either qualitative (SAR) or quantitative (QSAR).

Guidance from the international regulatory agencies (EFSA and FDA respectively for EU and US) requires a suite of *in vivo* and *in vitro* assessments that must be carried out for nanomaterial containing products. The guidance underlined how, currently, there are no *in vitro* methods that have been validated to be used for hazard assessment of ENMs. Indeed, the doses estimated, *in vitro* might not be relevant *in vivo* or *in vitro* cell lines might not be a good representative for the whole organism. However, *in vitro* tests may provide information on hazards, give indication on potential toxicity of an ENM, and may be used to elucidate possible mode of action to understand biological responses and mechanisms involved in toxicity. Absorption, distribution, metabolism and excretion parameters are likely to be influenced by both the chemical composition of the ENM as well as its physico-chemical properties (size, shape, solubility, surface charge and surface reactivity). For these reasons, both *in vivo* and *in vitro* tests provide necessary information that is complementarily needed to assess the ENMs mechanism of action and toxicity.

Legislation concerning ENMs is currently under consideration because of the variable nature of the molecules investigated. On February 10$^{th}$, 2009, the European Food and Safety Authority (EFSA) adopted a scientific opinion on "The potential risks arising from nanoscience and nanotechnologies on food and feed safety" in response to the growing need of regulation of those materials. The first guidance was released from EFSA scientific committee on May 10$^{th}$, 2011 concerning the risk assessment of the application of nanoscience and nanotechnologies in food chain and feed (EFSA, 2011)*,* in which the attention was focused on the evaluation of the methodologies relevant for all the phases of the risk assessment procedure (Tsuji *et al.* 2006), in six general cases here reported: i) no persistence of ENMs in preparations/formulations as marketed, ii) no migration from food contact materials, iii) complete ENMs transformation in the food/feed matrix before ingestion, iv) transformation during digestion, v) information on non-nanoform available, vi) no information on non-nanoform available. Conversely, United States Food and Drug Administration (FDA), on April 2012 approved two different draft guidance concerning regulation of nanomaterials in food and cosmetics,

allowing the use of ZnO ENMs and $TiO_2$ ENMs for sunscreens. On July 26th, 2013, the European Commission's (EC) Scientific Committee on Consumer Safety (SCCS) posted two documents available for comments regarding legislation of ZnO and $TiO_2$ ENMs, still under consideration. On December 20th, 2013, European Joint Research Center released online a web platform for the purpose of sharing and increasing the current knowledge concerning nanomaterials both for physico-chemical characterization of the pollutant and also risk assessment procedure (http://ihcp.jrc.ec.europa.eu/our_databases/web-platform-on-nanomaterials).

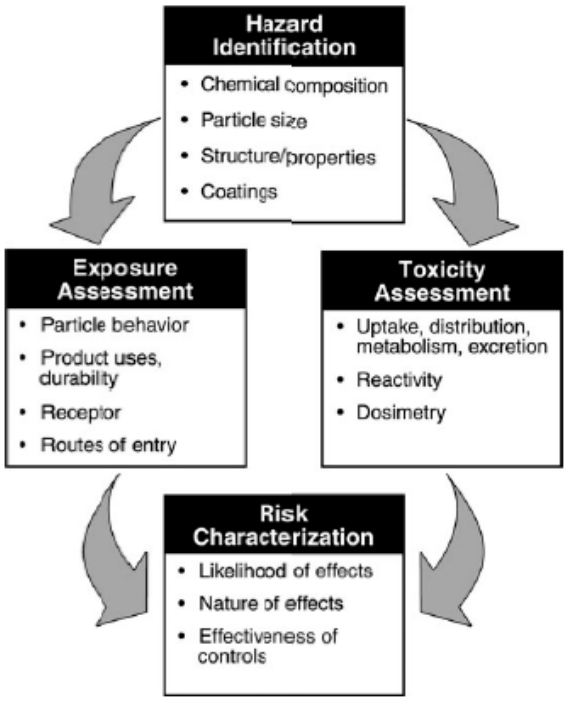


**Figure 2.** Risk assessment framework for nanomaterials (Tsuji *et al.* 2006).

Due to ongoing safety concerns regarding the use of nanomaterials, the National Nanotechnology Initiative (NNI) launched the Nanotechnology Environmental and Health Implications Working Group (NEHIWG) to manage the potential risks associated with nanotechnology. In order to help efficiently regulate potential nanotechnology research, the NEHIWG prepared the report "NNI-Strategy for nanotechnology related environmental, health and safety research" in 2008 (Davies *et al.* 2008). The strategy identified five priority areas for Environmental Health and Safety (EHS) research and for coordination of interested agencies:

1. Instrumentation, metrology and analytical methods: National Institute for Standards and Technology (NIST)

2. Nanomaterials and human health: National Institutes of Health (NIH)

3. Nanomaterials and the environment: Environmental Protection Agency (EPA)

4. Human and environmental exposure assessment: National Institute for Occupational Safety and Health (NIOSH)

5. Risk management methods: FDA and EPA.

To regulate nano-related materials, products, and processes, the FDA, EPA, NIOSH, the Occupational Safety and Health Administration (OSHA), and the Consumer Product Safety Commission (CPSC) have summarized EHS implications, risks and possible needs for regulations (Choi *et al*. 2010*).*

## 1.3 Synthesis of engineered nanomaterials

The nanofabrication methods are divided into two major categories: "top–down" and "bottom–up" methods according to the processes involved in creating nanoscale structures.

A top–down approach corresponds to using nanofabrication tools that are controlled by external experimental parameters to create nanoscaled structures/ functional devices with the desired shapes and characteristics starting from larger dimensions and reducing them to the required values. Various methods of lithography are used in the top–down approach, including serial and parallel techniques for patterning two-dimensional nanoscale features, but also scanning probe lithography, nanoimprint lithography and block co-polymer lithography (Gates *et al*. 2005; Mailly *et al*. 2009). On the other hand, bottom–up approaches seek to have molecular or atomic components built up into more complex nanoscale assemblies or directed self-assemblies based on complex mechanisms and technologies (Ariga *et al*. 2008). This area of nanofabrication uses atoms or small molecules as the building blocks of multi-level structures that perform various operations and is extremely promising since it could lead to no waste or unused materials.

## 1.4 Nanomaterials classification

A first classification of nanomaterials engineered and non- engineered can be performed according to their natural or manufactured source. The first category includes all the nanomaterials produced by geological (e.g. chemical and physical degradation of rock materials, neoformation, volcanic eruptions) or biological (e.g. nucleic acid, peptides, virus) processes. Handy *et al*. (2008) explains as the living organisms evolved in an environment where these natural nanomaterials are actively released and intact with other pollutants, water and organic matter. The ENMs are man-made nano-structures, designed to meet specific proprieties and characteristics and are synthetized through technological process. They can be subdivided furthermore by their composition in:

1. Carbon-based ENMs, including fullerenes, nanotubes and graphene;
2. Metal-based including single metals, metal oxides and nanocrystal, such as semiconductor quantum dots;
3. Hybrid ENMs, combining the two categories through functionalization or the use of a core/shell structure to modulate ENMs reactivity and target specificity.

## 1.5 Quantum dots

Quantum dots (QDs) are nanocrystals of semiconducting materials measuring around 2–10 nm, composed by metals belonging to groups II-V or III-V of the periodic table, consisting of a semiconductor inorganic core, an aqueous organic coated shell to improve optical properties, and fluorescence when stimulated by light. Quantum dots may bear a cap, which enables them improving their solubility in aqueous buffers. The core metal and the dimensions of the quantum dots determine the colour emitted and the outer shell is available for conjugation with biomolecules (Oh *et al.* 2016).

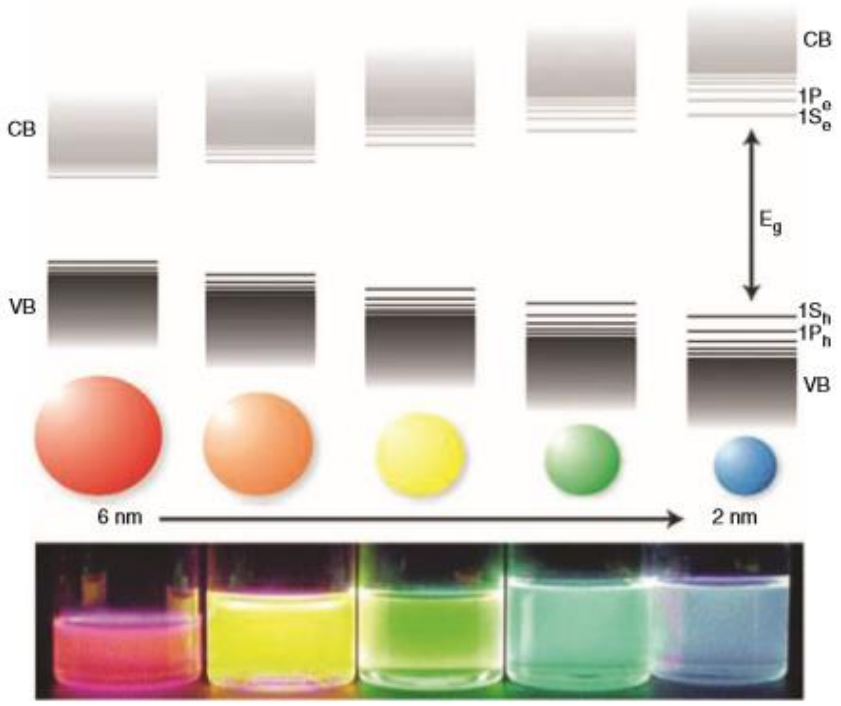


**Figure 3**. Schematic representation of the "quantum confinement" effect on the energy level structure of a semiconductor material. The lower panel shows colloidal suspensions of CdSe NCs of different sizes under UV excitation. (Reprinted with permission from Ref 25. Copyright 2011 The Royal Society of Chemistry)

Owing to the to their narrow emission waveband (Δλ), bright fluorescence, high photostability and broad UV excitation QDs have been adopted for tracking of intracellular process, for *in vitro* bioimaging and for real time monitoring. As far as the applications are concerned, QDs cover medical areas as diagnostic, therapeutic tool for *in vitro* and *in vivo* detection, and analysis of biomolecules, immunoassays, DNA hybridization, magnetic resonance imaging (MRI), time graded fluorescence imaging of tissue, development of non-viral vectors for gene therapy, labelling of cells, therapeutic tools for cancer treatment and transport vehicles for DNA, protein, drugs or cells (Bailey *et al.* 2004). In addition, they can be tagged with biomolecules and used as highly sensitive probes. Thanks to their tuneable absorption spectrum, combined with a high extinction coefficient, QDs find application in the synthesis of new generation aerogel components of photovoltaic panels (Xing *et al.* 2016). They are

widely used in the manufacturing of batteries, high resolution led screens and precision tuneable lasers (Zhai *et al.* 2010).

The Cadmium sulfide quantum dots (CdS QDs) used in this study were synthetized by IMEM-CNR (Istituto dei materiali per l'Elettronica e il Magnetismo, Parma, Italy). CdX (X = S, Se, Te) QDs are part of the group II-VI QDs. They were synthetized through a wet-chemistry approach, according to Villani *et al.* 2012, Cadmium acetate 99,99% (Cd(CH3CO2)), N,N-dimethylformamide 99% (HCON(CH3)2) and thiourea 99.5% (NH2CSNH2). These QDs have an average diameter of 4-5 nm, a density of 4,82 g $cm^{-3}$ and an average weight of 2,5 $10^{-18}$ g. They have the crystal structure of wurtzite (Villani *et al.* 2012). **The characterization of this batch of CdS QDs with HRTEM, XRD and ESEM/EDX is reported in appendix at page 79 of the thesis.**

In literature there are several evidence of quantum dots' toxic impact on human health and environment, which is correlated to their surface proprieties, functionalization, diameter, assay type and exposure time (Gong *et al.* 2016). For example, Marmiroli *et al. (*2014*)* compared the effects of CdS QD exposure on wild type (wt) and two mutant strains of *Arabidopsis*, *atnp01* and *atnp02*. The mutants were selected because their tolerance to CdS QDs at concentrations that significantly affect the growth of wt *Arabidopsis*. The mutants responded differently to each other and to the wt, and the tolerance response was characterized at a transcriptomic and proteomic level (Marmiroli *et al*. 2015). Paesano *et al*. (2016) characterized the cytotoxic and genotoxic effect of CdS QDs on HepG2 cells to understand the underlying mechanisms involved in the cellular response and to identify markers of exposure. QDs have been developed in bioimaging application for decades, such as cell imaging, tissue imaging, as well as body imaging (Oh *et al.* 2016). He *et al.* (2016) has reported a carbon shell CdSeTe/CdS/C QDs, which showed low cytotoxicity and good biocompatibility in live cells. By conjugating with AS1411-aptamer on the surface of QDs as the tumor cell target motif, they could be used for the target imaging of tumor cells, such as HeLa cells (Benayas *et al*. 2015). Recently, Foda *et al*. (2014) have developed a biocompatible and highly luminescent CuInS2/ZnS QDs embedded silica beads for cancer cell imaging, which possessed excellent PL and long colloidal stability in cell culture.

In addition of bioimaging application, near- infrared (NIR) semiconductor QDs have emerged as the representative NIR sensors possessing excellent fluorescence properties, such as broad excitation spectra but narrow emission bands, size-tunable photoluminescence, as well as robust photochemical stability. For example, Wang *et al.* (2016) have designed a NIR electrochemiluminescence aptasensor

for turn-on determination of thrombin, which was based on the electrochemiluminescence (ECL) resonance energy transfer (ECL-RET) of CdTe/CdS core small/shell thick QDs to gold nanorods (AuNRs). Owning to lower background interference, and reduced photochemical damage of NIR, this senor displayed a low detection limit and could be applied successfully to thrombin sensing in real serum samples. Zhang *et al*. (2016) have reported how in vivo and in vitro exposure of CdTe QDs in mice liver cells resulted in an increased level of lipid peroxide markers and in concentration and time dependent cytotoxic effect. An accumulation of reactive oxygen species (ROS) and the induction of apoptosis were also observed. The study of Fan J. *et al*. (2016) showed how CdTe/ CdS core/shell QDs activated autophagy instead of apoptosis in HL-7702, HepG2, HEK-293 and Raij cell lines, as confirmed by confocal and TEM microscopy. Accumulation of ROS was suggested as one of the causes of autophagy induction and cytotoxic effects.

## 1.6 *Arabidopsis thaliana* as model system for nanomaterial exposure in crop plants

*Arabidopsis thaliana* is an ideal test plant because it has a short generation time, small size, high seed production, and most importantly its genome sequence is published and available openly (Koornneef *et al.* 2010). *A. thaliana* has a relatively small genome of approximately 135 megabase pairs (Mbp) and five chromosomes. It was the first plant to have its genome sequenced. In addition, seed banks distribute *Arabidopsis* and a variety of its mutants; hence, many studies on plant-contaminant interactions have been performed using *Arabidopsis*.

ENMs have revolutionized almost every field of science and of course, plant science could not remain unaffected. In fact, Rico *et al*. (2011) highlighted the need to understand the exact mechanisms by which ENMs may be taken up and internalized by plants because of the numerous challenges and opportunities that plant biochemical pathways offer in the chemical modification of ENMs. The properties of ENMs can change as they travel through xylem, from intact ENMs, uncoated ENMs, salts or ions (Figure 4a) and any of these forms may be transported to the phloem. It is not clear as to what extent ENMs pass into the interior of the root via the apoplastic (extracellular) pathway (Figure 4b) (*Montes et al. 2017*). Several experiments led to understand the transport mechanisms and accumulation of Ag ENMs in *A. thaliana* both on the physiological and molecular point of view (Geisler-Lee *et al*. 2013; Kaveh *et al.* 2013). Applications of ENMs alone or along with short term chilling

treatment have been shown to improve growth, physiological and biochemical attributes of cold-stressed plants. In *Arabidopsis thaliana*, Khan *et al.* (2014), reported an enrichment of antioxidant activity for the genes, 35% of similar genes were regulated by both Ag ENMs and cold stress. Kim *et al.* (2015) observed that iron-NPs activate stomatal opening through activating plasma membrane $H^+$-ATPase in *A. thaliana*, maintained normal drought sensitivity, increased $CO_2$ assimilation.

ENMs such as Ag ENMs, $TiO_2$ ENMs, and ZnO ENMs, have been reported to induce the formation of new and larger poresin cell walls (Kurepa *et al*. 2010) and cuticles (Larue *et al*. 2014), and cause structural changes (e.g., ruptures and disruption of microfilaments) (Wang *et al*. 2015), which in turn facilitate the internalization of larger ENMs.

In conclusion, as reported in most of the current literature, the mechanisms involved in uptake and translocation of ENMs in the plant tissues and their physico-chemical forms inside the plant still remain largely unknown (Rico *et al*. 2011).

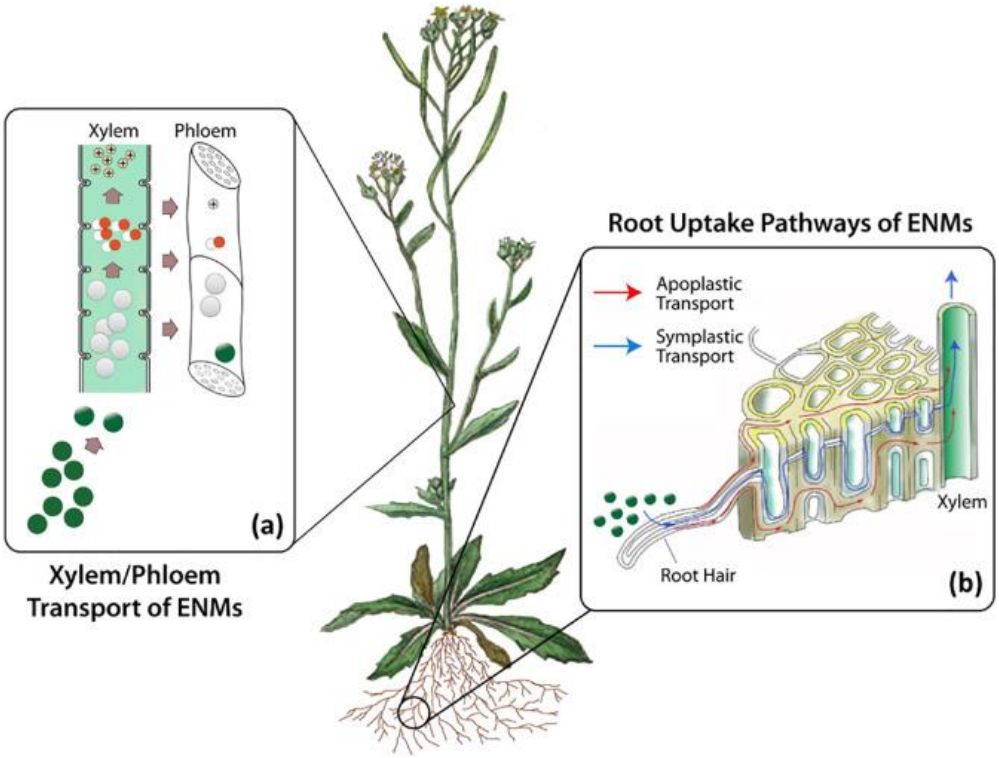


**Figure 4**. Uptake and transformation of ENMs in *Arabidopsis thaliana*. (a) A longitudinal section of the stem shows how the chemical form of ENMs at any location in the plant is unclear and may change as they travel through the xylem, existing as intact ENMs (green), possibly degrading (gray), present as salts (white/red) or free ions (+) and may be distributed through phloem tissue in any of these forms.

(b) The root tissue cross section depicts different pathways ENMs could travel through, apoplastic (red) or symplastic (blue) (Monte*s et al. 2017).*

### *1.7 Saccharomyces cereviasiae* as model system for the investigation of ENMs toxicity

*Saccharomyces cereviasiae* is a unicellular eukaryote and one of the most used model organisms for molecular biology. Its genome has a size of about 12Mb, subdivided in 16 chromosomes, which has been completely sequenced and annotated (Goffeau. 2000). Due to its easy to use, fast life cycle (one division each 90 minutes) and to availability of several molecular and genomic tools, yeast had been used as a platform for toxicological studies (Dos Santos *et al.* 2015). Furthermore the high level of functional conservation within higher eukaryotes genomes (either in human) make yeast a model system for the assessment of the mechanisms underlying the response to environmental pollutants as ENMs.

Similarly, to plants, the mechanisms involved in ENMs toxicity in yeast are still actually unknown. Furthermore, the variability of ENMs behaviour, along the different types of treatment applicable to yeast strains, led to increase the level of general complexity of the experimental approaches used. Several studies performed on yeast revealed the extreme variability of effects ascribable to different categories of ENMs, focusing the attention to several properties implicated in toxicity. Pasquali *et al.* (2017) established that the effect of CdS QD exposure in yeast increased the level of ROS and decreased the level of reduced vs oxidized glutathione (GSH/GSSG). Differences observed in the ENMs responses may be cause by the stability of the type of ENM tested: CuO ENM, for instance, showed an intrinsic instability, highlighting how the toxic effect consist in the $Cu^{2+}$ release. In this context it was also analyzed the effect of CuO ENM on some yeast strains deleted in genes involved in the detoxification pathway of $Cu^{2+}$ (Kasemets *et al.* 2012). Bayat *et al.* (2014) analysed the cytotoxic and morphological effects of $TiO_2$, CuO, ZnO, Ag ENMs and a single-walled carbon nanotubes (SWCNTs) on *S. cerevisiae*. CuO ENMs were highly cytotoxic, reducing the cell density by 80%, and inducing lipid droplet formation. Cells exposed to Ag-ENMs and $TiO_2$-ENMs contained dark deposits in intracellular vacuoles, the cell wall and vesicles, and reduced cell density (40 and 30%, respectively). ZnO-ENMs caused an increase in the size of intracellular vacuoles, despite not being cytotoxic. SWCNTs did not cause cytotoxicity or significant alterations in ultrastructure, despite high oxidative potential. Rong-Mullins *et al* (2017)

found that the response of *S. cerevisiae* to soluble copper was an improvement of the antimicrobial function of cellulosic copper nanoparticles. Cells exposed to c-CuNPs (cellulosic cupric nanoparticles) demonstrated greater sensitivity to Cu than cells exposed to soluble Cu, although Cu-resistant strains were more tolerant than Cu-sensitive strains of c-CuNP exposure. At the same level of growth inhibition, c-CuNPs led to the same internal Cu levels as did $CuSO_4$, offering evidence for alternative mechanisms of toxicity, perhaps through β-arrestin dependent endocytosis, which was supported by flow cytometry and fluorescence microscopy of c-CuNPs distributed both on the cell surface and within the cytoplasm.

# II PART

## 2.1 Proteomics

The proteome analysis was defined as "the analysis of the entire PROTEin complement expressed by a genOME" (Pennington *et al*. 1997). Proteomics can be defined as the systematic analysis of proteome, the protein complement of genome (Phizicky *et al*. 2003). This technology allows the global analysis of gene products in various tissues and physiological states of cells. With the completion of many genomes sequencing projects and the development of analytical methods for protein characterization, proteomics has become a major field of functional genomics (Park *et al*. 2004). Many different protein extraction methods have been developed from different prokaryotes, plant, and animal tissues and a large number of protein separation techniques have been developed in order to decrease the complexity of the proteome. However, the analysis of whole proteomes, including identification and quantitation, for any organism at a given time or biological state, has become not only possible but also faster than the earlier approaches. As the proteome may change with time, developmental conditions, and environmental effects, studies need to be designed in such a way that this dynamic behaviour of a biological system can be captured and understood. The genome remains fairly static, but the expression of genes in a specific context is more interesting, for which the proteome studies need to factor in time because of its ever-changing nature. Multiplexing various states by labelling techniques is therefore of utmost necessity for quantitative proteomics. The quantitative information for the proteins expressed can be used for modeling the cellular and metabolic response of an organism (Bantscheff *et al.* 2011) and thus can help in designing inhibitors for specific targets in a disease study (Boehm et al. 2007). With the improvement of qualitative techniques, many quantitative techniques are now in existence for high-throughput proteomics data sequencing that offer improved sensitivity, precision, and easy automation of experiments and analysis (Putz *et al.* 2005).

## 2.2 Protein separation techniques

In recent years, proteomics technology has undergone rapid development; in particular, many quantification strategies have been published (Gorg *et al.* 2004). These strategies provide different prospects and vary in their principal workflows. A common method used for decades is the well-established two-dimensional-PAGE (2D-PAGE). New and faster high-throughput techniques using stable isotope labelling and chromatography followed by mass spectrometry were developed over the turn of the millennium, e.g., isotope coded affinity tag (ICAT) (*Gygi et al. 1999*), stable isotope labelling with amino acids in cell culture (SILAC) (Ong *et al. 2002*), global internal standard technology (GIST) (Chakraborty *et al.* 2002), and isobaric tag for relative and absolute quantitation (iTRAQ) (Ross *et al.* 2004). The most prominent of these techniques, SILAC and iTRAQ, have different characteristics concerning workflow and data evaluation. For instance, in SILAC technique, the proteins are labelled in cell culture with stable isotopes and quantification is done in the MS1 spectrum. However, in the case of iTRAQ, peptides from previously digested protein samples are chemically labelled with isobaric tags, allowing identification and quantification of up to four or eight samples in the same MS/MS spectrum (Choe *et al.* 2007*;* Ross *et al.* 2004).

### 2.2.1 Two-dimensional electrophoresis

About 30 years ago, a protein separation technique called “2D- gel electrophoresis” was introduced, and this technique satisfied the resolving power requirement while conserving the quantitative aspect of the proteome. Two-dimensional gel electrophoresis has been the method of choice for the large-scale purification of proteins in proteomic studies since 1975, because it can potentially separate several thousand proteins in a single experiment (Görg *et al.* 1995*,* O’Farrell *et al*. 1997). Although the predictions for the number of genes in some genomes are high, it is generally believed that the number of genes expressed is, on average, between 5000 and 15,000 per cell type. However, these genes and post-translational modifications can lead to many forms of proteins, greatly increasing the complexity of the proteome (O’Farrell *et al*. 1997). Two-dimensional electrophoresis (2-D electrophoresis) sorts out proteins according to two independent properties in two discrete steps: the first-dimension step, isoelectric focusing (IEF), separates proteins according to their isoelectric points (pI). Proteins are

amphoteric molecules; they carry either positive, negative, or zero net charge, depending on the pH of their surroundings. The net charge of a protein is the sum of all the negative and positive charges of its amino acid side chains and amino- and carboxy-terminal. The isoelectric point (pI) is the specific pH at which the net charge of the protein is zero. Proteins are positively charged at pH values below their pI and negatively charged at pH values above their pI. The presence of a pH gradient is critical to the IEF technique. In a pH gradient, under the influence of an electric field, a protein will move to the position in the gradient where its net charge is zero, with a specific velocity. A protein with a positive net charge will migrate toward the cathode, becoming progressively less positively charged as it moves through the pH gradient until it reaches its pI. A protein with a negative net charge will migrate toward the anode, becoming less negatively charged until it also reaches zero net charge. If a protein should diffuse away from its pI, it immediately gains charge and migrates back. The second-dimension step, SDS-polyacrylamide gel electrophoresis (SDS-PAGE), separates proteins according to their molecular weights (Mr, relative molecular weight). Each spot on the resulting two-dimensional gel corresponds to a single protein species in the sample. Thousands of different proteins can thus be separated, and information such as the protein pI, the apparent molecular weight, and the amount of each protein is obtained. (Figure 5).

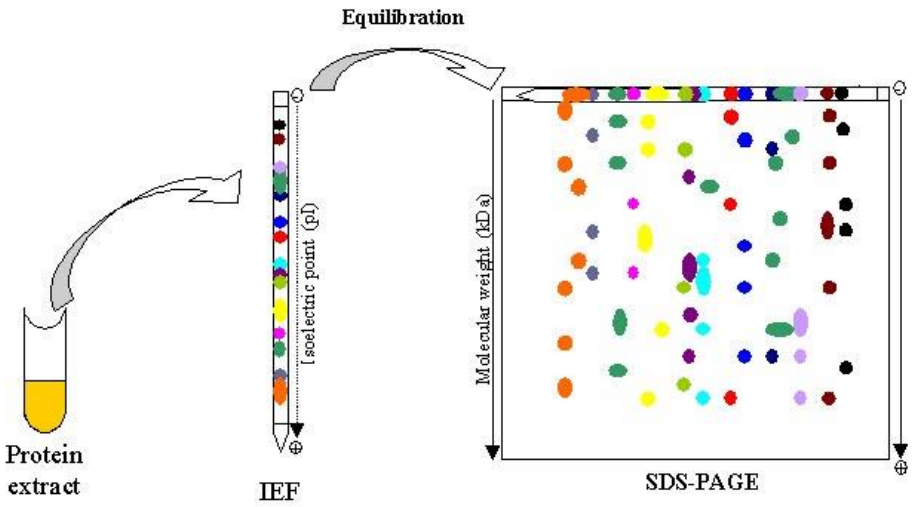


**Figure 5.** Two-dimensional gel electrophoresis, abbreviated as 2-DE, is a form of gel electrophoresis commonly used to analyze mixture of proteins by two properties in two dimensions respectively.

However, despite technological progress, there are still some shortcomings of the 2D electrophoresis methodology: Difference Gel Electrophoresis (DIGE) by Unlu *et al*. (1997) was an enormous valuable contribution to increase the reliability of qualitative and quantitative results of 2D gels: DIGE provides the use of an internal standard, which consists of all proteins contained in the entire experiment. In the DIGE method prior to electrophoresis the proteins of the different samples are pre-labelled with different fluorescent tags, which do not alter the isoelectric points and the migration in the second dimension. Differently labelled samples are mixed and separated in the same gel. The internal standard is generated prior to labelling: aliquots are taken from each sample, combined and labelled with one of the fluorescent dyes. The spot patterns are obtained with multi-fluorescence imagers.

### 2.2.2 iTRAQ (isobaric tag for relative and absolute quantitation)

Introduced in 2004, iTRAQ was developed as a multiplexed method for studying protein quantitation using isobaric tags containing a reporter and a balancer group. In iTRAQ, the amine groups at the N-terminal and lysine residues of the digested peptides are derivated by isobaric labels (4-plex, 6-plex, or 8-plex) after digestion and mixed before MS. Ross *et al.* (2004) introduced four different reporters having the masses of 114.1, 115.1, 116.1, and 117.1. Corresponding balancers with masses ranging from 28 to 31 Da add up to form the isobaric tag with the combined mass of 145.10 Da (Fig. 6a). It was extended later to 6-plex and 8-plex (Choe *et al*. 2007; Dayon *et al.* 2008). In 8-plex iTRAQ, four new reporters, 113.1, 118.1, 119.1, and 121.1, were added, supplemented with a corresponding balancer mass of 192–184 Da that takes the total mass to 305.10 Da (Fig. 6b). Reporter with a mass of 120.08 Da was omitted from 8-plex masses, as it is isobaric with phenylalanine immonium ion and could have contaminated the peak resulting in inaccurate quantitation. An iTRAQ reaction utilizes an N-hydroxysuccinimide (NHS) ester derivative to modify the primary amine groups by linking the balancer group (carbonyl group) and a reporter group (based on N-methylpiperazine) to the digested peptides by forming an amide bond (Wiese *et al.* 2007). During MS/MS fragmentation the balancer group is lost as a neutral loss and the reporter group is released. As the labels make the peptides isobaric, at MS1 level the peptide (+isobaric tag) appears as a single peak but during MS/ MS, the quantitation is

achieved when the reporter ions of different masses are released and seen in low-mass region of the fragment spectrum.

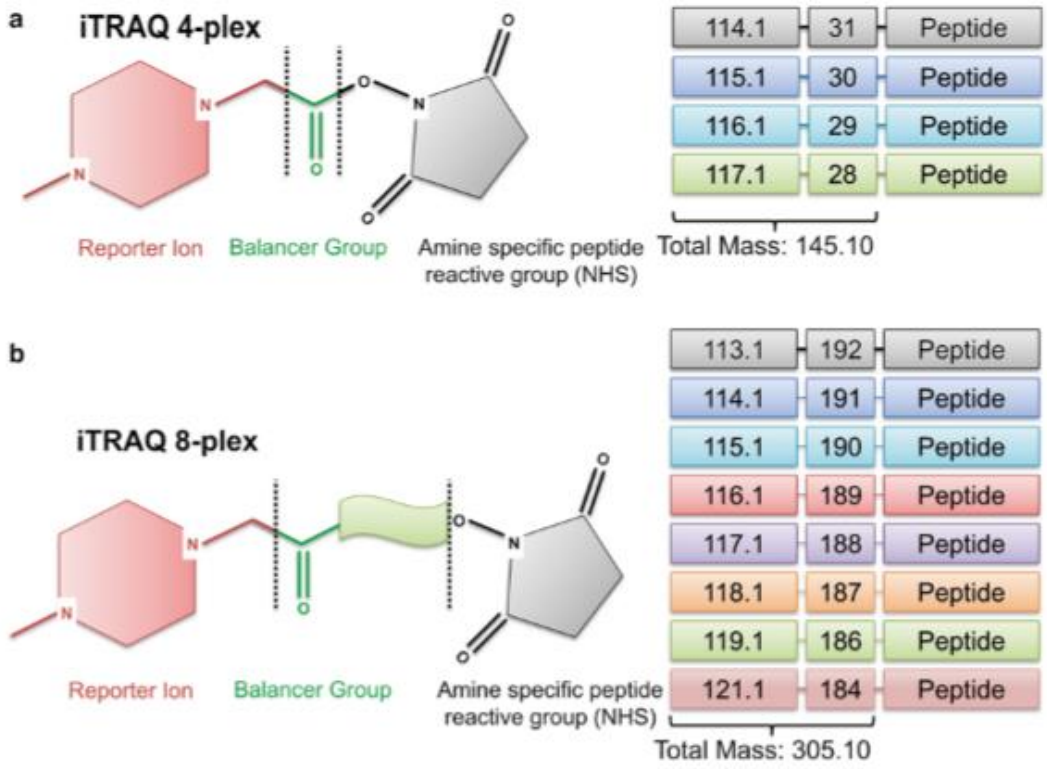


**Figure 6.** Chemical structures for iTRAQ (a) 4-plex and (b) 8-plex isobaric tags. Balancer + reporter ions add up to 145 Da in 4-plex and 304 Da in 8-plex experiments. In 8-plex, reporter mass of 120 is not present as it will give erroneous quantitation since phenylalanine immonium ion is also observed at a mass of 120 Da.

# *Arabidopsis thaliana*

# Materials and methods (I)

## 3.1 Seed Germination, Growth, and Treatments

Twenty-five seeds of *A. thaliana,* accession Landesberg erecta (Ler-0) wild type (wt) and the two mutants atnp01 and atnp02 (Marmiroli *et al*. 2014) were sawn on Petri dishes containing Murashige and Skoog (MS) nutrient medium (Duchefa Biochemie, Haarlem, Netherlands) containing 1% w/v sucrose and solidified with 0.8% w/v agar, then placed in the dark, under controlled conditions in a growth chamber. After germination, seedlings were grown at 24°C, with relative humidity of 30%, and under a 16-h photoperiod (light intensity 120 µM $m^{-2}$ $s^{-1}$ photosynthetic photon flux) in the same MS medium in the absence of CdS QDs for 14 days. Seedlings were transferred to MS medium containing 80 mg $L^{-1}$ CdS QDs (treatment) or 0 mg $L^{-1}$ (control) and grown for a further 21 days, as above. One gram of plant material for all six samples were collected: plantlets were then removed from the medium, carefully washed with Milli-Q deionized $H_2O$, frozen in liquid nitrogen and then stored at -80°C until use and used for protein extraction.

## 3.2 Proteins extraction

Crude proteins of wt and the two mutant lines in untreated and treated (80 mg $L^{-1}$ CdS QDs) conditions were extracted, using the following protocol.

Frozen samples were finely powdered in liquid nitrogen using mortar and pestle, 1 g were suspended in 6 ml of extraction buffer (700 mM sucrose, 500 mM Tris-HCl, pH 7.5, 50 mM EDTA, 100 mM KCl, 2% DTT, 0.1% Protease Inhibitor Cocktail), vortexed and mixed for 10 min on ice. An equal volume of 500 mM Tris-HCl buffered phenol was added and the solution was mixed for 10 min at room temperature (Giavalisco *et al*. 2004; Faurobert *et al.* 2007). The samples were centrifuged for 10 min at 5500 g and 4°C. The phenolic phase was collected in a new tube and back-extracted with 3 ml of extraction buffer. Proteins were precipitated from the phenolic phase overnight at -20°C by adding five volumes of 0.1 M ammonium acetate (J.T. Baker, Deventer, Holland) saturated in methanol. Precipitated proteins were centrifuged for 30 min at 5500g (4°C) and the pellet was washed with cooled methanol and then with cooled acetone. After each washing step, the samples were centrifuged for 5 min at 5500 x g and 4°C.

Finally, the pellets were dried using a Speed Vac Concentrator 5301 (Eppendorf AG, Barkhausenweg, Hamburg, Germany).

### 3.3 Protein quantification

The pellets were solved in 300 µl of isoelectofocusing (IEF) buffer containing 9 M urea, 4% CHAPS, 50 mM DTT, 0.001% protease inhibitor cocktail, 1% carrier ampholyte mixtures (pH 3-10, BioRad, USA). Protein concentration was evaluated according to a modified Bradford assay (Ramagli et al., 1985) based on the acidification of the sample buffer with 20 mM HCl. Bovine serum albumin (BSA) was used as standard.

### 3.4 2-D gel electrophoresis

IPG strips (11 cm, pH 5-8, ReadyStrip BioRad, USA) were rehydrated overnight with 250 µl of IEF buffer containing 400 mg of total proteins. Proteins were focused by PROTEAN® i12™ IEF System (BioRad, USA) applying 250 V (60 min), 1 kV (60 min), 8 kV (2 hours) and 8 kV for a total of 35 kV/h.

After focusing, the strips were incubated 15 min in 3 ml of reducing buffer containing 2% w/v DTT, 6 M Urea, 0.375 M Tris-HCl (pH 8.8), 20% w/v glycerol, 2% w/v SDS. They were subsequently incubated 15 min in 3 ml of alkylating buffer containing 2.5% w/v iodoacetamide, 6 M Urea, 0.375 M Tris-HCl (pH 8.8), 2% w/v glycerol. Electrophoresis in the second dimension was carried out using a Criterion™ Dodeca™ cell (BioRad, USA) and 12% Criterion™ XT Bis-Tris Gel (BioRad, USA) in MOPS (J.T. Baker, Deventer, Holland) buffer (1M 3-(N-morpholino) propanesulfonic acid, 1M Tris, 20 mM EDTA, 2% w/v SDS). 2-DE gels were stained with QC Colloidal Coomassie G-250 (BioRad, USA) and gel images were obtained with a ChemiDoc™ Imaging System (BioRad, USA). Image analysis was performed using the PDQuest software (BioRad, USA). Spot detection and matching between gels were performed automatically, followed by manual verification. The spots' densities were normalized by local regression method and subsequently against the whole gel's density. The percentage density of each spot was averaged for three replicates gels and Student's t-test analysis ($p<0.05$) was performed to find out statistically significant differences in proteins abundance. When matching the statistic criterion, spots were excised from the gels and digested with trypsin according to Shevchenko *et al.* (2006). The excised

spots were destained 30 min with 100 mM ammonium bicarbonate and acetonitrile (J.T. Baker, Deventer, Holland) (1:1 v/v). Digestion was carried out overnight at 37°C with a trypsin buffer containing 13 ng/µl trypsin, 10 mM ammonium bicarbonate (pH 7.8), 10% acetonitrile. The resulting tryptic fragments were extracted with 5% formic acid/acetonitrile 1:1 (v/v) incubating them15 min at 37°C in a termomixer at 700 rpm (Mixing Block MB-102, Bioer, Hangzhou, CN) and dried using a Speed Vac Concentrator 5301 (Eppendorf AG, Barkhausenweg, Hamburg, Germany).

### 3.5 MALDI-TOF Mass Spectrometry

The tryptic peptides were desalted and concentrated to a final volume of 4 µl with Zip-Tip C18 (Millipore Corporation, Billerica, MA, USA), according to the manufacturer's protocol, then dispersed into an α-cyano-4-hydroxycinnamic acid (4-HCCA) matrix, prepared by dissolving 4-HCCA in 50% acetonitrile/0.05% trifluoroacetic acid and spotted on a MALDI plate. The samples were subjected to mass spectrometry analysis utilizing a model 4800 MALDI-TOF/TOFTM MS analyzer (Applied Biosystems, Foster City, CA, USA). Peptide mass spectra were acquired in reflectron mode (500-4000 *m/z* range) and analyzed with the help of mMass v5.5 open source software (http://www.mmass.org/). For each feature, a peak list was created and then manually checked for the presence of signal from the matrix complex, trypsin and human keratin peptides. The main parameters were set as follows: digestion enzyme trypsin with one missed cleavage, mass type monoisotopic, 100 ppm peptide tolerance, cysteine carbamidomethylation and methionine oxidation were set to enzymatic cleavage as fixed and variable modifications respectively.

### 3.6 Protein identification and data analysis

Peptide mass fingerprinting analysis was carried out with the software Mascot (http://www.matrixscience.com) and proteins were identified by searching the Swiss-Prot Viridiplantae (Green Plants) taxonomic sub-database of 'nr' (nonredundant) database of the UniProtKB-Swissprot database (http://www.uniprot.org/uniprot/).

### 3.7 Data mining and analysis

Heat maps of selected proteins were generated using the open source program R v3.3.1 (www.r-project.org). The Gene Ontology analysis was performed through the Panther database (Mi et al. 2016; pantherdb.org/).

In modern plant biology, the most widely used ontologies are the Gene Ontology (GO) and Gene Ontology MapMan. MapMan Ontology was performed using the GoMapMan tool based on ITAG Release 2.3 234 (2011-04-26) of the A. thaliana genome sequence. MapMan 3.6.0RC1 software (mapman.gabipd.org/web/guest/mapman-download) was used to place proteins within a likely pathway.

# Results and discussion (I)

## 4.1 *Arabidopsis thaliana* proteome after CdS QDs treatment

The efficient separation, visualization, and identification of complex protein populations are prerequisites for successful proteome analysis. 2D electrophoresis (2-DE) and subsequent mass spectrometry (MS) to identify individual spots are classical approaches fulfilling these requirements (Usadel *et al.* 2012).

The 2-DE profiling generated overall about 600 visible features for each wt plants and for each of the two mutants, *atnp01* and *atnp02*, exposed or not exposed to CdS QDs.

To allow consistent MALDI-TOF analysis the effective number of the reproducible spots in the plant proteome of *Arabidopsis thaliana* were 258. Within the former set, 98 varied in intensity in response to the treatments (Figure 7): 61 of these were identified from the contrast wt nt *vs* wt + QDs, 31 from the contrast atn01 *vs* + atn01 QDs and 31 from the contrast atn02 *vs* + atn02 QDs (Figure 8).

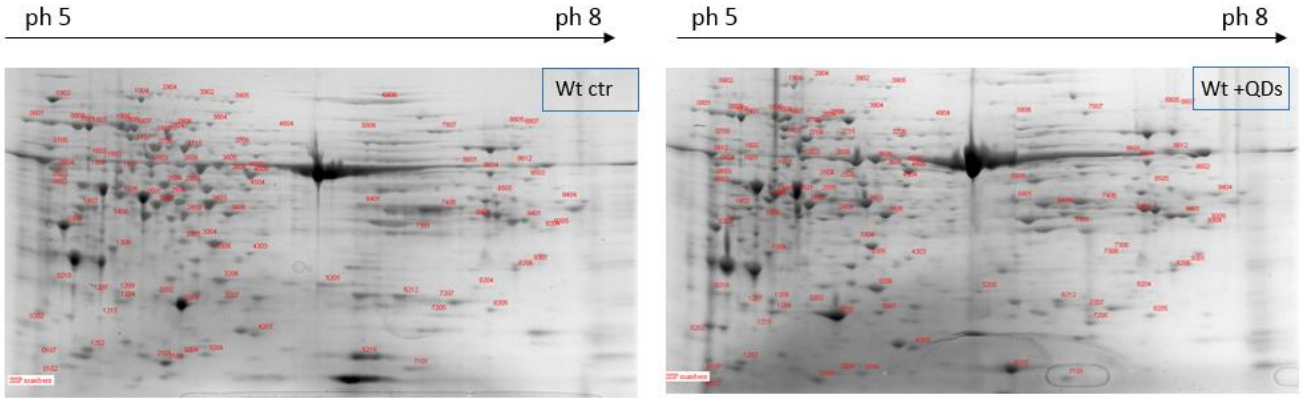


**Figure 7**. *Arabidopsis thaliana* proteins (400 µg loaded) were separated over pH range 5-8 (11 cm strips) and 12% SDS-polyacrylamide gel. These reference gel was stained with Comassie Brillant Blue. Red numbers in both gels indicate proteins showing quantitative differences, which were further identified by MS approach.

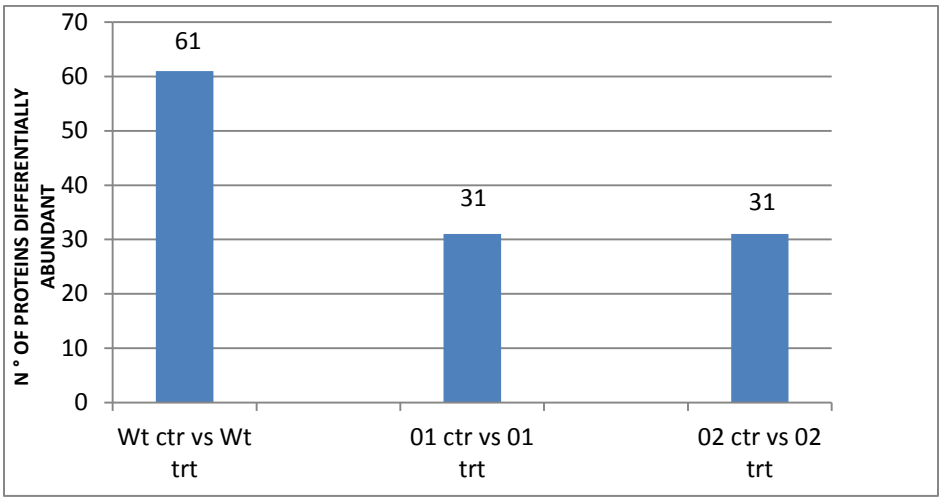


**Figure 8.** Proteins groups with statistically significant difference in abundance level (*p< 0.05)* according to *Student's test* in the three different comparisons.

The proteome of both mutants differed from that of the wt, either when the plants were grown under control conditions and when they were exposed to CdS QDs. In fact, only 1 of the variable features was in common among all comparisons, namely, a putative protein phosphatase 2C 58 (Figure 9). Two proteins were in common to both mutants in the treatment condition, namely bifunctional enolase 2/transcriptional activator and putative pectinesterase/pectinesterase inhibitor VGDH2 (Figure 9).

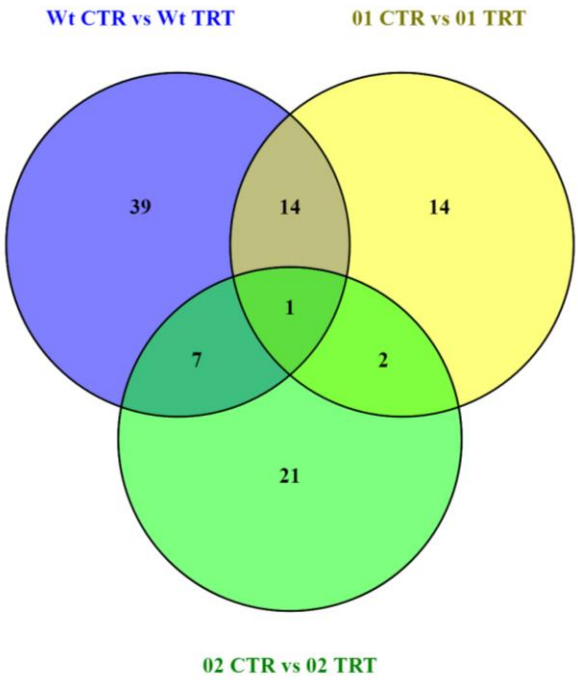


**Figure 9.** Venn diagrams for common and non-common proteins to wt and *atnp01*, to wt and *atnp02*, to a*tnp01* and *atnp02* and to all treatment conditions.

The identity set of variable features is given in Table 1 and Table 2, and the associated heat map illustrating their relative abundance is shown in Figure 10.

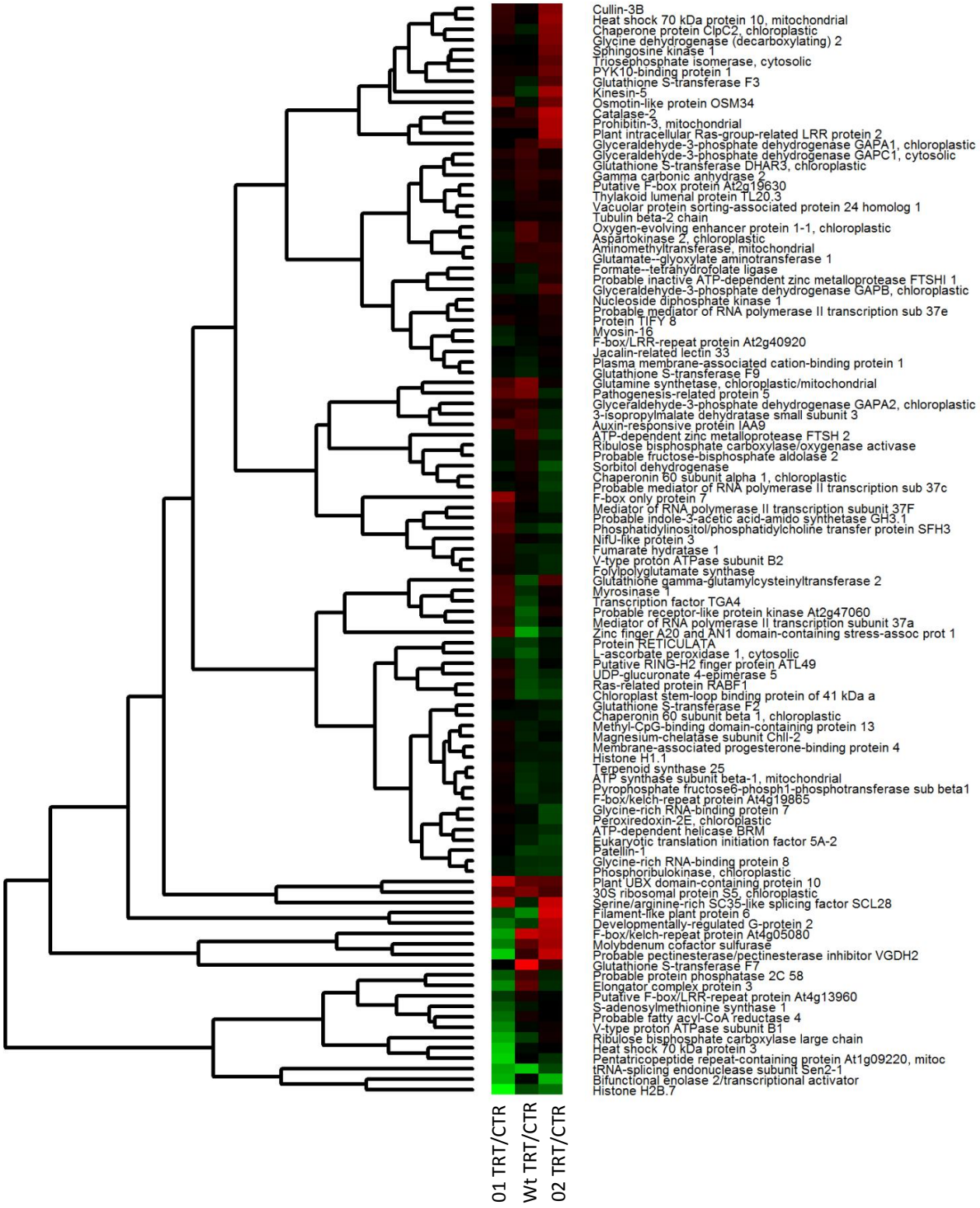


**Figure 10**. Heat map representing the effect on *A. thaliana* proteome of CdS QDs (80 mg $L^{-1}$) for wt and for the mutant lines *atnp01* and in *atnp02*.

For all the 258 proteins, the MapMan ontology BIN assignations are listed in Table 2.

In wt, the set of reprogrammed proteins were associated with the following bins: protein synthesis, protein folding, protein degradation, protein post-transcriptional modification, RNA regulation of transcription, DNA synthesis and chromatin structure, amino acid metabolism, hormone metabolism, redox ascorbate and glutathione biosynthesis, photosynthesis and abiotic stress and biotic stress.

In *atnp01*, the set of reprogrammed proteins were associated with protein synthesis, protein folding, protein degradation, protein post-transcriptional modification, RNA regulation of transcription, DNA synthesis and chromatin structure, hormone metabolism, redox ascorbate and glutathione biosynthesis, abiotic stress and biotic stress, and mitochondrial electron transport and ATP synthesis.

In *atnp02*, the set of reprogrammed proteins were associated with protein synthesis, protein folding, protein degradation, RNA regulation of transcription, hormone metabolism, redox ascorbate and glutathione biosynthesis, and abiotic stress and biotic stress and transport.

## 4.2 Proteome modulation in response to CdS QDs treatment

Most of the studies carried out so far primarily dealt with the overall plant response towards a specific ENMs stress showing differential abundance of proteins involved in oxidation-reduction, reactive oxygen species (ROS) detoxification, stress signaling, and hormonal pathways (Hossain *et al.* 2015). Exposure to ENMs resulted not only in extensive changes in the proteome, but also in the transcriptome, and in the metabolome (Marmiroli *et al.* 2014). When oxidative stress increases, due to the treatment with ENMs, the excessive concentration of ROS cause the utilization of most of the antioxidant molecules for their detoxification. At the same time, cell metabolism increases the biosynthesis of antioxidant enzymes and metabolites to replace those spent so far (Santos *et al.* 2012; Sharma *et al.* 2012).

Two *A. thaliana* mutants (*atnp*01 and *atnp*02) able to tolerate a level of CdS QDs sufficient to strongly compromise the growth of a wt plant, were found by screening a transposon-mutagenized line of A. thaliana (Marmiroli *et al.* 2014). Comparing the transcriptomes and the proteomes of these mutants with that of the wt has provided a ready means to define genes and/or proteins up- or down-regulated in one or both of the mutants, in non-stressed conditions and under CdS QDs exposure (Marmiroli *et al*. 2014; Marmiroli *et al*. 2015). Here, the analysis has been extended to the

protein level, by exploiting a platform able to identify not only specific gene products but also their post-translationally modified forms. Combining these data with those acquired from other "omics" platforms is one of the main goal of current system biology strategies, which aims at defining the complex pathways and networks involved in response to different external stimuli (Jorrín-Novo *et al*. 2015; Wang *et al.* 2015) and identifying potential biomarkers of exposure to the ENMs.

According to MapMan ontology, most of the proteins in wt were down-regulated annotating processes such as the biotic and abiotic stress response, protein folding and protein degradation. Conversely, proteins in both mutants did not show any particular changes in the proteome: about half of the proteins were down-regulated and the other half up- regulated.

In wt and in both mutants, proteins from cellular metabolism such as glyceraldehyde-3-phosphate dehydrogenase-C subunit (GAPA1, GAPA2, GAPB), Pyrophosphate fructose6-phosph1-phosphotransferase subunit beta1 (PFP-BETA1), 30S ribosomal protein S5, Glycine dehydrogenase decarboxylating 2 (GLDP2) and Bifunctional enolase 2/transcriptional activator (ENO2) were modulated. In general, GAPA1 has a role in the glycolytic pathway, but at the same time, it can interact with $H_2O_2$ thus becoming part of the ROS signaling cascade (Rius *et al.* 2008). The alteration of several proteins involved in primary metabolism suggests that CdS QDs exposure had moderately influenced carbon metabolism. These include the up-regulation in wt of GAPA1, PFP-BETA1, and 30S ribosomal protein S5. This observation further supported that CdS QDs exerted oxidative stress by reacting with cellular proteins and enzymes and subsequently generated free radicals (Garcìa-Sànchez). As supported by Tiwari M. (2016), the disruption or malfunction of electron transport system in mitochondria (V-type proton ATPase subunit B1 and B2, Prohibitin-3, and Gamma carbonic anhydrase 2) and chloroplast (Phosphoribulokinase, Chaperonin 60 subunit beta 1), by QDs, when they moved inside the cell, could be a probable mechanism of ROS production by the QDs. ENO2 and V-type proton ATPase subunit B1 were on the other hand down-regulated in both mutants. A study on Arabidopsis mitochondrial proteomics identified enolase among the enzymes, associated with the outer mitochondrial membrane (Giegé *et al.* 2003) and enolase is also proven to interact with the tonoplast through direct association with V-ATPase subunits, specifically the regulatory subunit VHA-B (Barkla *et al.* 2009). Therefore, our findings support the involvement of the mitochondria respiration process in CdS QDs response mechanism acting in both mutants.

Interestingly, four glutathione S-transferases (GSTs), representative of λ and φ classes of GST family, have been identified in the proteome analysis. In wt, two members of GST family, GST F2 and GST F9, decreased, whereas a significant increase in GST F7 and GST-DARH3 concentration was noticed in treatment condition. The GST family in plants is notable for its structural and functional diversity and the biochemical and physiological functions of specific members remain to be elucidated. As well as or instead of catalysing conjugase reactions, some GSTs may have antioxidative functions. The DHAR type of GST is one example, while several subclasses of GST have peroxidase activity (Wagner *et al.* 2002; Dixon *et al.* 2009). The detection of a large numbers of GSTs in *A. thaliana* proteome is particularly important, in fact the function of GSHs in the maintenance of the cell's redox balance, in xenobiotic detoxification and flavonoids subcellular transport is well known. It is also likely that induction of multiple GSTs is associated with the necessity of GSH molecules to reduce CdS QDs toxicity and chelate Cd ions that might be released by the nanoparticles.

Nanoparticle exposure may result in the change of transcription of genes involved in biosynthesis or signal transduction of plant hormones, e.g., of auxin repressor or auxin response genes, abscisic acid (ABA) biosynthetic genes or ethylene signaling components (Syu *et al.* 2014). In this study, at the proteome-level in *A. thaliana* wt there was an up-regulation of the proteins involved in the biosynthesis of auxin (Auxin-responsive protein IAA9) and a down regulation in proteins involved in the biosynthesis of ABA (Myrosinase 1) and jasmonate (Jacalin-related lectin 33). In plants, Protein phosphatase 2C (PP2C) has been implicated in the negative regulation of protein kinase cascades that are activated because of stress. The members of the family PP2Cs, such as ABI1 and ABI2, are involved in ABA signal transduction. Abscisic acid is a plant hormone crucial to mediate the plant responses to environmental stresses (Chandler *et al.* 1994). In this work we found that this protein is over abundant in the wt and under abundant in both mutants in condition of the treatment with CdS QDs. For instance, human PP2C catalysis the dephosphorylation and subsequent inactivation of the AMP-activated protein kinase (AMPK) (Moore *et al.* 1991). AMPK is a central component of a protein kinase cascade, which is activated by cellular stresses, especially those that deplete ATP levels (Corton *et al.* 1994).

The modulation of these proteins by CdS QDs treatment highlights the importance of hormones and signaling in the response mechanisms to the nanoparticles.

## 4.3 MapMan pathways identified under QDs treatment

Metabolic pathways associated with the cellular status of *Arabidopsis thaliana* wt and both mutants were derived using MapMan software, based on the "Ath_AGI_TAIR9_Jan2010" database. The highest scoring processes were "cell function overview" and "biotic stress pathway" for the three groups of genetic backgrounds. The "cell function overview" assigned 57 of 61 mapped proteins in the wt to 14 processes, namely: "DNA synthesis", "cell organization", "stress biotic and abiotic", "regulation of transcription", "development", "protein synthesis and amino acid activation", "hormone", "regulation", "protein modification", "protein degradation", "redox", "metal handling", "transport" and "enzyme families", leaving the remaining four proteins either without any ontology or having an unknown function (Figure 11A). Of the 31 atnp01 proteins classified within the "cell function overview" category, 29 could be assigned to 12 processes "cell division and cell cycle", DNA synthesis", "stress biotic and abiotic", "regulation of transcription", "hormone", "protein modification", "protein degradation", "redox", "transport" and "enzyme families", leaving the remaining 4 proteins either without any ontology or having an unknown function (Figure 11B). Of the 31 atnp02 proteins classified within the "cell function overview" category, 28 could be assigned to 13 processes: "DNA synthesis", "cell organization", "stress biotic and abiotic", "regulation of transcription", "protein synthesis and amino acid activation", "hormone", "regulation", "protein modification", "protein degradation", "redox", "metal handling", and "enzyme families", leaving the remaining 3 proteins either without any ontology or having an unknown function (Figure 11C).

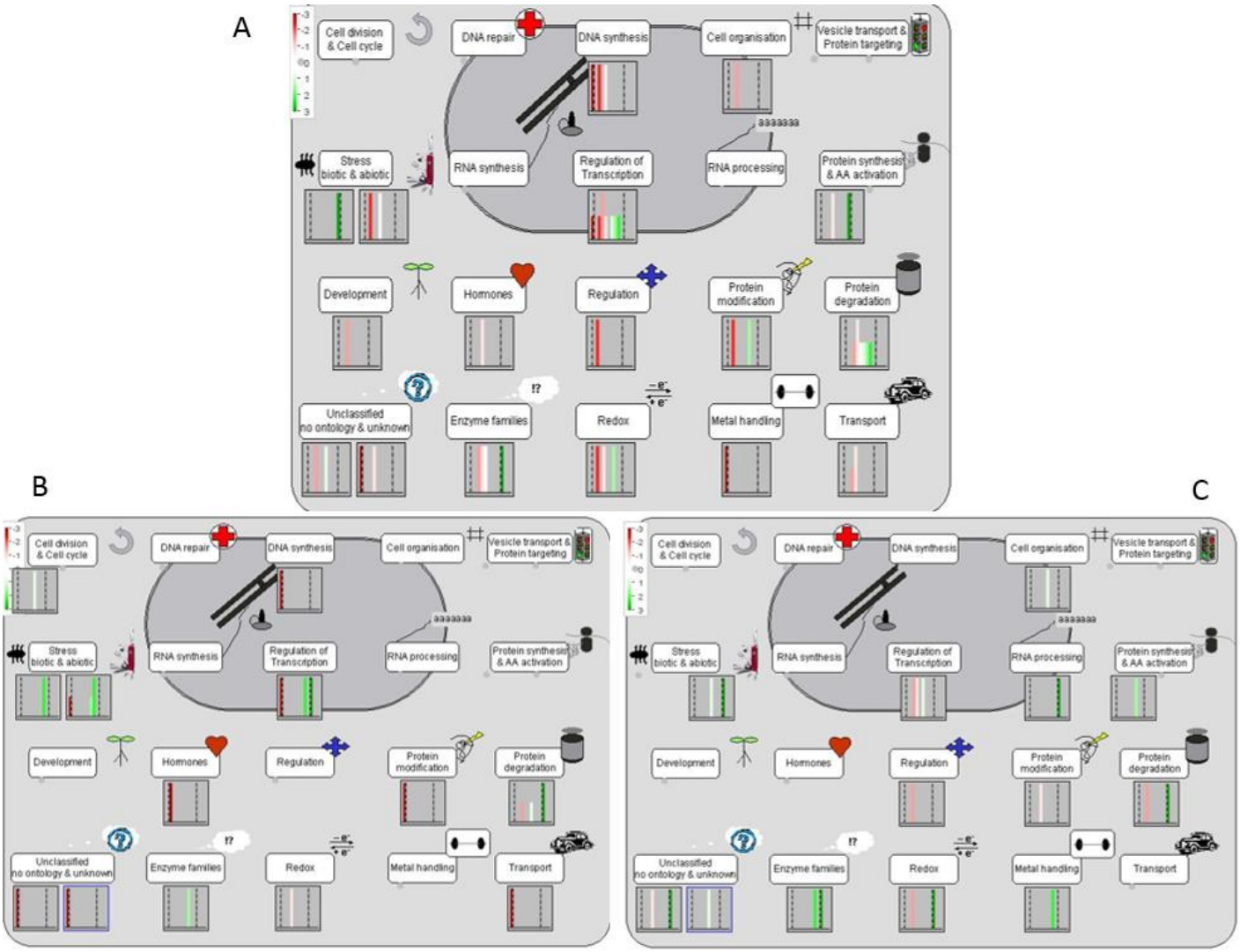


**Figure 11**. Cell function overview map after CdS QDs exposure. Cell functions associated with the proteomic changes affecting *Arabidopsis thaliana* after CdS QDs exposure in wt (A) *atnp01* (B) and in *atnp02* (C) using MapMan software. The represented spots are only for proteins showing a significant change in protein abundance between the treatment and the untreated control that were attributed to the respective bins by MapMan. Over- and under- abundant proteins are indicated in red and green, respectively.

The 23 wt proteins assigned to the "biotic stress pathway" were associated with "hormone signaling", "cell wall", "proteolysis", "heat shock proteins" "redox", "abiotic stress" "signaling" "transcription

factor" and "secondary metabolites" (Figure 12A). The 16 atnp01 proteins assigned to the "biotic stress pathway" were associated with "hormone signaling", "transcription factor" and "secondary metabolites" (Figure 12B). The 10 atnp02 proteins assigned to the "biotic stress pathway" were associated with "cell wall", "proteolysis", "heat shock proteins" "redox" and "abiotic stress" (Figure 12C). Proteins that have been experimentally indicated to be involved in biotic stress are collected in the main panel (colored with dark grey), while proteins and pathways that are putatively involved in biotic stress are shown on sides (colored in light grey).

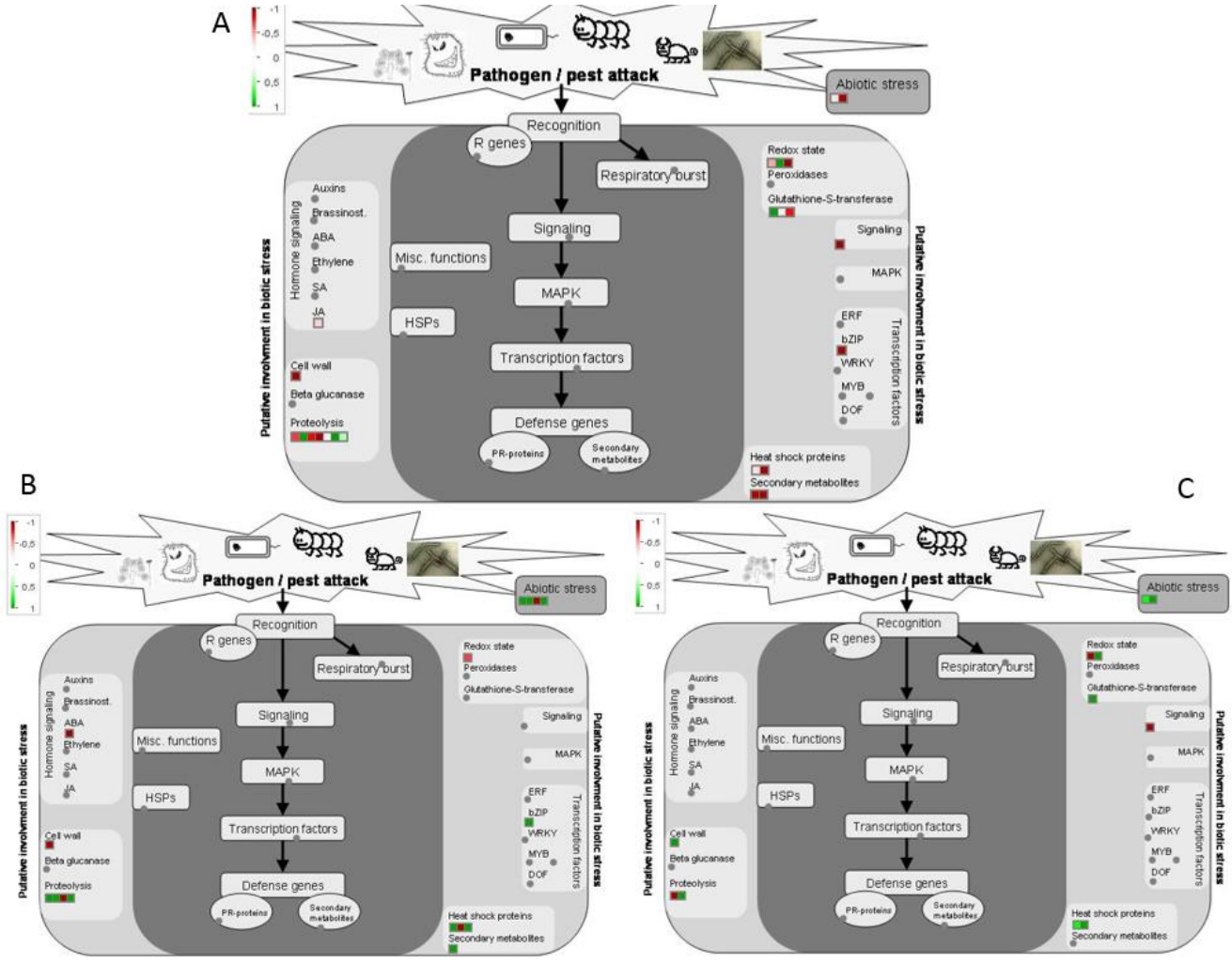


**Figure 12**. Biotic stress overview map after CdS QDs exposure. Stress response associated with the proteomic changes affecting *A. thaliana* after CdS QDs exposure in wt (A) atnp01 (B) and in atnp02 (C)

using MapMan software. The represented spots are only for proteins showing a significant change in protein abundance between the treatment and the untreated control that were attributed to the respective bins by MapMan. Over- and under- abundant proteins are indicated in red and green, respectively.

The MapMan pathway analysis highlighted the distinct behavior adopted by wt in respect to both mutants after CdS QDs exposure. Proteins implicated in the biotic stress response were reprogrammed in wt and mutants, but there were differences with respect to the number and type of the major classes of proteins involved. For example, transcription regulation, protein degradation, and redox were prominent in wt, whereas in both mutants, the main categories were protein degradation, biotic and abiotic stress and hormones.

### 4.4 Gene Ontology

The Gene Ontology (GO) analysis, performed with PANTHER™ Version 12.0 (released 2017-07-10), identified the biological process that were functionally enriched after the treatment with CdS QDs in wt and in the two mutants using a p-values <0,01 (Figure 13). The main biological processes enriched were: response to stimulus (34,3%), response to chemical (27,3%), response to stress (22.2%), response to abiotic stimulus (16,2%), response to hormone (15,2%). Response to stimulus and response to abiotic stimulus include several dehydrogenases (GAPB and GAPA1) and oxidoreductases (CSP41A and GDCST). Response to stress includes glutathione transferases (GSTF2, GSTF7 and GSTF9), heat shock protein (HSP70-10) one catalase (CAT2) and one enolase (ENO2), with a protective role by oxidative damage.

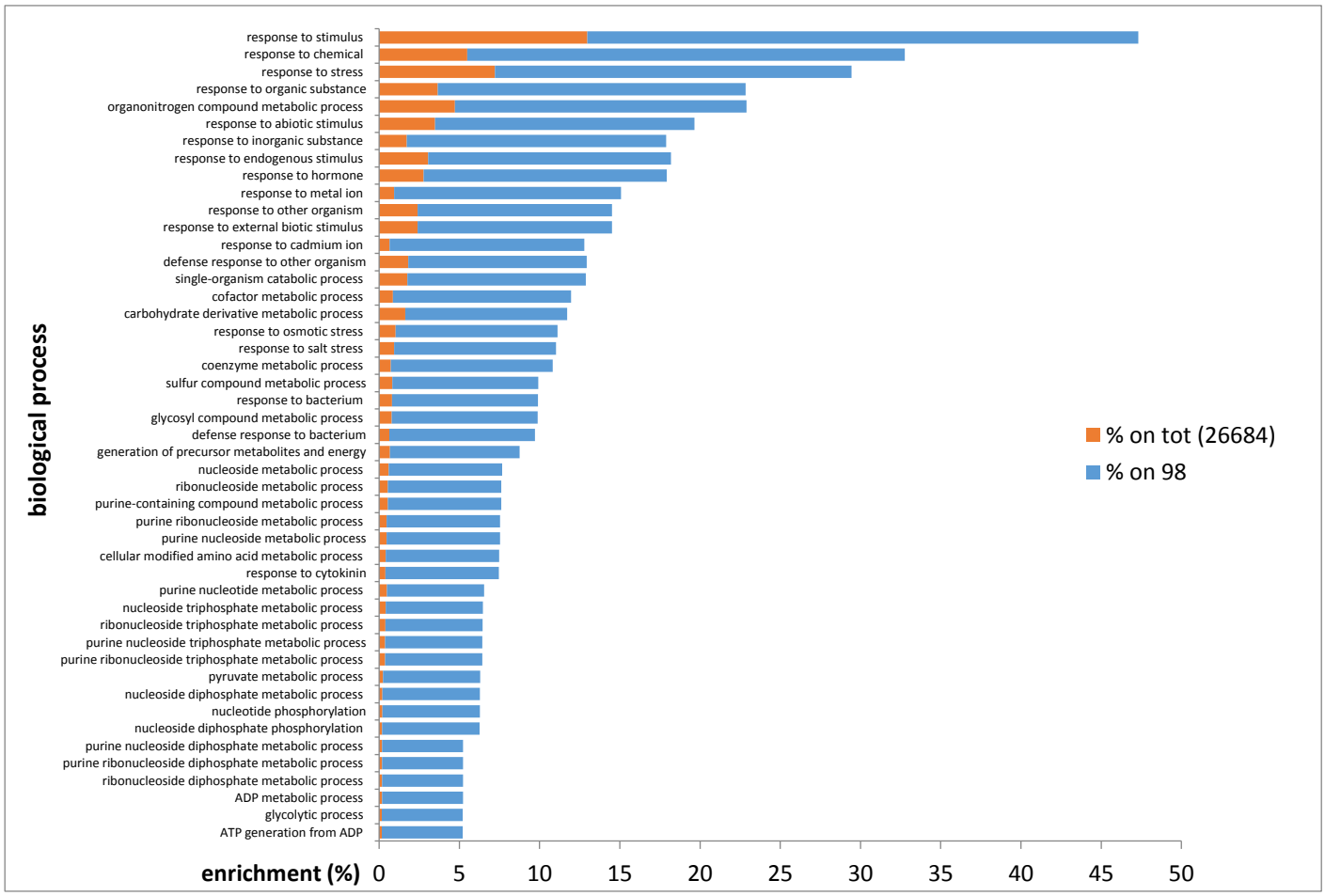


**Figure 13**. Gene ontology analysis of functionally enriched biological process in response to CdS QDs exposure. Blue bars represent the frequency of the genes belonging to each category in the cluster, while orange bars represent the frequency on the entire genome of *A. thaliana.*

*Saccharomyces cerevisiae*

# Materials and methods (II)

## 5.1 Yeast strains and growth conditions

The experiments discussed in this part used *Saccharomyces cerevisiae* strain BY4742 (MATα his3Δ1 leu2Δ0 lys2Δ0 ura3Δ0) (Giavier *et al.* 2014). Yeast cells were inoculated in a liquid YPD (Yeast extract Peptone Dextrose) medium pre-culture (1% w/v yeast extract, 2% w/v peptone, 2% w/v dextrose), and grown for 9 hours (exponential phases) at 28°C under shaking at 130 rpm.

The proteomic analysis was performed on cells grown in 50 ml of YPD without any further supplementation or supplementation of: 0.25 mg $L^{-1}$ nystatin, 100 mg $L^{-1}$ CdS QDS and 0.25 mg $L^{-1}$nystatin plus 100 mg $L^{-1}$ CdS QDS.

## 5.2 Yeast growth on different CdS QDs exposure

A spot assay was performed in 25 mL Petri dishes on YPD agar 2% w/v (yeast extract 1% w/v, peptone 2% w/v, dextrose 2% w/v) and on SD (Synthetic Defined) agar 2% w/v (6.7 g/L yeast nitrogen base w/v, glucose 2% w/v, histidine 20 mg/L w/v, leucine 120 mg/L w/v, lysine 60 mg/L w/v, uracil 20 mg/L w/v). Starting from cultures pre-grown in YPD, five serial 10-fold dilutions ($10^7$-$10^3$) of wilt type were spotted onto growth media alone, or supplemented with 25/50/100/200 mg $L^{-1}$ CdS QDS. After 72 h of incubation at 28°C, the presence/absence of growth at each cell dilution was assessed.

To increase the permeability of the yeast membranes and facilitate the CdS QDs intake we decided to supplement the growth media with a concentration of nystatin according to Marmiroli *et al*. (2016). Nystatin is an antibiotic, isolated for the first time in 1954 from *Streptomyces noursei* and belonging to the class of polyenic macrolides, able to bind ergosterol present in the fungal cell membrane and lead to the formation of pores that alter the physical characteristics of transport and permeability of the membrane itself. Thanks to these peculiarities, the use of a sub-lethal concentration of nystatin should allow an easier intake of the nanoparticles within the yeast cell.

To determine the toxicity of the CdS QDs different growth curves were plotted, using concentrations ranging from 0 to 200 mg $L^{-1}$ with and without nystatin. Yeast was grown starting from liquid cultures

pre-grown in YPD at an optical density, at 600 nm [$OD_{600}$] of 14 OD after 12 h was estimated. Then the cells were diluted to $OD_{600}$ = 0.2/ml in 10 ml YPD medium alone and supplemented with 25/50/100/200 mg $L^{-1}$ CdS QDS at 28 °C with shaking (200 rpm) for 48 h.

### 5.3 Protein extraction for 2d gel

Cells were sampled at the exponential phase (9 h). The growth medium was eliminated by centrifugation at 5000 g for 15 min. Cell pellets were collected, washed with distilled cold water and stored frozen at -80°C. After storage, cells were resuspended in 300 µl of denaturing IEF buffer containing 7 M urea, 2 M thiourea, 2% CHAPS detergent, 1% ampholytes (pH 3–10, GE Healthcare), 75 mM DTT (added just before use) and supplemented with 5 µl of protease inhibitor cocktail (SIGMA-P8215) per 10 mL of buffer (Slibinskas *et al.* 2013*)*. The cells were broken by vortexing six times 60 s (the samples were cooled on ice for 30 s between each vortexing step) in the presence of glass beads in a volume equivalent to that of the cell pellet. Glass beads insoluble material and cell debris were eliminated by centrifugation for 30 min at 4 °C 12000 g.

### 5.4 Protein quantification

Supernatants protein concentrations were determined according to a modified Bradford assay (Ramagli *et al.* 1985) based on the acidification of the sample buffer with 20 mM HCl. Bovine serum albumin (BSA) was used as standard. Further sample preparation depended on the separation strategy, i.e., 2D-gel or iTRAQ-labeling.

### 5.5 2-D gel electrophoresis

IPG strips (11 cm, pH 4-7, ReadyStrip BioRad, USA) were rehydrated overnight with 250 µl of IEF buffer containing 250 mg of total proteins. Proteins were focused by PROTEAN® i12™ IEF System (BioRad, USA) applying 250 V (60 min), 1 kV (60 min), 8 kV (5 hours) and 8 kV for a total of 35 kV/h.

After focusing, the strips were incubated 15 min in 3 ml of reducing buffer containing 2% w/v DTT, 6 M Urea, 0.375 M Tris-HCl (pH 8.8), 20% w/v glycerol, 2% w/v SDS. Subsequently they were incubated 15 min in 3 ml of alkylating buffer containing 2.5% w/v iodoacetamide, 6 M Urea, 0.375 M Tris-HCl (pH 8.8), 2% w/v glycerol. Electrophoresis in the second dimension was carried out using a Criterion™ Dodeca™ cell (BioRad, USA) and 12% Criterion™ XT Bis-Tris Gel (BioRad, USA) in MOPS (J.T. Baker, Deventer, Holland) buffer (1M 3-(N-morpholino ) propanesulfonic acid, 1M Tris, 20 mM EDTA, 2% w/v SDS).

2-DE gels were stained with QC Colloidal Coomassie G-250 (BioRad, USA) and gel images were obtained with a ChemiDoc™ Imaging System (BioRad, USA). Image analysis was performed using the PDQuest software (BioRad, USA). Spot detection and matching between gels were performed automatically, followed by manual verification. The spot densities were normalized by local regression method and subsequently against the whole gel densities. The percentage density of each spot was averaged for three replicates gels and Student's t-test analysis ($p<0.05$) was performed to find out statistically significant differences in proteins abundance. Spots, compliant with the statistics requirements, were excised from the gels and digested with trypsin according to Shevchenko *et al.* (2006). The excised spots were destained 30 min with 100 mM ammonium bicarbonate and acetonitrile (J.T. Baker, Deventer, Holland) (1:1 v/v). Digestion was carried out overnight at 37°C with a trypsin buffer containing 13 ng/µl trypsin, 10 mM ammonium bicarbonate (pH 7.8), 10% acetonitrile. The resulting tryptic fragments were extracted with 5% formic acid/acetonitrile 1:1 (v/v) incubating them15 min at 37°C in a termomixer at 700 rpm (Mixing Block MB-102, Bioer, Hangzhou, CN) and dried using a Speed Vac Concentrator 5301 (Eppendorf AG, Barkhausenweg, Hamburg, Germany).

## 5.6 MALDI-TOF Mass Spectrometry

The tryptic peptides were desalted and concentrated to a final volume of 4 µl with Zip-Tip C18 (Millipore Corporation, Billerica, MA, USA), according to the manufacturer's protocol, then dispersed into an α-cyano-4-hydroxycinnamic acid (4-HCCA) matrix, prepared by dissolving 4-HCCA in 50% acetonitrile/0.05% trifluoroacetic acid and spotted on a MALDI plate. The samples were subjected to mass spectrometry analysis utilizing a model 4800 MALDI-TOF/TOFTM MS analyzer (Applied

Biosystems, Foster City, CA, USA). Peptide mass spectra were acquired in reflectron mode (500-4000 *m/z* range) and analyzed with the help of mMass v5.5 open source software (http://www.mmass.org/). For each feature, a peak list was created and then manually checked for the presence of signal from the matrix complex, trypsin and human keratin peptides. The main parameters were set as follows: digestion enzyme trypsin with one missed cleavage, mass type monoisotopic, 100 ppm peptide tolerance, cysteine carbamidomethylation and methionine oxidation were set to enzymatic cleavage as fixed and variable modifications respectively.

## 5.7 Protein extraction for iTRAQ labelling

Cells were sampled at the exponential phase (9 h). The growth medium was remuved by centrifugation at 5000 g for 15 min. Cell pellets were collected, washed with distilled cold water and stored frozen at -80°C. After storage, cells were resuspended in 250 µl extraction buffer containing 7 M urea, 2 M thiourea, 2% CHAPS detergent, 20 mM Tris, and supplemented with 5 µl of protease inhibitor cocktail (SIGMA-P8215) per 10 mL of buffer. The cells were broken by vortexing six times 60 s (the samples were cooled on ice for 30 s in between the vortex steps) in the presence of glass beads in a volume equivalent to that of the cell pellet. Glass beads insoluble material and cell debris were eliminated by centrifugation for 30 min at 4 °C at top speed.

To clean up the samples (100 µg of proteins) an acetone precipitation was performed to add six volumes of cold acetone and incubated the tube at –20 °C until precipitate forms for 1 hours. Used the precipitated pellets as samples for iTRAQ analysis.

## 5.8 iTRAQ

The proteins (100 µg) were solubilized in 0.05 M triethylammonium bicarbonate containing 1% sodium deoxycholate (Sigma). Their disulfide bonds were reduced for 1 h at 60 °C in the presence of 5 mM tris (2-carboxyethyl) phosphine, and the resulting free thiol groups were alkylated at room temperature for 15 min by methyl methanethiosulfonate (10 mM). The proteins were hydrolyzed for 16 h at 37 °C in the presence of 5% trypsin in 50 mM triethylammonium bicarbonate. The solutions were acidified by the addition of trifluoroacetic acid (TFA) to a final concentration of 0.5% and centrifuged to remove the

sodium deoxycholate. The resulting supernatants were transferred to new tubes and dried under vacuum. The dried peptides from the yeast samples were dissolved in 100 µl of a mixture consisting of 25% 250 mM triethylammonium bicarbonate and 75% (v/v) ethanol and transferred to different vials containing the different iTRAQ reagents (114–117; AB SCIEX, Foster City, CA). After 1 h of incubation at room temperature, the reaction was stopped by the addition of 100 µl of Milli-Q water. The iTRAQ-labeled yeast samples were pooled, and the mixtures were dried under vacuum. The iTRAQ labeling of the peptides from the other biological replicate was performed in the same conditions, except that the labels were inverted to reduce bias between samples.

### 5.9 Strong Cation Exchange (SCX) Fractionation of the iTRAQ-labeled Peptides

The dried iTRAQ-labeled peptides were resuspended in 3 ml of sample loading buffer (10 mM ammonium formate, 20% acetonitrile, pH 3.0) and loaded on a 1-ml Nuvia$^{TM}$S cartridge (Bio-Rad; prepared according to the manufacturer's instructions) at 0.5 ml/min using a syringe pump. After sample loading, the cartridges were washed with 5 ml of sample loading buffer at 0.5 ml/min, washing was followed by elution at the same flow rate with consecutive 1.5-ml ammonium formate salt plugs at pH 3.0 (30, 50, 80, 100, 125, 150, 175, 200, 225, 250, 275, 300, 325, 350, and 400 mM in 20% acetonitrile). The eluent from each salt plug was dried using a SpeedVac centrifugal vacuum concentrator, and the peptides were purified on a PepClean C-18 column (Thermo Fischer Scientific, USA) prior to mass spectrometry (MS) analysis.

### 5.10 Nano-LC-MS/MS Analysis of the Strong Cation Exchange Fractions

Peptide analysis was performed with reverse-phase LC–electrospray ionization–MS/MS using a nanoACQUITY Ultra Performance Liquid Chromatography system coupled to a Q-TOF mass spectrometer (Xevo Q-TOF, Waters, Milford, USA). The purified strong cation exchange fractions were resuspended in 0.1% TFA and loaded on a C18 trap column (Symmetry 180 µm × 20 mm, 5 µm; Waters, Milford, USA) that was then washed with 1% (v/v) acetonitrile, 0.1% (v/v) formic acid at 15 µl/min for 10 min. The samples eluted from the trap column were separated on a C18 analytical column (75 µm ×

100 mm, 1.7 µm; Waters, Milford, USA) at 350 nl/min using 0.1% formic acid as solvent A and 0.1% formic acid in acetonitrile as solvent B in a stepwise gradient: 0.1%–10% B (0–10 min), 10%–30% B (10–110 min), 30%–40% B (110–120 min), 40%–85% B (120–125 min), 85% B (125–130 min), and 85%–0.1% B (130–135 min). The eluting peptides were sprayed in the mass spectrometer (capillary and cone voltages set to 4 kV and 35 V, respectively), and MS/MS spectra were acquired using automated data-directed switching between the MS and MS/MS modes using the instrument software (MassLynx V4.0 SP4). The five most abundant signals of a survey scan (350–1500 *m*/*z* range, 0.9-s scan time) were selected by charge state, and collision energy was applied accordingly for sequential MS/MS fragmentation scanning (50–1800 *m*/*z* range, 0.9-s scan time).

## 5.11 Data Processing, Protein Identification, and Quantification

As described by Srivastava *et al.,* (2013) an extensive search scheme was used to rigorously profile the MS data following the strategy presented in Figure 14*.* The MS raw data files were processed using Mascot Distiller (version 2.4.3.2, Matrix Science, London, UK). The resulting ".mgf" files were converted into the ".mzXML" file format using msconvert (Kessner *et al.* 2008). The ".mzXML" files were searched by MyriMatch (Tabb *et al*. 2007*)* (version 2.1.120) and X!Tandem (*Craig et al*. 2010) (version 2011.12.01.1, LabKey, Insilicos, ISB, Seattle, WA) using the *Saccharomyces cerevisiae* protein database and the following settings: trypsin specific digestion with two missed cleavages allowed, peptide tolerance of 100 ppm, fragment tolerance of 0.2 Da, iTRAQ 4-plex for peptide N-t and Lys as fixed modifications, and, in variable mode, iTRAQ 4-plex on Tyr and oxidized Met and methylthio on Cys. For quantitative analysis, all iTRAQ reporter ion intensities were extracted using the Trans-Proteomic Pipeline (TPP) tool *Libra* and the isotopic correction factors from the iTRAQ reagent manufacturer. Normalization of iTRAQ channels was performed by summing all intensities of reporter ions in each iTRAQ channel (for peptides above the Libra probability cutoff) and equalizing each channel contribution by dividing individual reporter ion intensities by the corresponding channel-specific correction factor. All ".pep.xml" files obtained from PeptideProphet were combined using iProphet (Shteynberg *et al.* 2011*).* A protein list was assembled using ProteinProphet (Nesvizhskii *et al*. 2003*),* and the final protein ratios were calculated using Libra. In all searches a concatenated target-decoy

database-search strategy was used to check the false positive rate, which was found to be less than 1% in all cases. Peptide sequences were exported for each protein, with a protein and peptide probability cutoff of 0.95. Peptides matching two or more proteins (shared peptides) were excluded from the analysis. Proteins with no unique peptides (*i.e.*only identified by shared peptides) were also excluded. A protein was considered as identified if it contained at least one unique peptide. Only proteins identified by two or more unique peptides were used for quantification. The method of Ross *et al.* (2004) was used for statistical analysis of the quantitative data. Briefly, the 115/114, 116/114 and 117/114 ratio of each protein was calculated for each of the two biological replicates and log2 transformed to obtain a normal distribution. All the values in each comparison dataset were then normalized to the median log values, and global means and standard deviations were calculated for each biological replicate. Proteins whose average ratios fell outside a standard deviation of ±1 from the global mean in at least two out of three biological replicates were considered significantly enriched, therefore chosen for the further analysis.

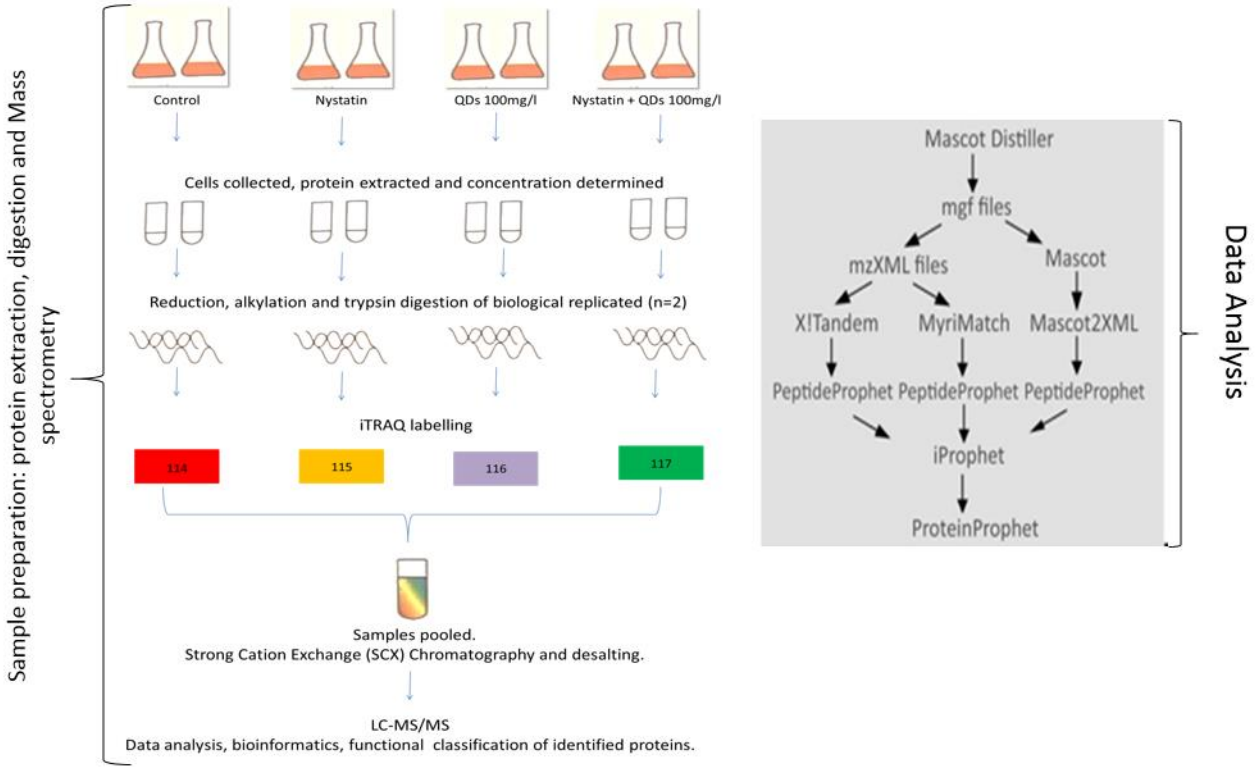


**Figure 14.** Experimental set-up and strategy used for data analysis in the iTRAQ and LC-MS/MS workflow.

## 5.12 Data mining and analysis

The proteins identified were then subjected to metabolic pathway enrichment analysis, which was conducted according to the instructions from the Kyoto Encyclopedia of Genes and Genomes (KEGG) Pathway Database. The Gene Ontology analysis was performed through the Panther database (www.pantherdb.org/).

# Results and discussion (II)

## 6.1 Growth on different CdS QDs concentrations

BY4742 cells were able to grow on YPD at every dilution tested, unless the concentration of CdS QDs in the media exceeded the 100 mg $L^{-1}$. Similarity, the cells were able to grow on SD medium at every dilution tested, unless the concentration of CdS QDs in the media exceeded the 50 mg $L^{-1}$ (Figure 15).

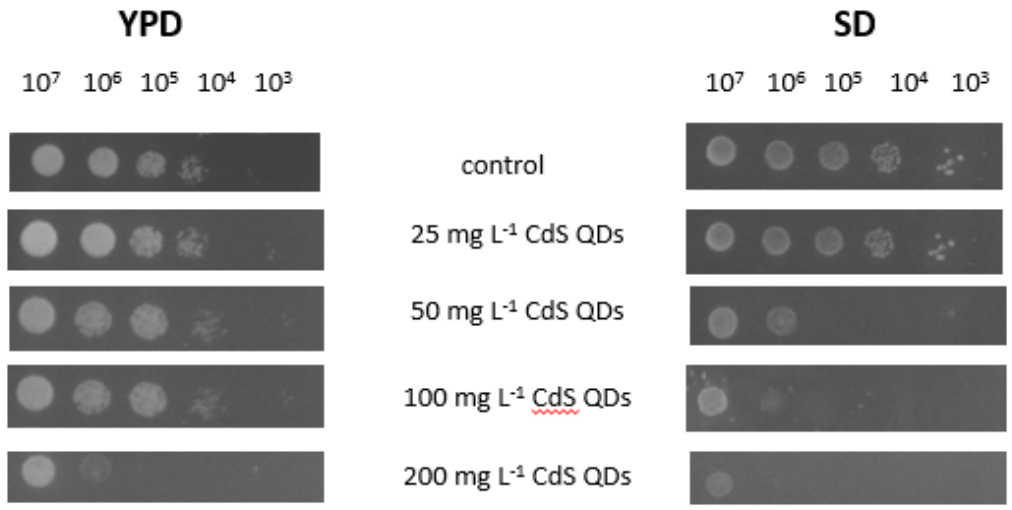


**Figure 15**. BY4742 grown on different growth media: YPD and SD. This panel shows how the growth at different cells dilutions was affected by the treatment conditions tested: control, 25, 50, 100, 200 mg $L^{-1}$. Cells concentrations, used for the different tests, are indicated in the first row of the panel.

Yeast growth better on YPD than on SD media, therefore YPD was chosen as medium for subsequent proteomics analysis.

To determine the toxicity of the CdS QDs two different growth curves were carried out, using concentrations ranging from 0 to 200 mg $L^{-1}$ with and without nystatin (Figure 16).

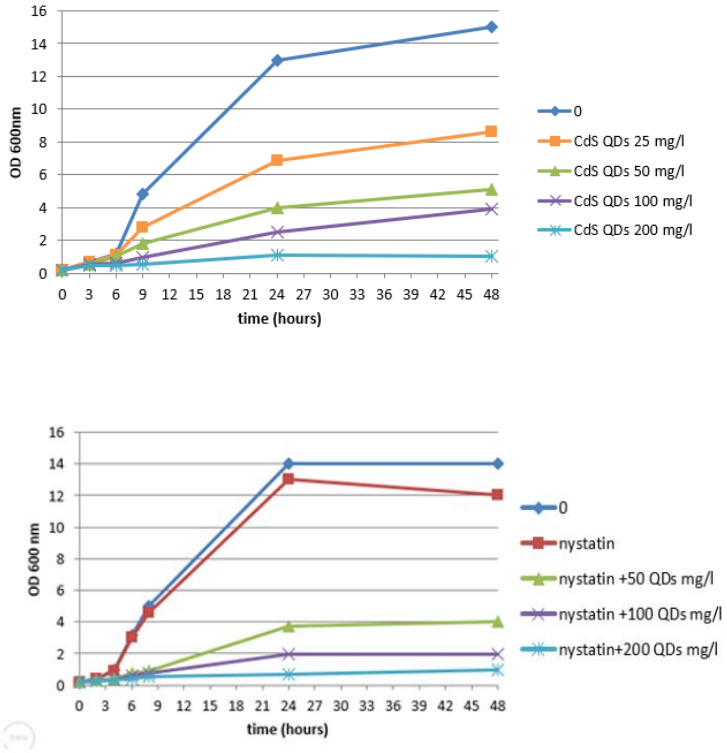


**Figure 16.** Grow curves with (up) and without (down) nystatin at different concentration of CdS QDs for 48 h.

According to Pasquali *et al.* (2017) the concentration of 100 mg $L^{-1}$, with and without nystatin, was chosen for the subsequent proteomic analysis. The time length of the treatment was set at 9 hours.

## 6.2 Proteomic analysis of yeast in response to CdS QDs

To highlight yeast proteome qualitative and quantitative changes during CdS QDs treatment, two techniques were applied: the gel-based method 2D-PAGE and gel-free method stable isotope labeling approach iTRAQ.

### 6.2.1 2D-PAGE Analysis and Identification of Differentially Expressed Proteins

The primary 2D-PAGE approach of yeast cells exposed to CdS QDs uncovered about 900 visible features for each samples. Subsequent MALDI-TOF MS/MS analysis evidenced an effective number of reproducible spots to be 270 (Figure 17). Among the former set, 100 varied in intensity in response to the treatments: 80 of these were identified from the comparison nt (no treated) *vs* QDs; 77 from the contrast nt *vs* nystatin + QDs; 11 from the contrast nt *vs* nystatin and 71 from the contrast nystatin *vs* nystatin + QDs (Figure 19, orange bars). The treatment with CdS QDs (100 mg $L^{-1}$) modulates a greater number of proteins compared to treatment with only nystatin. The identity of the set of identified proteins is given in Table 3 and Table 5.

In the past decades, 2D-PAGE has evolved to the standard method for separation and visualization of closely relative proteomes (Gorg *et al.* 2004).

However, in the 2D-PAGE approach, the identification of several proteins per spot might occur therefore, when using only 2D-PAGE, there still could be uncertainty about which protein is responsible for the changes in the spot intensity, hence the need to use other more selective protein isolation methods. Therefore, stable isotope labeling was chosen to circumvent the limitations of 2D-PAGE and to cover a higher proportion of the yeast proteome.

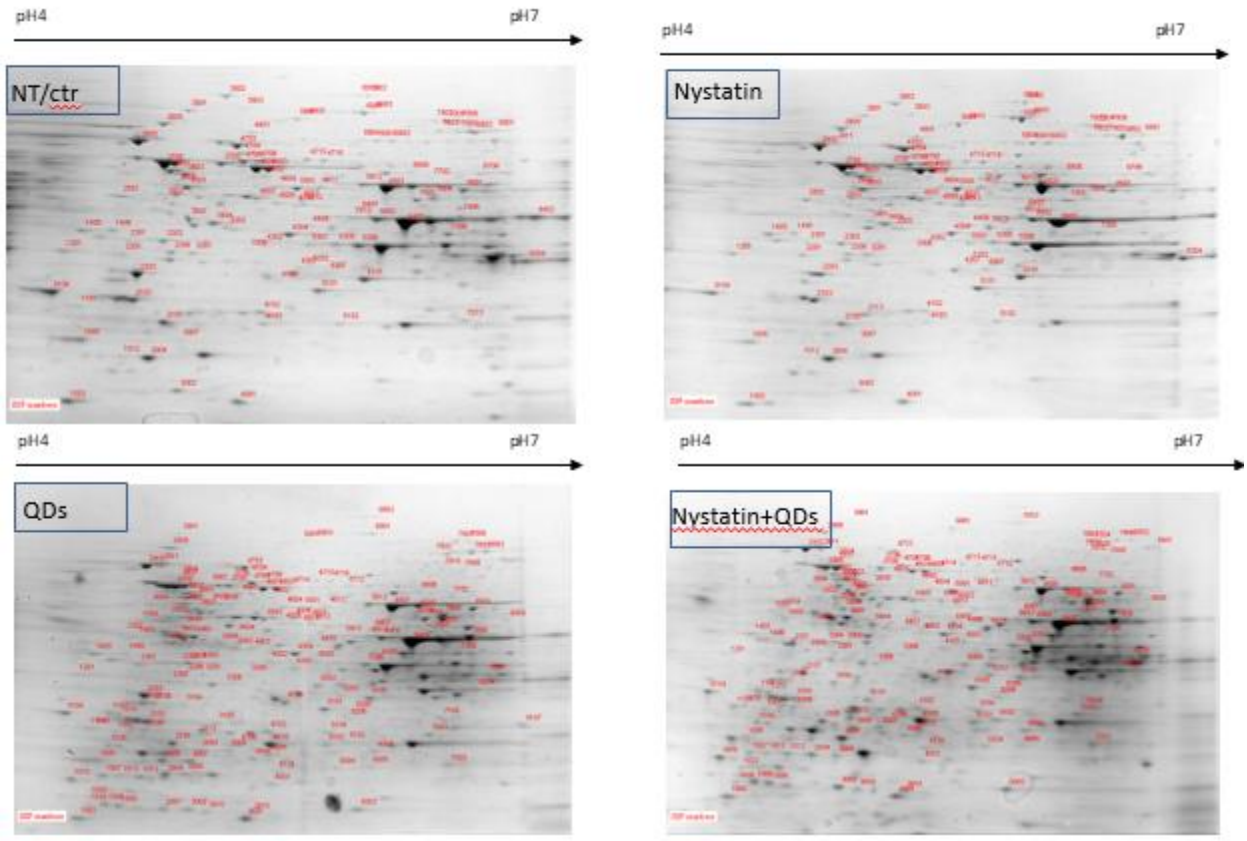


**Figure 17:** Yeast proteins (250 µg loaded) were separated over pH range 4-7 (11 cm strips) and 12% SDS-polyacrylamide gel. The gel was stained with Comassie Brillant Blue. Red numbers in the gels indicate proteins showing quantitative differences, which were further identified by MS approach.

### 6.2.2 iTRAQ Study and Identification of Differentially Expressed Proteins

In a second approach, iTRAQ experiments were carried out to obtain further quantitative information on the proteins regulated by the treatment with CdS QDs. Two biological replicates (BR1 and BR2) were conducted to strengthen the informative value of the analysis. To avoid an impact of possible different characteristics of the different iTRAQ reagents, the samples were labeled alternating. The experiments were conducted and evaluated independently of each other. Using iTRAQ, the quantification at the peptide level enables direct mapping of the identification and the quantification of the results, because both information originate from the same MS/MS spectrum. Moreover, isobaric tags have an advantage compared with other stable isotope labeling techniques, namely, that no increase in sample complexity occurs during chromatographic separation and mass spectrometry (Ross *et al*. 2004). In several other

iTRAQ studies about a thousand proteins were identified (Tafelmeyer *et al*. 2008; Radosevich *et al*. 2007). Using the workflow described in the materials and methods (II) section, proteins having more then one unique peptide identification were filtered. Far more than a thousand proteins were detected within each single iTRAQ experiment. Overall 1479 proteins were identified, of which 712 proteins were detected in both experiments (Figure 18), and thus we achieved a double quantification result.

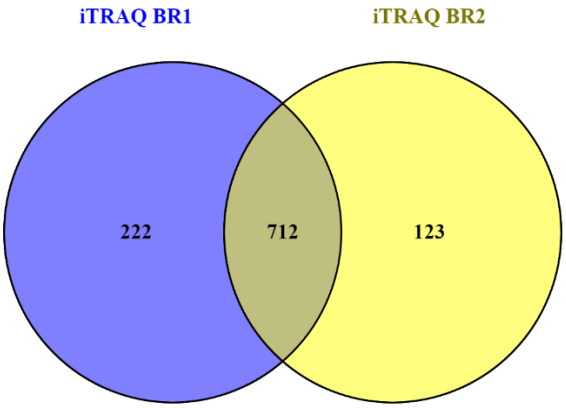


**Figure 18**: Venn diagram of the number of proteins identified with the iTRAQ experiments. Thereof 712 proteins were identified in all two iTRAQ experiments (BR1 and BR2).

The iTRAQ-based quantitative analysis revealed that the actual total number of proteins enriched in yeast in response to the treatments was 93: 80 of these were identified from the comparison nt *vs* QDs, 77 from the contrast nt *vs* nystatin + QDs, 11 from the contrast nt *vs* nystatin and 71 from the contrast nystatin *vs* nystatin + QDs (Figure 19, blue bars). In addition, in this case the treatment with CdS QDs modulates a greater number of proteins compared to treatment with only nystatin. The identity of the set of identified proteins is given in Table 4 and Table 5.

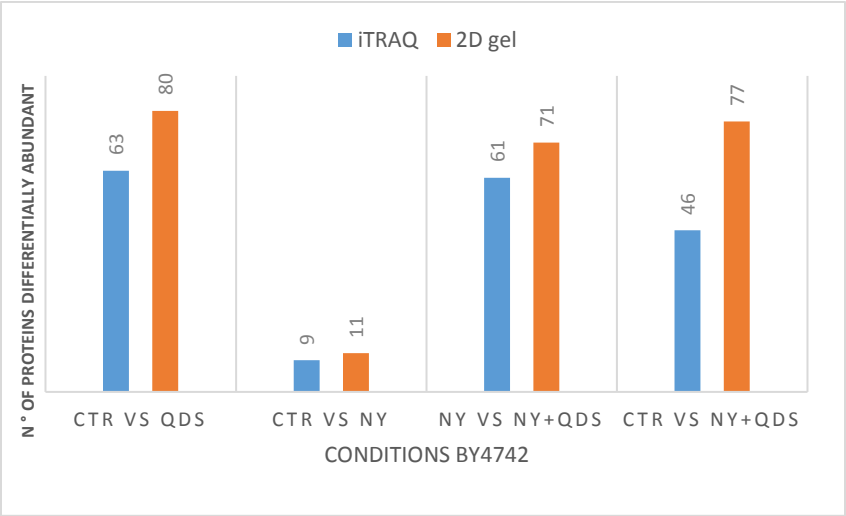


**Figure 19**. Comparison of the proteins enriched in response to the treatments with CdS QDs as identified using 2D-gel or iTRAQ method.

### 6.3 Comparison of the Strategies Used: 2D-PAGE and iTRAQ

The choice of the proteins separation methods to be utilized depends on their different properties. Complementary analyzing strategies have already been used in other proteome studies yielding compatible results (Moebius *et al.* 2005). In proteomics studies using different methods such as DIGE (Difference Gel Electrophoresis), iTRAQ, and ICAT (Isotope-coded affinity tag) have lead to the identification of a large number of proteins (Wu *et al.* 2006). The remarkable differences of the methods applied here can be highlighted by their advantages: in the 2D-PAGE approach the separation is conducted at the proteome level (Gorg *et al.* 2004). iTRAQ instead enables the multiplexing of up to eight samples (Choe *et al*. 2007). These complementary properties become remarkable in the results: proteins identified and quantified with 2D-PAGE and iTRAQ differ substantially. Thus, the combined use of different techniques uncovers a higher proportion of the proteome of an organism (Pütz *et al*. 2012). Still the complementarity of the methods raises the question whether they provide different results concerning the amount of identified and regulated proteins. The number of proteins detected with the different techniques and how many of them were identified by both, is shown in a Venn diagram (Figure 20A). Altogether, 1323 proteins were identified, of which 1057 by iTRAQ constituting majority of the whole proteins. The methods 2D-PAGE and iTRAQ, provide slightly overlapping results, 193 proteins

were isolated by both methods, of which only 4 were significantly modulated according to the set statistical parameters explained in materials and methods (II) section, with mass spectrometry. However, in the 2D-PAGE experiment only proteins already partially modulated were analyzed because the spot isolation methods intrinsically factors in the concentration of each protein corresponding to a spot on the 2D-gel. To investigate how many modulated proteins were isolated by the two strategies and how many were also identified, a Venn diagram representation was used (Figure 20B). Altogether, 189 regulated proteins were significantly modulated out of 1323 isolated in total.

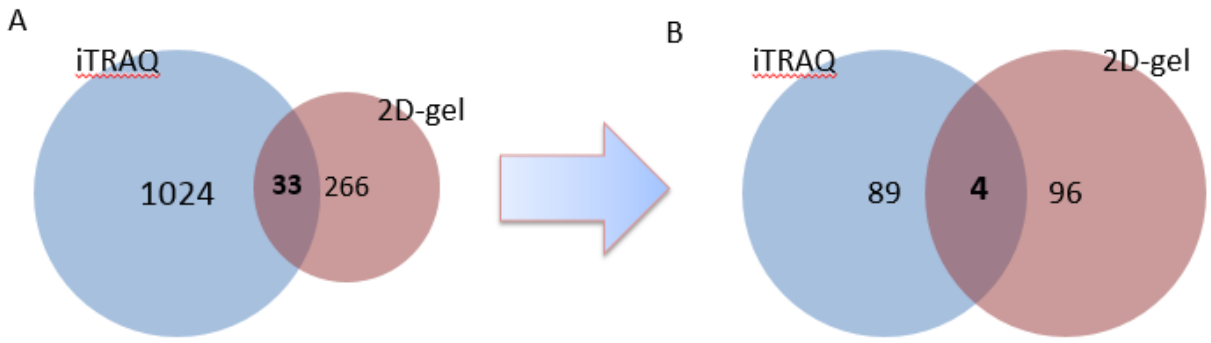


**Figure 20:** Comparison of the number of proteins isolated and identified with iTRAQ and 2D-PAGE. The Venn diagram (A) depicts the numbers of isolated proteins. The Venn diagram (B) depicts the numbers of significant and modulated proteins.

As expected, iTRAQ and 2D-PAGE provide complementary results. The four proteins in common between the two methods were: ATP-dependent molecular chaperone HSP82, uncharacterized oxidoreductase YMR226C (YMR226C), fructose-bisphosphate aldolase (FBA1), and homocysteine/cysteine synthase (MET17) (Table 3, 4 and 5).

## 6.4 Gene Ontology

The Gene Ontology (GO) analysis, performed with SGD *Saccharomyces* Genome Database (https://www.yeastgenome.org) identified the commons molecular functions and the biological processes between the two techniques. The main common molecular functions were: transferase activity (GRX1, KRE2, MET17), oxidoreductase activity (COX1 and 5A, ERG1,4 and 27, ALD4, GRX1) hydrolase activity (HSP82, SIR2, CAR1) (Figure 21), (Table 3, 4 and 5).

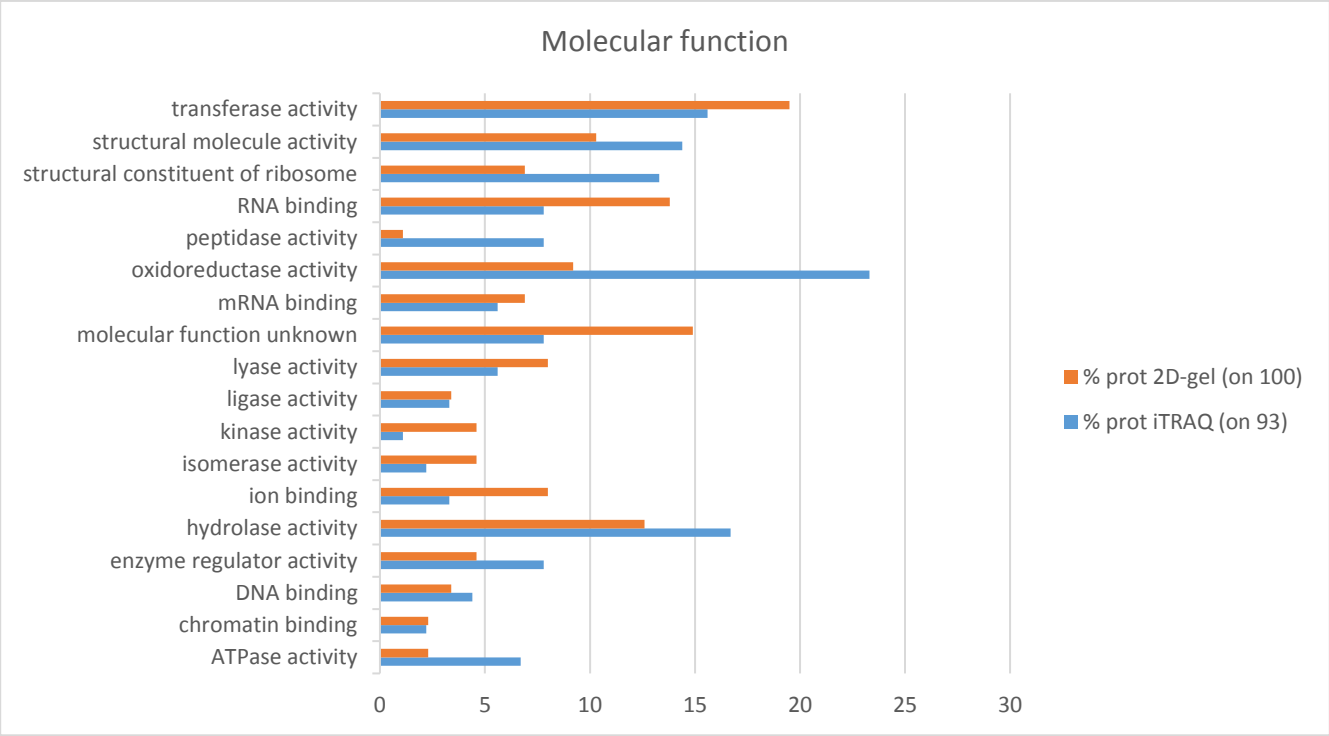


**Figure 21:** Gene ontology analysis of molecular functions in response to CdS QDs exposure. Blue bars represent the percentage of the proteins, find with iTRAQ, belonging to each category in the cluster, while orange bars represent the percentage of the proteins, find with 2D gel, belonging to each category in the cluster.

The main common biological process were: nucleobase–containing small molecule metabolic process (ADE1, FBA1, ADE12 and 17, COX5A, ENO1 and ENO2), response to chemical (GRX1, GAL3, KAR2), monocarboxylic acid metabolic process, mitochondrion organization (GIC2, TIM54, HSP78, ATP25), generation of precursor metabolites and energy (FBA1, ENO1 and ENO2), cytoplasmic translation,

cellular amino acid metabolic process (MET3, MET5 and MET17, LYS12, HIS6) and carbohydrate metabolic process (TDH1 and TDH3, FBA1, GAL3, ENO1 and ENO2) (Figure 22) (Table3, 4 and 5).

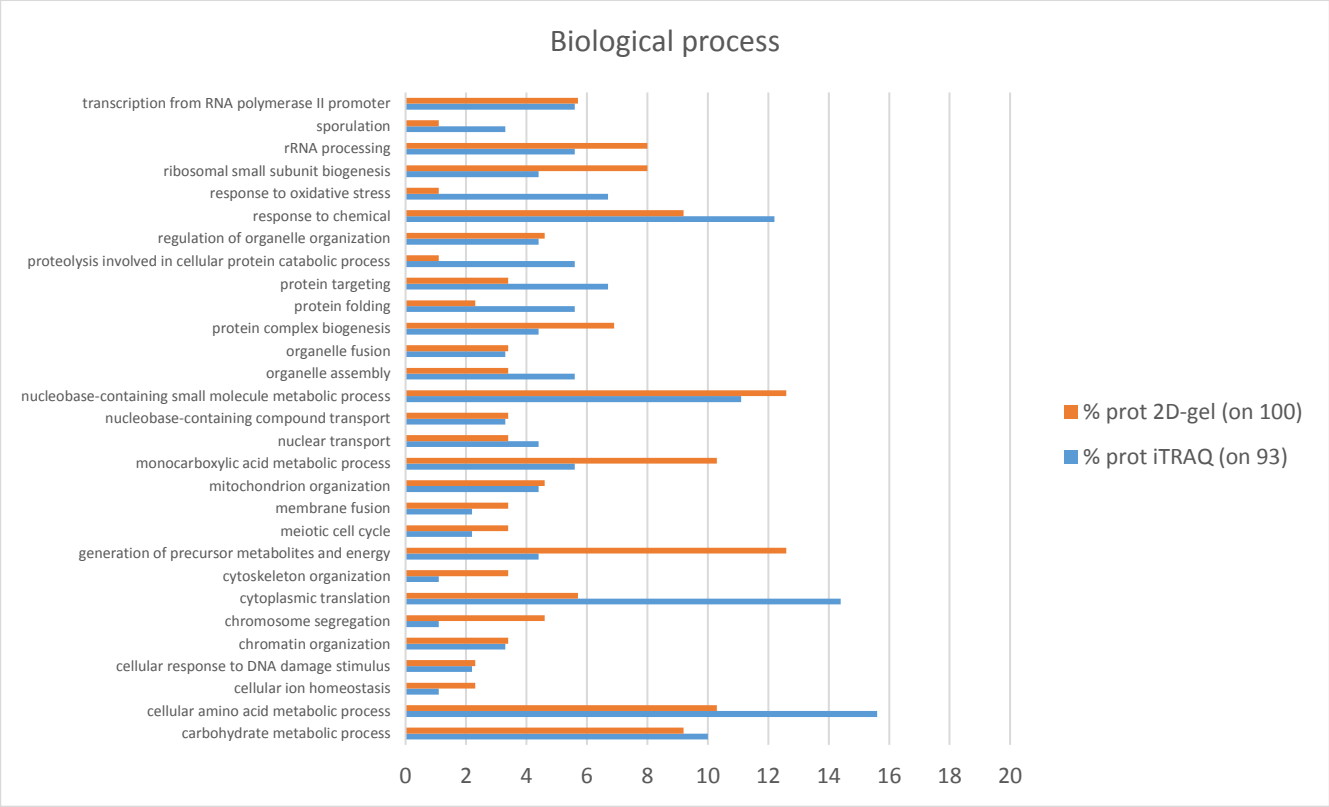


**Figure 22:** Gene ontology analysis of biological process in response to CdS QDs exposure. Blue bars represent the percentage of the proteins, find with iTRAQ, belonging to each category in the cluster, while orange bars represent the percentage of the proteins, find with 2D gel, belonging to each category in the cluster.

## 6.5 Pathway analysis

Metabolic pathway analysis was performed searching KEGG database (http://www.kegg.jp) for Saccharomyces cerevisiae to identify the pathways that were represented mostly. The main common pathway classes between 2D-gel and iTRAQ were: general metabolic pathway, biosynthesis of the secondary metabolites, biosynthesis of amino acids, glycolysis and gluconeogenesis, ribosome, carbon metabolism, and protein processing in endoplasmic reticulum (ER). There were some pathway classes

exclusive to iTRAQ or 2D-gel. RNA transport, MAPK kinase and autophagy were exclusive to iTRAQ, mitochondrial biogenesis, endocytosis and ubiquitin mediated proteolysis were found only through 2D-gel (Figure 23).

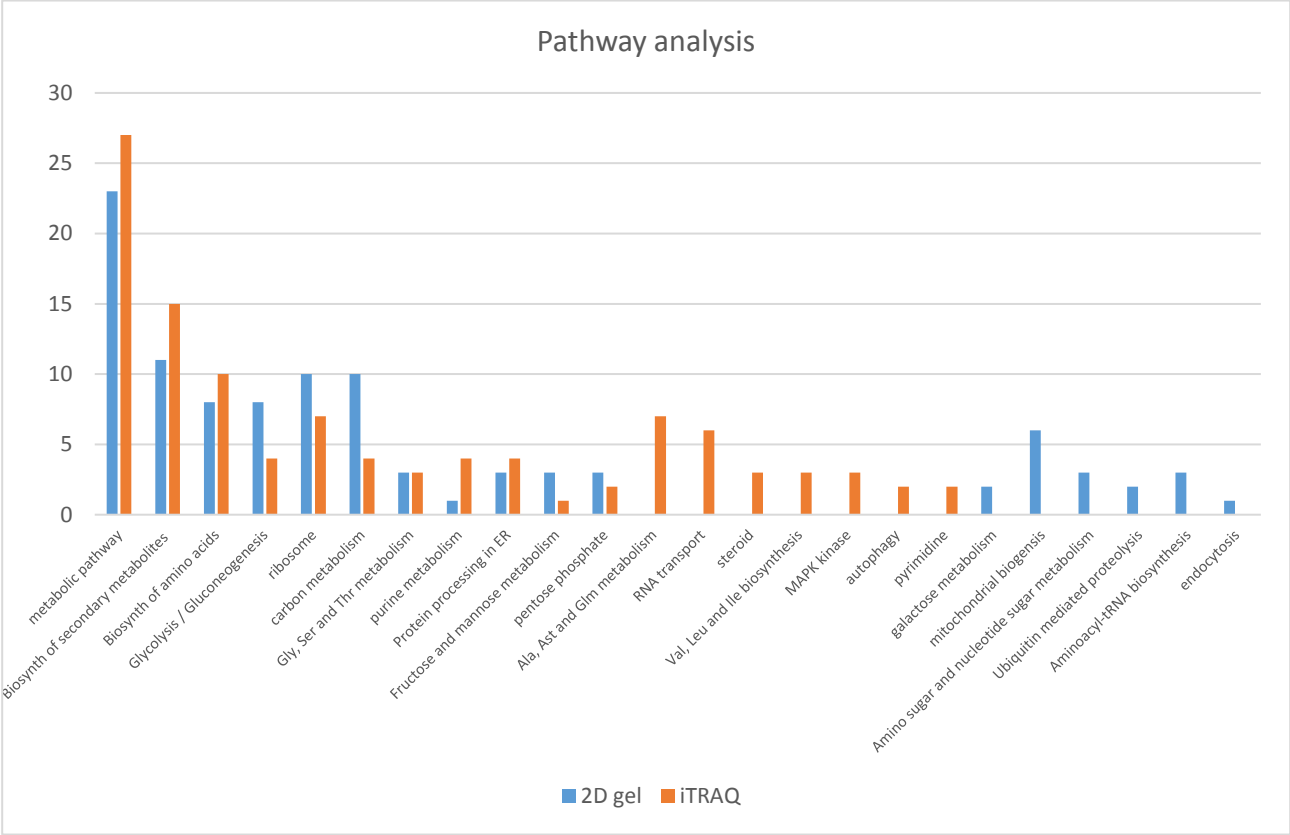


**Figure 23:** Pathway analysis class in response to CdS QDs exposure. Blue bars represent the numbers of the proteins in pathway classes, find with 2D gel, while orange bars represent the numbers of the proteins in pathway classes, found by iTRAQ.

Of particular interest was the "glycolysis and gluconeogenesis" pathway (Figure 24), which included 14 proteins (10 from 2D- gel and 4 from iTRAQ). Majority of the enzymes in the first part of the pathway were under abundant (G6PI, ENO1, ENO2, G3P3, TDH1, PFKA2, FBA1, GLK1), those at the end were over abundant (ADH6, ADH7, PDC1, ALD4, G6PI). The common enzyme between 2D-gel and iTRAQ, fructose-bisphosphate aldolase, was under abundant with both iTRAQ and 2D-gel. As reported Gomez *et al.* ENMs treatments inhibited glycolysis pathway and stimulated fermentation (Gomes *et al.* 2006). *In vitro*

inhibition studies of GAPDH in presence of QDs suggest that the binding of QDs to the enzyme molecules slows down the rate of the reactions catalysed by the enzyme, evidencing QDs as a potential enzyme inhibitor. For example, when human cancer cells are exposed to QDs, loss of cellular GAPDH activity causes metabolic perturbation during glycolysis, therefore the inhibition of GAPDH leads to the decrease of glycolysis rates. This suggests a possible mechanism of impaired energy homeostasis during QDs-mediated cellular injury to the process of cell dysfunction and death (Ghosh *et al.* 2014).

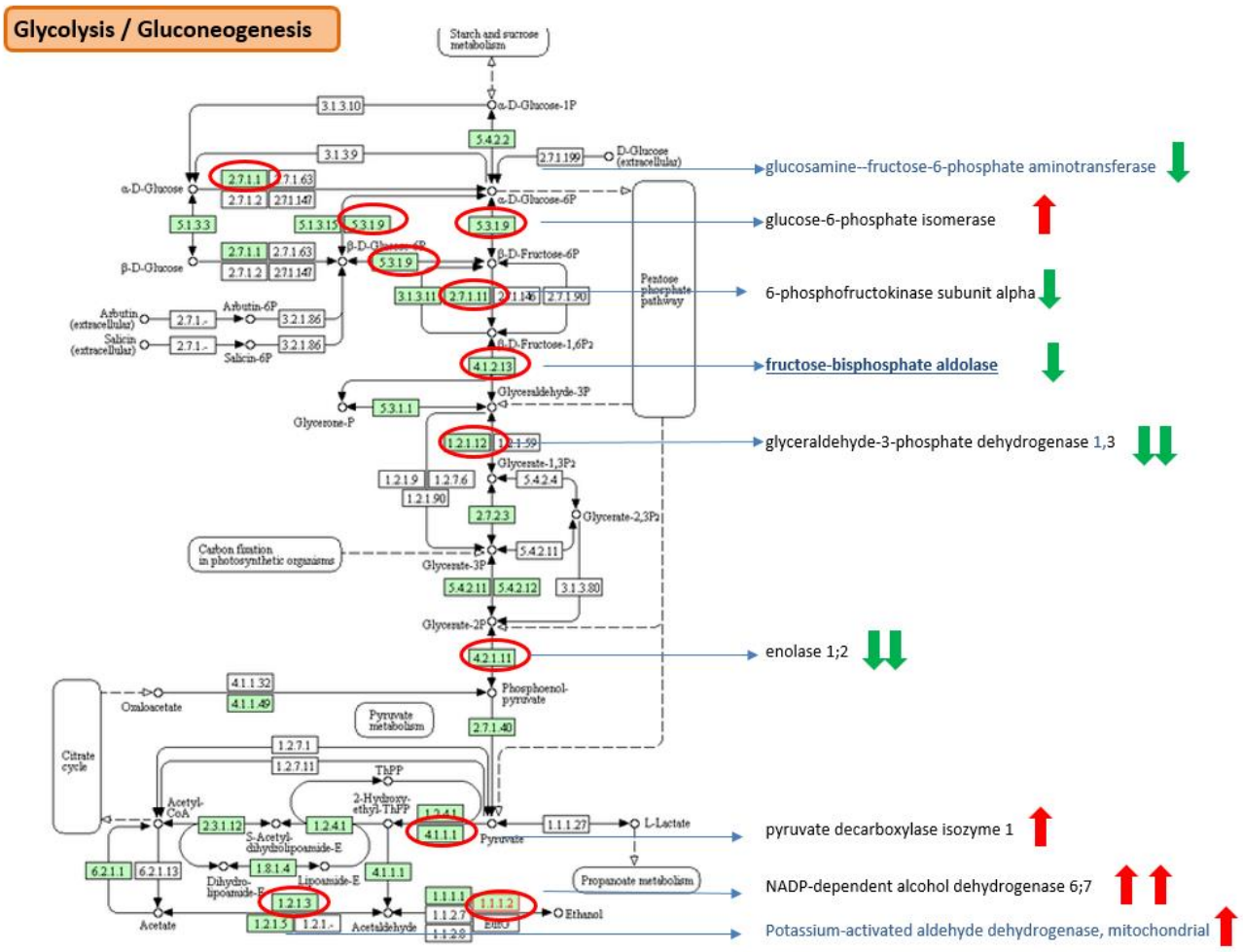


**Figure 24.** Glycolysis and Gluconeogenesis pathway. In black the proteins identified with 2D-gel, in blue the proteins identified with iTRAQ, and in blue bold and underlined the common proteins. With the red arrows were indicated the over abundant proteins, with the green arrows were indicated the under abundant proteins.

Another pathway of particular interest was “protein processing in ER”, which included 4 over abundant proteins (KAR2, HSP26, SHP1, SLS1) and 2 under abundant protein (HSC82, CDC48) (Figure 25). The common enzyme between 2D-gel and iTRAQ, ATP-dependent molecular chaperone HSC82, was found under abundant with both iTRAQ and 2D-gel. The results obtained by Wei *et al*. (2017) on human cancer cells suggest that ENMs are capable of inducing autophagy affecting the ER which is involved in cell autophagy. Schütz *et al.* (2016) had reported that internalized Silica nanoparticles (Si -NPs) might be accumulated in lysosomes, resulting in lysosomal dysfunction in HeLa cells. Similarly, Si NPs accumulating in ER may indicate that those nanoparticles should have an effect on ER structure, through mechanisms of action still unknown. Furthermore, ER is closely connected with cell autophagy, one of the principal cell death mechanism triggered by ENMs.

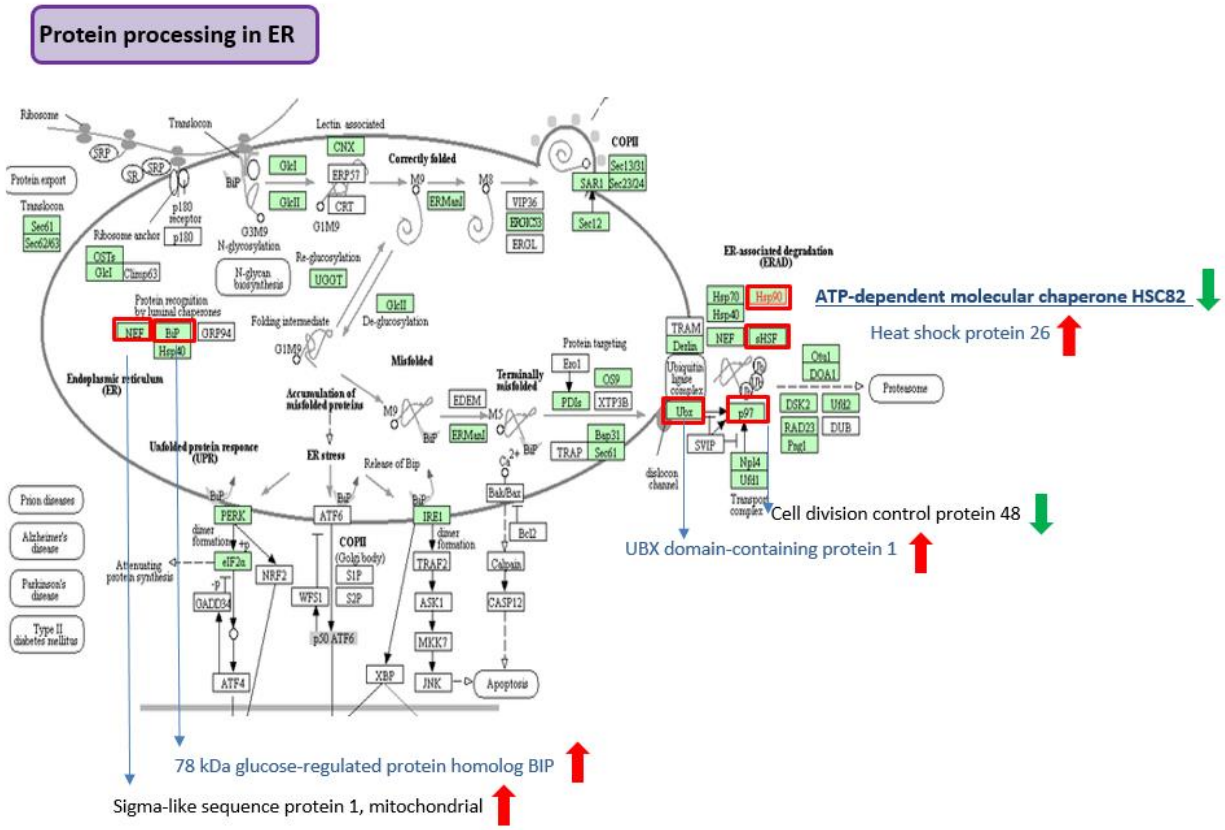


**Figure 25.** Protein processing in ER pathway. In black the proteins identified with 2D-gel, in blue the proteins identified with iTRAQ, and in blue bold and underlined the common proteins. With the red

arrows were represented the over abundant proteins, with the green arrows are represented the under abundant proteins.

Consistenly, HSC82 was found to be one of the main hubs in the CdS QDs- sensitive yeast mutants transcriptomic networks found in Marmiroli *et al.* (2016).

## Conclusions

Proteomic analysis carried out in *A. thaliana* showed several differences in proteins abundance modulation between the wild type and two resistant mutants (*atnp01, atnp02*): 61 proteins in wt against 31 in both mutants were reprogrammed by CdS QDs treatment. Interestingly, the proteome of wt was more affected by CdS QDs treatment than the proteomes of the two resistant mutants. There was however little overlapping among these protein sets: one protein only (Probable protein phosphatase 2C 58) was in common among the three types of plants and thus it can be used as probable biomarker of exposition to CdS QDs. Two proteins (Bifunctional enolase 2/transcriptional activator and Probable pectinesterase/pectinesterase inhibitor VGDH2) were in common between the two mutants and these proteins can be used as possible biomarkers of resistance to CdS QDs and maybe to other ENMs. However, Aslani *et al.* (2014), recommends assessing ENMs exposure, effects, and risk on a case-by-case basis. In fact, Pagano *et al.* (2016) showed different responses between zucchini and tomato upon exposure to different ENMs ($CeO_2$, $La_2O_3$, and CuO), both at the physiological and molecular level. This data obtained from *A. thaliana* can provide important information required for assessing the environmental and public health risks related to ENMs exposure. In addition, the use of plants as model organisms to investigate the environmental and biological effect of ENMs exposure, coupled with the exploitation of resistant (or tolerant) mutants, provides a convenient means to discriminate between non-essential and essential molecular functions involved in ENMs response (Marmiroli *et al.* 2015).

Several proteins identified in this study are involved in oxidative stress response, which is already known to be a major factor of nanomaterials toxicity in cells. In the present work, it emerged that the toxicity induced by CdS QDs in *A. thaliana* could be summarized as the concomitant action of two main stresses. One type of stress showed the specific mechanisms of oxidative stress, the other stress can be considered as “general stress”, an evolutionarily conserved process through which diverse organisms rapidly respond to the initial effects of external perturbations (Kultz, 2005; Lopez-Maury *et al*., 2008). Previous efforts have identified several candidate components of general stress response (GSR) signaling cascades, including hormones, calcium bursts, transcription factor, and kinase cascades (Fujita *et al*., 2006). Indeed, a type of general stress response mechanism here evidenced, especially in the mutants, was the hormone response and signalling (IAA9). The specific-stress, in this case oxidative stress response caused byincreased ROS production and oxidative damage to cellular components, was

present in wt type and in both mutants. CdS QDS treatments reprogrammed proteins known to be involved in oxidative stress response. For example, DHAR3 in wt, GAMMACA2 in *atnp01*, CAT2 in *atnp02*.

*Saccharomyces cerevisiae* proved to be a suitable model organism for nanotoxicology analysis and thanks to the presence of a high number of orthologue genes conserved in higher eukaryotes, could be an ideal platform for proteomic study and pathway analysis.

Two comparative proteomic analyses were used to identify differences in protein abundance correlated with the CdS QDs treatments. The remarkable differences in the results obtained using 2D-PAGE or iTRAQ methods are due to the methods' level of interaction with different parts of the proteome. 2D-PAGE interacts with the proteome more directly but less sensibly than iTRAQ. Protein profiling on yeast cell lysates displayed limited overlapping among proteins identified by the two methods, only four proteins, suggesting the complementary nature of these methods.

A further proof of the complementarity of the two techniques was that the proteins sets identified and quantified with the two methods had a scant overlap. Thus, the combined use of different techniques uncovers a higher proportion of the proteome responsive to treatments.

Future improvement in instrumentation sensitivity, labelling chemistry, and chromatography is clearly needed to enable routine quantification of proteins/peptides by mass spectrometry. Nevertheless, the complementary information obtained through different methods should potentially provide a better portrait of the biological system under investigation.

However, despite the proteins sets did overlap poorly, the pathways involved are shared by the two proteins groups**:** glycolysis and gluconeogenesis, biosynthesis of amino acids, ribosome, carbon metabolism, and protein processing in endoplasmic reticulum (ER). The same results were found for Biological function, where the main classes involved were: nucleobase–containing small molecule metabolic process, response to oxidative stress, monocarboxylic acid metabolic process, mitochondrion organization, generation of precursor metabolites and energy, cytoplasmic translation, cellular amino acid metabolic process and carbohydrate metabolic process. These results are in agreement with both transcriptomic and physiologic data on CdS QDs treatment in yeast. Notably the protein HSC82 has already been highlighted as one of the main hubs in the transcriptomic networks of CdS QDs sensitive yeast mutants in Marmiroli *et al.* (2016). Moreover, Pasquali *et al.* (2017) evidenced that yeast strains

treated with CdS QDs showed disruption of the mitochondrial network, accumulation of ROS and the decrease of glutathione redox state.

*A. thaliana* and *S. cerevisiae* have been proven to be reliable and effective model systems to study and understand the molecular interaction of the two main types of eukaryotic cells (plant and animal) with ENMs. One of the main outcomes of this approach bearing important practical applications is the identification of biomarkers of ENMs exposition, resistance, and sensitivity to be used in environmental and human health risk assessment.

## Aknowledgements

I wish to thank Prof. Nelson Marmiroli for introducing me to this project, allowing to me to grow as well as researcher as person. I also thank my tutor Prof. Marta Marmiroli to help me during these years of work. I also thank all the colleagues, in particular Dr. Francesca Mussi, Dr. Davide Imperiale, Dr. Luca Pagano and Dr. Graziella Pira, for their help and suggestion during these three years of Ph.D.

I would like to thank Dr. Vaibhav Srivastava and all the colleagues of the KTH University, Division of Glycoscience in Stockholm, for giving me the opportunity to spend three months of my Ph.D in their laboratories and for help and mentor me during my period of training in Stockholm.

I wish to thank also Dr. Andrea Zappettini and Dr. Marco Villani of the IMEM-CNR (Parma, Italy) for providing certified CdS QDs, useful comments and suggestions on the physics of nanomaterials.

## References


Ariga K., Hill JP., Lee MV., Vinu A., Charvet R., Acharya S. Challenges and breakthroughs in recent research on self-assembly. *Sci Technol Adv Mater* 2008; 9:014109.

Aslani F., Bagheri S., Muhd Julkapli N., Juraimi AS., Hashemi FS., Baghdadi A. Effects of engineered nanomaterials on plants growth: an overview. Scientific World Journal. 2014; 641759. doi: 10.1155/2014/641759.

Bailey RE., Smith AM., Nie S. Quantum dots in biology and medicine. *Physica E*. 2004; 25:1–12.

Bantscheff M., Hopf C., Savitski MM., Dittmann A., Grandi P., Michon AM., Schlegl J., Abraham Y., Becher I., Bergamini G., Boesche M., Delling M., Dümpelfeld B., Eberhard D., Huthmacher C., Mathieson T., Poeckel D., Reader V., Strunk K., Sweetman G., Kruse U., Neubauer G., Ramsden NG., Drewes G. Chemoproteomics profiling of HDAC inhibitors reveals selective targeting of HDAC complexes. *Nat. Biotechnol*. 2011; 29:255–265.

Barkla B.J., Vera-Estrella R., Hernández-Coronado M., Pantoja O. Quantitative Proteomics of the Tonoplast Reveals a Role for Glycolytic Enzymes in Salt Tolerance. *The Plant Cell*. 2009; 21: 4044–4058

Bayat N., Rajapaskse K., Marinsek-Logar R., Drobne D., Cristobal S. The effects of engineered nanoparticles on the cellular structure and growth of *Saccharomyces cerevisiae*. *Nanotoxicology.* 2014. 8(4):363-73.

BCC Research. 2017. Market Research Report and industry analysis. *ReportsnReports.*

Benayas A., Ren F., Carrasco E., Marzal V., del Rosal B., Gonfa B.A., Juarranz A., Sanz-Rodriguez F., Garcia-Sole DJ.J., Ma D. PbS/CdS/ZnS quantum dots: a multifunctional platform for *in vivo* nearinfrared low-dose fluorescence imaging. *Adv. Funct. Mater*. 2015; 25:6650–6659.

Boehm AM., Putz S., Altenhofer D., Sickmann A., Falk M. Precise protein quantification based on peptide quantification using iTRAQ. *BMC Bioinformatics.* 2007; 8:214

Chakraborty A., Regnier F. E. Global internal standard technology for comparative proteomics. *J. Chromatogr.* 2002; 949 (1−2):173−84.

Chandler PM., Robertson M. Gene expression regulated by abscisic acid and its relation to stress tolerance. *Annu. Rev. Plant Biol. Plant Mol. Biol*. 1994; 45: 113–141.

Cherkasov A., Muratov EN., Fourches D., Varnek A., Baskin II., Cronin M., Dearden J., Gramatica P., Martin YC., Todeschini R., Consonni V., Kuz'min VE., Cramer R., Benigni R., Yang C., Rathman J., Terfloth L., Gasteiger J., Richard A., Tropsha A. QSAR modeling: where have you been? Where are you going to? *J. Med. Chem.* 2014; 57(12):4977-5010. doi: 10.1021/jm4004285

Choe L. D'Ascenzo M., Relkin N. R., Pappin D., Ross, P., Williamson B., Guertin S., Pribil P., Lee K. H. 8-Plex quantitation of changes in cerebrospinal fluid protein expression in subjects undergoing intravenous immunoglobulin treatment for Alzheimer's disease. *Proteomics.* 2007; 7 (20): 3651−60.

Choi H., Frangioni J. V. Nanoparticles for Biomedical Imaging: Fundamentals of Clinical Translation. *Mol. Imaging*. 2010; 9(6): 291–310.

Corton JM., Gillespie JG., Hardie DG. Role of the AMP activated protein kinase in the cellular stress response. *Current Biology*. 1994; 4: 315–324.

Craig R., Beavis R. C. TANDEM: matching proteins with mass spectra. *Bioinformatics*. 2004; 20, 1466–1467

Davies JC. Nanotechnology oversight an agenda for the new administration. Project on emerging nanotechnologies. 2008; http://www.nanotechproject.org/publications/

Dayon L., Hainard A., Licker V., Turck N., Kuhn K., Hochstrasser DF., Burkhard PR., Sanchez JC. Relative quantification of proteins in human cerebrospinal fluids by MS/MS using 6-plex isobaric tags. *Anal. Chem*. 2008; 80:2921–293.

Dearden JC., Hewitt M., Bresnen GM., Gregg CN. Improved correlation between animal and human potency of non-steroidal anti-inflammatory drugs using quantitative structure-activity relationships (QSARs). *SAR QSAR Environ Res*. 2017; 28(7):557-565. doi: 10.1080/1062936X.2017.1351391.

Dos Santos S. C., Sá-Correia I. Yeast toxicogenomics: lessons from a eukaryotic cell model and cell factory. *Curr Opin Biotechnol*. 2015; 33, 183-191.

EFSA Scientific Committee. Guidance on the risk assessment of the application of nanoscience and nanotechnologies in the food and feed chain. *EFSA Journal*. 2011; 9(5): 2140-2176.

EU Commission recommendation of 18 October 2011 on the definition of nanomaterial (2011/696/EU). *Official journal of the European Union.*

Fan J., Sun Y. Inhibition of autophagy overcomes the nanotoxicity elicited by cadmium-based quantum dots. *Biomaterials.* 2016; 78:102-14.

Faurobert M., Mihr C., Bertin N., Pawlowski T., Negroni L., Sommerer N. Major Proteome Variations Associated with Cherry Tomato Pericarp Development and Ripening. *Plant Physiol.* 2007; 143:1327–46.

Foda MF., Huang L., Shao F., Han HY. Biocompatible and highly luminescent near-infrared CuInS2/ZnS quantum dots embedded silica beads for cancer cell imaging. *ACS Appl. Mater Interfaces* 2014; 6:2011–2017.

Fujita M., Fujita Y., Noutoshi Y., Takahashi F., Narusaka Y., Yamaguchi-Shinozaki K. Shinozaki K. Crosstalk between abiotic and biotic stress responses: a current view from the points of convergence in the stress signaling networks. *Curr. Opin. Plant Biol.* 2006; 9:436–442.

Garcìa-Sànchez S., Bernales I., Cristobal S. Early response to nanoparticles in the Arabidopsis transcriptome compromises plant defence and root-hair development through salicylic acid signaling. *BMC Genomics* 2015; 16:341

Gates BD., Qiaobing X., Stewart M., Ryan D., Willson C.G., Whitesides GM. *Chem Rev*. 2005;105:1171.

Geisler-Lee J., Wang Q., Yao Y., Zhang W., Geisler M., Li K., Huang Y., Chen Y., Kolmakov A., Ma X. Phytotoxicity, accumulation and transport of silver nanoparticles by *Arabidopsis thaliana. Nanotoxicology. 2*013; 7: 323-337.

Ghosh S., Ray M., Rani M. Das, Chakrabarti A., Khan A.H., Sarmad D. D., Acharya S. Modulation of glyceraldehyde-3-phosphate dehydrogenase activity by surface functionalized quantum dots. *Phys. Chem. Chem. Phys*. 2014; 16: 5276

Giaever G., Nislow C. The yeast deletion collection: a decade of functional genomics. *Genetics*. 2014; 197 (2):451–465.

Giavalisco P., Nordhoff E., Lehrach H., Gobom J., Klose J**.** Extraction of proteins from plant tissues for two-dimensional electrophoresis analysis. *Electrophoresis.* 2003;24(1-2):207-16.

Giegé P., Heazlewood, J.L., Roessner-Tunali U., Millar A.H., Fernie A.R., Leaver C.J., Sweetlove L.J. Enzymes of glycolysis are functionally associated with the mitochondrion in Arabidopsis cells. *Plant Cell*. 2003; 15: 2140–2151.

Goffeau A. Four years of post-genomic life with 6,000 yeast genes. *FEBS Lett*. 2000; 480(1):37-41.

Gomes A., Sengupta J., Datta P., Ghosh S., Gomes A. Physiological Interactions of Nanoparticles in Energy Metabolism, Immune Function and Their Biosafety: A Review. *J Nanosci and Nanotech*. 2016; 16: 92–116.

Gong X.W., Yang Z.Y., Walters G., Comin R., Ning Z.J., Beauregard E., Adinolfi V., Voznyy O., Sargent E.H. Highly efficient quantum dot near-infrared light emitting diodes. *Nat Photon.* 2016:10:253–257.

Görg A., Boguth G., Obermaier C., Posch A., Weiss W. Two-dimensional polyacrylamide gel electrophoresis with immobilized pH gradients in the first dimension (IPG-Dalt): The state of the art and the controversy of vertical versus horizontal systems. *Electrophoresis.* 1995; 16:1079–1086.

Görg A., Weiss W., Dunn M. J. Current two-dimensional electrophoresis technology for proteomics. *Proteomics.* 2004; 4 (12), 3665−85.

Gygi S. P., Rist B., Gerber S. A., Turecek F., Michael H., Aebersold R. Quantitative analysis of complex protein mixtures using isotope-coded affinity tags. *Nat. Biotechnol*. 1999; 17: 994−999.

Handy RD., Owen R., Valsami-Jones E. The ecotoxicology of nanoparticles and nanomaterials: current status, knowledge gaps, challenges, and future needs. *Ecotoxicology*. 2008; 17(5):315-25. doi: 10.1007/s10646-008-0206-0.

He L., Li L., Wang W., Abdel-Halimc ES., Zhang J., Zhu J.J. Highly luminescent and biocompatible nearinfrared core–shell CdSeTe/CdS/C quantum dots for probe labeling tumor cells. *Talanta.* 2016; 146:209–215.

Hett A. Nanotechnology: small matters, many unknowns. *Swiss Reinsurance Company*. 2004.

Hossain Z., Mustafa G., Komatsu S. Plant Responses to Nanoparticle Stress. *Int. J Mol. Sci*. 2015; 16(11), 26644-6653.

http://ihcp.jrc.ec.europa.eu/our_databases/web-platform-on-nanomaterials.

Jorrín-Novo, J. V., Pascual, J., Sánchez-Lucas, R., Romero-Rodríguez, M. C., Rodríguez-Ortega, M. J., Lenz, C., Valledor L. Fourteen years of plant proteomics reflected in Proteomics: moving from model species and 2DE-based approaches to orphan species and gel-free platforms. *Proteomics.* 2015; 15: 1089–1112. doi: 10.1002/pmic.201400349.

Kasemets K., Suppi S., Kunnis-Beres K., Kahru A. Toxicity of CuO Nanoparticles to Yeast *Saccharomyces cerevisiae* BY4741 Wild-Type and Its Nine Isogenic Single-Gene Deletion Mutants. *Chem. Res. Toxicol*. 2012; 26(3): 356-367.

Kaveh R., Li Y.S., Ranjbar S., Tehrani R., Brueck C. L., Van Aken B. Changes in *Arabidopsis thaliana* gene expression in response to silver nanoparticles and silver ions. *Environ. Sci. Technol*. 2013; 47: 10637-10644.

Kessner D., Chambers M., Burke R., Agus D., Mallick P. ProteoWizard: open source software for rapid proteomics tools development. *Bioinformatics*. 2008; 24, 2534–2536.

Khan M.N., Mohammad F., Mobin M., Saqib M.A. Tolerance of plants to abiotic stress: a role of nitric oxide and calcium. Nitric Oxide in Plants: Metabolism and Role. *Springer International Publishing Switzerland.* 2014;

Kim J.H., Oh Y., Yoon H., Hwang I., Chang Y.-S. Iron nanoparticle-induced activation of plasma membrane Hþ-ATPase promotes stomatal opening in *Arabidopsis thaliana*. *Environ. Sci. Technol.* 2015; 49: 1113-1119.

Koornneef M., Meinke D. The development of Arabidopsis as a model plant. *Plant J*. 2010; 61 (6)909-921.

Kultz, D. Molecular and evolutionary basis of the cellular stress response. *Annu. Rev. Physiol.* 2005; 67:225–257.

Kurepa J., Paunesku T., Vogt S., Arora H., Rabatic BM., Lu J., Wanzer MB., Woloschak GE., Smalle JA. Uptake and distribution of ultrasmall anatase $TiO_2$ alizarin reds nanoconjugates in *Arabidopsis thaliana. Nano Lett.* 2010; 10, 2296–2302

Larue C., Castillo-Michel H., Sobanska S., Trcera N., Sorieul S., Cécillon L., Ouerdane L., Legros S., Sarret G. Fate of pristine TiO2 nanoparticles and aged paint-containing $TiO_2$ nanoparticles in lettuce crop after foliar exposure. *J. Hazard. Mater.* 2014; 273: 17–26

Lopez-Maury L., Marguerat S., Bahler J. Tuning gene expression to changing environments: from rapid responses to evolutionary adaptation. *Nat. Rev. Genet.* 2008; 9:583–593.

Mailly D., Eur Phys J. *Special Topics*. 2009; 172:333.

Marmiroli M., Pagano L., Pasquali F., Zappettini A., Tosato V., Bruschi CV., Marmiroli N. A genome-wide nanotoxicology screen of Saccharomyces cerevisiae mutants reveals the basis for cadmium sulphidequantum dot tolerance and sensitivity. *Nanotoxicology*. 2016; 10 (1):84–93.

Marmiroli M., Imperiale D., Pagano L., Villani M., Zappettini A., Marmiroli N. The Proteomic Response of Arabidopsis thaliana to Cadmium Sulfide Quantum Dots, and Its Correlation with the Transcriptomic Response. *Front. Plant Sci*. 2015; 16; 6:1104. doi: 10.3389/fpls.2015.01104.

Marmiroli M., Pagano L., Savo Sardaro M. L., Villani M., and Marmiroli N. Genome-wide approach in *Arabidopsis thaliana* to assess the toxicity of cadmium sulfide quantum dots. *Environ. Sci. Technol*. 2014; 48, 5902–5909. doi: 10.1021/es404958r

Moebius J., Zahedi R. P., Lewandrowski U., Berger C., Walter U., Sickmann A. The human platelet membrane proteome reveals several new potential membrane proteins. *Mol. Cell Proteomics*. 2005; 4 (11): 1754−61.

Montes A., Bisson M.A., Joseph A., Gardella J.A., Diana S., Aga D. S. Uptake and transformations of engineered nanomaterials: Critical responses observed in terrestrial plants and the model plant *Arabidopsis thaliana. Sci. Tot. Environ.* 2017; 607–608; 1497–1516

Moore F., Weekes J., Hardie DG. Evidence that AMP triggers phosphorylation as well as direct allosteric activation of rat liver AMP-activated protein kinase. *Europ. J. Biochem* 1991; 199: 691–697.

Nesvizhskii A. I., Keller A., Kolker E., Aebersold R. ProteinProphet: a statistical model for identifying proteins by tandem mass spectrometry. *Anal. Chem*. 2003; 75, 4646–4658

O'Farrell PZ., Goodman HM., O'Farrell PH. High resolution two dimensional electrophoresis of basic as well as acidic proteins. *Cell.* 1977; 12:1133–42.

Oh E., Liu R., Nel A., Gemill K.B., Bilal M., Cohen Y., Medintz I.L. Meta-analysis of cellular toxicity for cadmium-containing quantum dots. *Nature Nanotechnology.* 2016; 11, 479–486.

Ong S. E., Blagoev B., Kratchmarova I., Kristensen D. B., Steen H., Pandey A., Mann M. Stable isotope labeling by amino acids in cell culture, SILAC, as a simple and accurate approach to expression proteomics. *Mol. Cell. Proteomics.* 2002; 1 (5): 376−86.

Paesano L., Perotti A., Buschini A., Carubbi C., Marmiroli M., Maestri E., Iannotta S., Marmiroli N., Markers for toxicity to HepG2 exposed to cadmium sulphide quantum dots; damage to mitochondria. *Toxicology*. 2016; 37:418-28.

Pagano L., Servin A.D., De La Torre-Roche R., Mukherjee A., Majumdar S., Hawthorne J., Marmiroli M., Maestri E., Marra R.E., Isch S.M., Dhankher O.P., White J.C., Marmiroli N. Molecular Response of Crop Plants to Engineered Nanomaterials. Environ Sci Technol. 2016; 5; 50(13):7198-207. doi: 10.1021/acs.est.6b01816.

Park O.K. Proteomic Studies in Plants. *J Biochem Mol Biol*, 2004; 37(1):133-8.

Pasquali F., Agrimonti C., Pagano L., Zappettini A., Villani M., Marmiroli M., White J.C., Marmiroli N. Nucleo-mitochondrial interaction of yeast in response to cadmium sulfide quantum dot exposure. *J Hazard Mater*. 2017; 324(Pt B):744-752.

Pennington S.R., Wilkins M.R., Hochstrasser D.F., Dunn M.J. Proteome analysis: From protein characterization to biological function. *Trends in Cell Biology*. 1997; 7: 168–173.

Phizicky E., Bastiaens P. I., Zhu H., Snyder M. Fields, S. Protein analysis on a proteomic scale. *Nature*. 2003; 422: 208-215.

Pütz S. M., Boehm A. M., Stiewe T., Sickmann A. iTRAQ Analysis of a Cell Culture Model for Malignant Transformation, Including Comparison with 2D-PAGE and SILAC*. J. Proteome Res.* 2012; 11:2140−2153.

Pütz S. M., Reinders J., Reinders Y., Sickmann A. Mass spectrometry-based peptide quantification: applications and limitations. *Expert Rev. Proteomics*. 2005; 2 (3), 381−92.

Radosevich T. J., Reinhardt T. A., Lippolis J. D., Bannantine J. P., Stabel J. R. Proteome and differential expression analysis of membrane and cytosolic proteins from Mycobacterium avium subsp. paratuberculosis strains K-10 and 187. J. Bacteriol. 2007; 189 (3): 1109−17.

Ramagli LS., Rodriguez LV. Quantitation of microgram amounts of protein in SDS -mercaptoethanol-tris electrophoresis sample buffer. *Electrophoresis*. 1985; 559–563

Ramšak Ž., Baebler Š., Rotter A., Korbar M., Mozetič I., Usadel B. GoMapMan: Integration, consolidation and visualization of plant gene annotations within the MapMan ontology. *Nucleic Acids Res.* 2014; 42:1167–75.

Rico C. R, Majumdar S., Duarte-Gardea M., Peralta-Videa J.R. Gardea-Torresdey J. L. Interaction of nanoparticles with edible plants and their possible implications in the food chain*. J Agric. Food Chem*. 2011; 59: 3485-3498.

Rius S. P., Casati P., Iglesias A. A., Gomez-Casati D. F. Characterization of *Arabidopsis* lines deficient in GAPC-1, a cytosolic NAD-dependent glyceraldehyde-3-phosphate dehydrogenase. *Plant Physiol*. 2008; 148: 1655–67.

Rong-Mullins X., Winas M. J., Lee JB., Lonergan ZR., Pilolli VA., Weatherly LM., Carmenzind TW., Jiang L., Cumming JR., Oporto GS., Gallagher JEG. Proteomic and genetic analysis of the response of *S. cerevisiae* to soluble copper leads to improvement of the antimicrobial function of cellulosic copper nanoparticles. *Metallomics.* 2017; 9:1304-15.

Ross P. L., Huang Y. N., Marchese J. N., Williamson B., Parker K., Hattan S., Khainovski N. Pillai, S., Dey S., Daniels, S., Purkayastha S., Juhasz, P., Martin S., Bartlet-Jones, M., He, F., Jacobson, A., Pappin D. J. Multiplexed protein quantitation in *Saccharomyces cerevisiae* using amine-reactive isobaric tagging reagents. *Mol. Cell Proteomics*. 2004; 3 (12): 1154−69.

Santos A. R., Miguel A. S., Fevereiro P., Oliva, A. Evaluation of cytotoxicity of 3-Mercaptopropionic acid-modified quantum dots on *Medicago sativa* cells and tissues. Nanoparticles in Biology and Medicine, Methods and Protocols. *Springer Protocols*. 2012; 435–449.

Schütz I., Lopez-Hernandez T., Gao Q., Puchkov D., Jabs S., Nordmeyer D., Schmudde M., Rühl E., Graf CM., Haucke V. Lysosomal dysfunction caused by cellular accumulation of silica nanoparticles. *J Biol. Chem*. 2016; 291(27):14170-84. doi: 10.1074/jbc.

Sharma P., Bhushan Jha A., Shanker Dubey R., Pessarakli M. Defense Mechanism in Plants under Stressful Conditions. *J Botany*. 2012; Article ID 217037.

Shevchenko A., Tomas H., Havlis J., Olsen J. V., Mann M. In-gel digestion for mass spectrometric characterization of proteins and proteomes. *Nat. Protoc*. 2006; 1:2856– 68760.

Shteynberg D., Deutsch E. W., Lam H., Eng J. K., Sun Z., Tasman N., Mendoza L., Moritz R. L., Aebersold R., Nesvizhskii A. I. iProphet: multi-level integrative analysis of shotgun proteomic data improves peptide and protein identification rates and error estimates. *Mol. Cell. Proteomics.* 2011; 10, M111.007690.

Silva G. A. Neuroscience nanotechnology: progress, opportunities and challenges. *Nat. Rev. Neurosci*. 2016; 7:65-74.

Slibinskas R., Ražanskas R, Zinkevičiūtė R, Čiplys E. Comparison of first dimension IPG and NEPHGE techniques in two-dimensional gel electrophoresis experiment with cytosolic unfolded protein response in *Saccharomyces cerevisiae*. *Proteome Sci*. 2013; 11(1):36. doi: 10.1186/1477-5956-11-36.

Srivastava V., Malm E., Sundqvist G., Bulone V. Quantitative proteomics reveals that plasma membrane microdomains from poplar cell suspension cultures are enriched in markers of signal transduction, molecular transport, and callose biosynthesis. *Mol. Cell Proteomics.* 2013; 12(12):3874-85. doi: 10.1074/mcp.M113.029033.

Stone V., Johnstone H. J., Balharry D., Gernand JM., Gulumian M. Approaches to develop alternative testing strategies to inform human health risk assestement of nanomaterials. *Risk Anal*. 2016; 36(8)1535-50.

Tabb D. L., Fernando C. G., Chambers M. C. MyriMatch: highly accurate tandem mass spectral peptide identification by multivariate hypergeometric analysis. *J Proteome Res*. 2007; 8:654–661

Tafelmeyer P., Laurent C., Lenormand P., Rousselle J. C., Marsollier L., Reysset G., Zhang R., Sickmann A., Stinear T. P., Namane A., Cole S. T. Comprehensive proteome analysis of Mycobacterium ulcerans and quantitative comparison of mycolactone biosynthesis. *Proteomics.* 2008; 8 (15):3124−38.

Tiwari M., Krishnamurthy S., Shukla D., Kiiskila J., Jain A., Datta R., Sharma N., Sahi SV. Comparative transcriptome and proteome analysis to reveal the biosynthesis of gold nanoparticles in Arabidopsis. *Scientific Reports*. 2016; 6: 21733.

Tsuji J.S., Maynard A.D., Howard P.C., James J.T., Lam C., Warheit D.B., Santamaria A.B. Research strategies for safety evaluation of nanomaterials, part IV: risk assessment of nanoparticles. *Toxicol. Sciences*. 2006; 89(1): 42-50.

Unlu M, Morgan ME, Minden JS. Difference gel electrophoresis: A single gel method for detecting changes in protein extracts. *Electrophoresis.* 1997; 18:2071–7.

Usadel B., Schwacke R., Nagel A., Kersten B. GabiPD – the GABI Primary Database integrates plant proteomic data with gene-centric information. *Front. Plant Sci*. 2012; 3:154.

Villani M., Calestani D., Lazzarini L., Zannotto L., Mosca R., Zappettini A. Extended functionality of ZnO nanotetrapods by solution-based coupling with CdS nanoparticles. J. *Mater. Chem*. 2012; 22, 5694.

Wang J., Jiang X., Han H. Turn-on near-infrared electro chemiluminescence sensing of thrombin based on resonance energy transfer between CdTe/CdS coresmall/shell thick quantum dots and gold nanorods. *Biosens. Bioelectron.* 2016; 82:26–31.

Wang P., Menzies NW., Lombi E., Sekine R., Blamey FP., Hernandez-Soriano MC., Cheng M., Kappen P., Peijnenburg WJ., Tang C., Kopittke PM. Silver sulfide nanoparticles (Ag2S-NPs) are taken up by plants and are phytotoxic. *Nanotoxicology*. 2015; 9:1041–1049.

Wang X.-C., Li Q., Jin X., Xiao G.-H., Liu G.-J., Liu N.-J. Quantitative proteomics and transcriptomics reveal key metabolic processes associated with cotton fiber initiation. J. Proteomics. 2015; 114: 16–27. doi: 10.1016/j.jprot.2014.10.022.

Wani I. A., Ahmad T. Understanding toxicity of Nanomaterials in Biological Systems. In applying nanotechnology for environmental sustainability. *IGI global*. 2017; Sung Hee Joo (University of Miami, USA) (403-427); DOI: 10.4018/978-1-5225-0585-3.

Wei F., Wang Y., Zewei L. Z., Li Y., Duan Y. New findings of silica nanoparticles induced ER autophagy in human colon cancer cell. *Sci. Rep.* 2017; 7, 42591; doi: 10.1038/srep42591.

Wiese S., Reidegeld KA., Meyer HE., Warscheid B. Protein labeling by iTRAQ: a new tool for quantitative mass spectrometry in proteome research. *Proteomics*. 2007; 7:340–350.

Wu W. W., Wang G., Baek S. J., Shen, R. F. Comparative study of three proteomic quantitative methods, DIGE, cICAT, and iTRAQ, using 2D gel- or LC-MALDI TOF/TOF. *J Proteome Res.* 2006; 5 (3): 651−8.

Xing W., Chen Y., *Wang X., Lv L., Ouyang X., Ge Z., Huang H.* $MoS_2$ Quantum Dots with a Tunable Work Function for High-Performance Organic Solar Cells. *ACS Appl. Mater. Interfaces*. 2016; *8* (40): 26916–26923.

Y.Y. Syu, J.H. Hung, J.C. Chen, H.W. Chuang Impacts of size and shape of silver nanoparticles on Arabidopsis plant growth and gene expression. *Plant Physiol. Biochem*. 2014; 83: 57-64.

Zhai T., Fang X., *Xu J, Zhang Q., Bando Y, Golberg D., Ma Y., Zhai T*. One-dimensional CdS nanostructures: synthesis, properties, and applications. *Nanoscale*. 2010; 2, 168-187.

Zhang X., Wang Y., Xue Y., Lei B., Yan D., Li N., Liu Z., Du Y., Cai R. Ultrathin lanthanide oxides nanomaterials: synthesis, properties and applications*. Sci. Bull*. 2016; 61(18):1422-1434.

# Appendix

## Synthesis and characterization of CdS QDs

The method used to synthesize CdS QDs followed Villani *et al.*, and the synthesis was performed by IMEM-CNR (Parma, Italy). X-ray diffraction was performed using an ARL-X'Tra device (Thermo Fisher Scientific, 81 Wyman Street, Waltham, MA USA). A field emission high resolution (Scherzer resolution of ~0.19 nm) JEM-2200 FS transmission electron microscope (JEOL ltd., 3-1-2 Musashino, Akishima, Tokyo, JAPAN) operating at 200 kV, was used to examine the structure of the CdS QDs.

An ESEM Quanta 250FEG, FEI with Bruker QUANTAX EDS XFlash® 6T detector series and ESPRIT 2 analytical methods interface (FEI company, 5350 NE Dawson Creek Drive Hillsboro, Oregon 97124 USA, Bruker, Am Studio 2D, 12489 Berlin, Germany) was utilized to determine CdS quantum dots group morphology and elemental content. Single drops of 1 mL containing 80 mg $L^{-1}$ of CdS Quantum dots were left to dry on SEM stub covered with carbon tape in a protected environment. Seven stubs were analyzed during one round of experiments.

Figures 1 represents CdS QDs at different magnifications, with their EDX spectra.

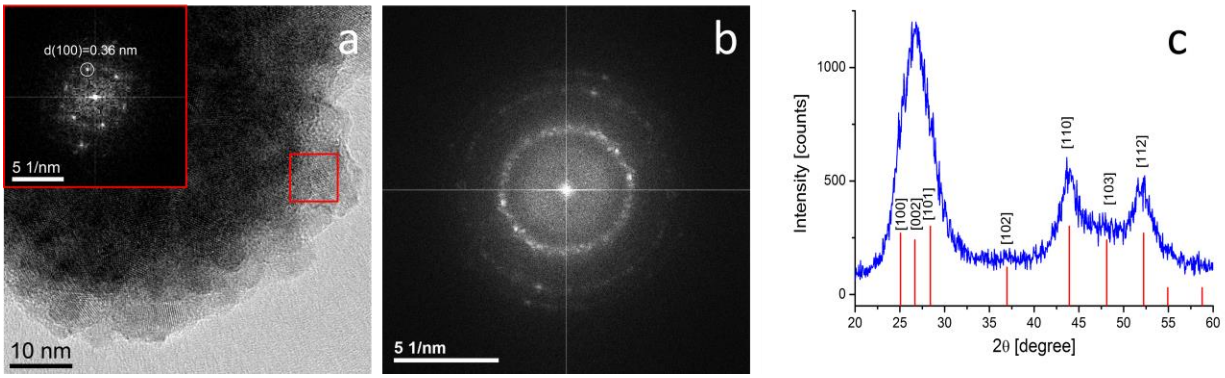

**Figure 1.** HRTEM image of ligand-free QDs assembly**. (a)** QDs aggregation is observed upon solvent evaporation due to the lack of capping molecules at QDs surface. The corresponding reduced Fourier transform (FT) in the inset confirms the hexagonal structure (greenockite, P63mc) of as-synthesized CdS QDs (d=0.36 nm in agreement with (JCPDS no. 80-0006). **(b)** The FT of the whole HRTEM image is presented in panel. The expected ring feature coming from the random orientation of the CdS crystallites is observed, as is the overlap of (100), (002) and (101) reflections of the wurtzite structure (at high *d* values) due to low-dimension peak broadening. Such features are in agreement with XRD pattern reported in panel **(c)**. All peaks have been indexed according to greenockite structure and no other reflections arising from possible impurities are observed. Scherrer calculation, based on FWHM of the three main peaks of the reported pattern, results in an average size of about 6 nm.

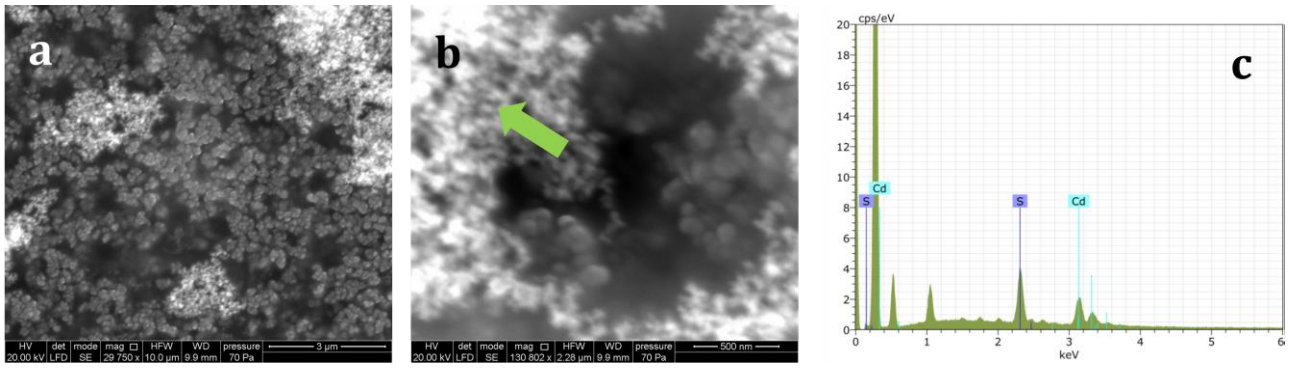


**Figure 2.** ESEM/EDX image of ligand-free CdS QDs assemblycentrationat 80 mg $L^{-1}$ c. **(a)** SEM image at 29750x magnification of CdS QDs drop. **(b)** SEM image at 130802x magnification of CdS QDs drop: nanocrystals are grouped into small agglomerates of 50-100 nm. **(c)** EDX spectra of the point indicated by the green arrow in fig S3(b): X-ray emission lines for Cd Lα1 and Lβ1 are clearly visible at 3.133 and 3.316 eV. For S Kα1 and Kβ1 lines at 2.308 and 2.464 eV are also visible.

## Table 1. MALDI-TOF/TOF data associated with differentially abundant proteins identified in *Arabidopsis thaliana*

| Spot n° | Protein name | Protein code | Gene name | mass | pI | score | expect | match | coverage (%) |
|---|---|---|---|---|---|---|---|---|---|
| 7305 | **30S ribosomal protein S5, chloroplastic** | RR5_ARATH | RPS5 | 32682 | 8,99 | 43 | 0,76 | 13 | 43 |
| 1207 | **3-isopropylmalate dehydratase small subunit 3** | LEUD3_ARATH | At2g43090 | 27059 | 6,33 | 44 | 0,61 | 6 | 35 |
| 9404 | **Aminomethyltransferase, mitochondrial** | GCST_ARATH | GDCST | 44759 | 8,55 | 107 | 2,90E-07 | 15 | 37 |
| 102 | **Aspartokinase 2, chloroplastic** | AK2_ARATH | AK2 | 60137 | 6,38 | 58 | 0,021 | 8 | 25 |
| 3605 | **ATP synthase subunit beta-1, mitochondrial** | ATPBM_ARATH | At5g08670 | 59805 | 6,18 | 215 | 4.6E-18 | 38 | 57 |
| 202 | **ATP-dependent helicase BRM** | BRM_ARATH | BRM | 246173 | 8 | 48 | 0,2 | 21 | 15 |
| 1707 | **ATP-dependent zinc metalloprotease FTSH 2** | FTSH2_ARATH | FTSH2 | 74282 | 6 | 67 | 0,0029 | 9 | 18 |
| 7306 | **Auxin-responsive protein IAA9** | IAA9_ARATH | IAA9 | 36781 | 6,06 | 36 | 4 | 7 | 31 |
| 3606 | **Bifunctional enolase 2/transcriptional activator** | ENO2_ARATH | ENO2 | 48974 | 5,54 | 54 | 0,0062 | 9 | 27 |
| 8612 | **Catalase-2** | CAT2_ARATH | CAT2 | 57237 | 6,63 | 149 | 1,80E-11 | 18 | 39 |
| 3902 | **Chaperone protein ClpC2, chloroplastic** | CLPC2_ARATH | CLPC2 | 105902 | 6,06 | 79 | 0,00018 | 16 | 21 |
| 705 | **Chaperonin 60 subunit alpha 1, chloroplastic** | CPNA1_ARATH | CPN60A1 | 62205 | 5,09 | 166 | 3,60E-13 | 25 | 40 |
| 2706 | **Chaperonin 60 subunit beta 1, chloroplastic** | CPNB1_ARATH | CPN60B1 | 64169 | 6,21 | 55 | 0,049 | 13 | 20 |
| 7301 | **Chloroplast stem-loop binding protein of 41 kDa a** | CP41A_ARATH | CSP41A | 44074 | 8,54 | 55 | 0,044 | 9 | 23 |
| 8807 | **Cullin-3B** | CUL3B_ARATH | CUL3B | 86069 | 7,59 | 56 | 3,90E-02 | 13 | 25 |
| 2806 | **Elongator complex protein 3** | ELP3_ARATH | HAG3 | 64395 | 8 | 43 | 0,74 | 8 | 21 |
| 4203 | **Eukaryotic translation initiation factor 5A-2** | IF5A2_ARATH | ELF5A-2 | 17358 | 5,55 | 75 | 0,00049 | 10 | 55 |
| 1408 | **F-box only protein 7** | FBX7_ARATH | FBX7 | 47188 | 9,23 | 43 | 7,40E-01 | 7 | 27 |
| 3403 | **F-box/kelch-repeat protein At4g19865** | FBK84_ARATH | At4g19865 | 45182 | 8,78 | 38 | 2,40E+00 | 8 | 25 |
| 4505 | **F-box/LRR-repeat protein At2g40920** | FBL37_ARATH | At2g40920 | 50489 | 6,64 | 45 | 0,48 | 8 | 29 |
| 6906 | **Filament-like plant protein 6** | FPP6_ARATH | FPP6 | 119778 | 4,9 | 89 | 2,00E-05 | 38 | 32 |
| 2715 | **Folylpolyglutamate synthase** | FPGS1_ARATH | FPGS1 | 63876 | 0,11 | 51 | 0,11 | 10 | 25 |
| 7807 | **Formate--tetrahydrofolate ligase** | FTHS_ARATH | THFS | 68329 | 6,26 | 77 | 0,00031 | 18 | 26 |
| 9502 | **Fumarate hydratase 1** | FUM1_ARATH | FUM1 | 53479 | 8,01 | 68 | 2,30E-04 | 15 | 26 |
| 8206 | **Gamma carbonic anhydrase 2** | GCA2_ARATH | GAMMACA2 | 30161 | 6,71 | 64 | 0,0062 | 12 | 57 |
| 8601 | **Glutamate--glyoxylate aminotransferase 1** | GGT1_ARATH | GGAT1 | 53780 | 6,49 | 142 | 9,10E-11 | 22 | 53 |
| 1508 | **Glutamine synthetase, chloroplastic/mitochondrial** | GLN2_ARATH | GLN2 | 47780 | 6,43 | 45 | 1,2 | 11 | 37 |
| 1603 | **Glutathione gamma-glutamylcysteinyltransferase 2** | PCS2_ARATH | PCS2 | 53435 | 6,58 | 41 | 1,10E+00 | 9 | 29 |
| 1209 | **Glutathione S-transferase DHAR3, chloroplastic** | DHAR3_ARATH | DHAR3 | 28724 | 7,5 | 77 | 3,10E-04 | 12 | 48 |

| | | | | | | | | | |
|---|---|---|---|---|---|---|---|---|---|
| 5210 | **Glutathione S-transferase F2** | GSTF2_ARATH | GSTF2 | 24114 | 5,92 | 102 | 9,10E-07 | 13 | 65 |
| 6212 | **Glutathione S-transferase F3** | GSTF3_ARATH | GSTF3 | 24106 | 6,25 | 69 | 0,002 | 9 | 33 |
| 7205 | **Glutathione S-transferase F7** | GSTF7_ARATH | GSTF7 | 23583 | 6,14 | 68 | 0,0021 | 7 | 32 |
| 7207 | **Glutathione S-transferase F9** | GSTF9_ARATH | GSTF9 | 27131 | 6,17 | 57 | 0,21 | 9 | 31 |
| 9305 | **Glyceraldehyde-3-phosphate dehydrogenase GAPA1, chloroplastic** | G3PA1_ARATH | GAPA1 | 42748 | 7,62 | 68 | 0,0024 | 12 | 28 |
| 9304 | **Glyceraldehyde-3-phosphate dehydrogenase GAPA2, chloroplastic** | G3PA2_ARATH | GAPA2 | 43105 | 8,16 | 58 | 2,10E-02 | 11 | 30 |
| 6401 | **Glyceraldehyde-3-phosphate dehydrogenase GAPB, chloroplastic** | G3PB_ARATH | GAPB | 48086 | 6,33 | 82 | 9,80E-05 | 20 | 35 |
| 8404 | **Glyceraldehyde-3-phosphate dehydrogenase GAPC1, cytosolic** | G3PC_ARATH | GAPC1 | 37005 | 6,62 | 57 | 0,026 | 8 | 25 |
| 3905 | **Glycine dehydrogenase (decarboxylating) 2** | GCSP2_ARATH | GLDP2 | 114672 | 6,18 | 44 | 0,65 | 24 | 21 |
| 3204 | **Glycine-rich RNA-binding protein 7** | RBG7_ARATH | RBG7 | 16937 | 5,85 | 49 | 1,9 | 6 | 45 |
| 2103 | **Glycine-rich RNA-binding protein 8** | RBG8_ARATH | RBG8 | 16626 | 5,58 | 52 | 0,093 | 4 | 32 |
| 2705 | **Heat shock 70 kDa protein 10, mitochondrial** | HSP7J_ARATH | HSP70-10 | 73174 | 5,63 | 43 | 0,51 | 12 | 17 |
| 801 | **Heat shock 70 kDa protein 3** | HSP7C_ARATH | HSP70-3 | 71559 | 4,97 | 73 | 0,00075 | 20 | 34 |
| 2501 | **Histone H1.1** | H11_ARATH | At1g06760 | 289929 | 10,77 | 51 | 0,12 | 12 | 36 |
| 2204 | **Histone H2B.7** | H2B7_ARATH | At3g46030 | 15902 | 10,02 | 46 | 0,36 | 12 | 54 |
| 1309 | **Jacalin-related lectin 33** | JAL33_ARATH | JAL33 | 32003 | 5,09 | 62 | 9,10E-03 | 13 | 39 |
| 8805 | **Kinesin-5** | ATK5_ARATH | ATK5 | 89166 | 7,25 | 73 | 0,00071 | 16 | 22 |
| 5205 | **L-ascorbate peroxidase 1, cytosolic** | apx1_ARATH | APX1 | 27829 | 5,72 | 163 | 7,20E-13 | 18 | 69 |
| 1402 | **Magnesium-chelatase subunit ChlI-2** | CHLI2_ARATH | CHLI2 | 46468 | 5,36 | 41 | 1,1 | 8 | 30 |
| 1805 | **Mediator of RNA polymerase II transcription subunit 37a** | MD37A_ARATH | MED37A | 73869 | 5,8 | 35 | 5,8 | 6 | 13 |
| 1806 | **Mediator of RNA polymerase II transcription subunit 37F** | MD37F_ARATH | MED37F | 73801 | 5,11 | 47 | 0,7 | 15 | 20 |
| 2205 | **Membrane-associated progesterone-binding protein 4** | MAPR4_ARATH | MAPR4 | 27492 | 8,46 | 26 | 41 | 7 | 29 |
| 1904 | **Methyl-CpG-binding domain-containing protein 13** | MBD13_ARATH | MBD13 | 83290 | 9,34 | 34 | 5,4 | 13 | 15 |
| 5806 | **Molybdenum cofactor sulfurase** | MOCOS_ARATH | ABA3 | 92772 | 6,56 | 58 | 0,039 | 11 | 16 |
| 2904 | **Myosin-16** | myo16_ARATH | XI-J | 142294 | 5,75 | 47 | 0,29 | 25 | 17 |
| 2804 | **Myrosinase 1** | BGL38_ARATH | TGG1 | 62664 | 5,61 | 75 | 0,00046 | 12 | 25 |
| 210 | **Oxygen-evolving enhancer protein 1-1, chloroplastic** | PSBO1_ARATH | PSBO1 | 35349 | 5,55 | 119 | 1,80E-08 | 17 | 50 |
| 8205 | **Osmotin-like protein OSM34** | OSL3_ARATH | OSM34 | 27528 | 6,08 | 72 | 0,00098 | 8 | 36 |
| 902 | **Patellin-1** | PATL1_ARATH | PATL1 | 64121 | 4.82 | 101 | 1,10E-06 | 25 | 38 |
| 107 | **Pathogenesis-related protein 5** | PR5_ARATH | At1g75040 | 26148 | 4,6 | 35 | 4,6 | 4 | 38 |

| | | | | | | | | | |
|---|---|---|---|---|---|---|---|---|---|
| 2608 | **Pentatricopeptide repeat-containing protein At1g09220, mitoc** | PPR24_ARATH | PCMP-E25 | 57781 | 8,77 | 39 | 6,2 | 15 | 28 |
| 1202 | **Peroxiredoxin-2E, chloroplastic** | PRX2E_ARATH | PRXIIE | 24783 | 9 | 78 | 0,00023 | 9 | 28 |
| 4602 | **Phosphatidylinositol/phosphatidylcholine transfer protein SFH3** | SFH3_ARATH | SFH3 | 63191 | 8,71 | 36 | 3,4 | 10 | 18 |
| 2403 | **Phosphoribulokinase, chloroplastic** | KPPR_ARATH | At1g32060 | 44721 | 5,71 | 60 | 0,016 | 10 | 29 |
| 8604 | **Plant intracellular Ras-group-related LRR protein 2** | PIRL2_ARATH | PIRL2 | 52621 | 4,82 | 52 | 0,089 | 7 | 10 |
| 6406 | **Plant UBX domain-containing protein 10** | PUX10_ARATH | PUX10 | 52998 | 4,85 | 44 | 0,63 | 14 | 20 |
| 3706 | **Probable fatty acyl-CoA reductase 4** | FACR4_ARATH | FAR4 | 56467 | 9,07 | 27 | 29 | 12 | 19 |
| 3406 | **Probable fructose-bisphosphate aldolase 2** | ALFC2_ARATH | FBA2 | 43132 | 6,78 | 117 | 2,90E-08 | 21 | 45 |
| 1801 | **Probable inactive ATP-dependent zinc metalloprotease FTSHI 1** | FTSI1_ARATH | FTSHI1 | 100705 | 7 | 45 | 0,49 | 11 | 19 |
| 809 | **Probable mediator of RNA polymerase II transcription sub 37c** | MD37D_ARATH | MED37D | 72000 | 5,03 | 54 | 0,051 | 13 | 29 |
| 1803 | **Probable mediator of RNA polymerase II transcription sub 37e** | MD37E_ARATH | MED37E | 71712 | 5,03 | 65 | 0,0041 | 15 | 23 |
| 503 | **Probable pectinesterase/pectinesterase inhibitor VGDH2** | PME37_ARATH | VGDH2 | 63374 | 8,7 | 51 | 0,11 | 7 | 15 |
| 3305 | **Probable protein phosphatase 2C 58** | P2C58_ARATH | At4g28400 | 31170 | 7,79 | 38 | 2,3 | 8 | 34 |
| 7406 | **Probable receptor-like protein kinase At2g47060** | Y2706_ARATH | At2g47060 | 40248 | 6,95 | 53 | 0,076 | 8 | 30 |
| 9301 | **Prohibitin-3, mitochondrial** | PHB3_ARATH | PHB3 | 30381 | 6,99 | 69 | 0,0019 | 12 | 40 |
| 2409 | **Protein RETICULATA** | RETIC_ARATH | RE | 46999 | 7,46 | 50 | 0,15 | 7 | 28 |
| 1607 | **Protein TIFY 8** | TIF8_ARATH | TIFY8 | 38766 | 9,4 | 60 | 0,015 | 8 | 37 |
| 9401 | **Putative F-box protein At2g19630** | FB113_ARATH | At2g19630 | 35047 | 8,85 | 56 | 3,60E-02 | 15 | 41 |
| 612 | **Putative F-box/LRR-repeat protein At4g13960** | FBL72_ARATH | At4g13960 | 50186 | 6 | 56 | 0,034 | 1,20E+01 | 33 |
| 2504 | **Putative RING-H2 finger protein ATL49** | ATL49_ARATH | ATL49 | 47884 | 7,5 | 37 | 2,9 | 8 | 20 |
| 3304 | **PYK10-binding protein 1** | JAL30_ARATH | PBP1 | 32138 | 5,46 | 85 | 4,60E-05 | 11 | 53 |
| 2603 | **Pyrophosphate fructose6-phosph1-phosphotransferase sub beta1** | PFPB1_ARATH | PFP-BETA1 | 61991 | 5,8 | 46 | 0,4 | 8 | 25 |
| 2202 | **Ras-related protein RABF1** | RABF1_ARATH | RABF1 | 21989 | 6,16 | 38 | 0,21 | 4 | 35 |
| 4504 | **Ribulose bisphosphate carboxylase large chain** | RBL_ARATH | rbcL | 53435 | 5,88 | 183 | 7,20E-15 | 31 | 44 |
| 1506 | **Ribulose bisphosphate carboxylase/oxygenase activase** | RCA_ARATH | RCA | 52347 | 5,87 | 67 | 0,0029 | 16 | 41 |
| 4303 | **S-adenosylmethionine synthase 1** | METK1_ARATH | SAM1 | 43587 | 5,51 | 58 | 0,023 | 10 | 25 |
| 8204 | **Serine/arginine-rich SC35-like splicing factor SCL28** | SRC28_ARATH | SCL28 | 28125 | 11,44 | 34 | 5,6 | 10 | 29 |
| 502 | **Sorbitol dehydrogenase** | DHSO_ARATH | SDH | 40028 | 5,67 | 46 | 0,37 | 8 | 30 |
| 8416 | **Sphingosine kinase 1** | SPHK1_ARATH | SPHK1 | 54121 | 6,39 | 56 | 0,038 | 14 | 25 |
| 3804 | **Terpenoid synthase 25** | TPS25_ARATH | TPS25 | 70693 | 5,6 | 40 | 1,3 | 9 | 19 |
| 1204 | **Thylakoid lumenal protein TL20.3** | TL203_ARATH | TL20.3 | 30388 | 8,72 | 45 | 6,70E-01 | 9 | 45 |

| | | | | | | | | | |
|---|---|---|---|---|---|---|---|---|---|
| 2509 | **Transcription factor TGA4** | TGA4_ARATH | TGA4 | 41953 | 6,69 | 25 | 48 | 4 | 12 |
| 3206 | **Triosephosphate isomerase, cytosolic** | TPIS_ARATH | CTIMC | 27380 | 5,39 | 109 | 1,80E-07 | 14 | 67 |
| 2305 | **tRNA-splicing endonuclease subunit Sen2-1** | SEN21_ARATH | SEN1 | 27741 | 8,42 | 44 | 0,53 | 6 | 20 |
| 2505 | **UDP-glucuronate 4-epimerase 5** | GAE5_ARATH | GAE5 | 48191 | 9,88 | 41 | 1,2 | 8 | 18 |
| 3207 | **Vacuolar protein sorting-associated protein 24 homolog 1** | VP241_ARATH | VPS24-1 | 26037 | 5,58 | 42 | 0,83 | 8 | 47 |
| 1602 | **V-type proton ATPase subunit B1** | VATB1_ARATH | VHA-B1 | 54188 | 4,98 | 86 | 3,40E-05 | 13 | 36 |
| 1601 | **V-type proton ATPase subunit B2** | VATB2_ARATH | VHA-B2 | 54385 | 5,03 | 61 | 0,01 | 14 | 30 |
| 2101 | **Zinc finger A20 and AN1 domain-containing stress-assoc prot 1** | SAP1_ARATH | SAP1 | 18379 | 8,94 | 57 | 0,03 | 6 | 45 |

## Table 2. MapMan BIN assignation and description of differentially abundant proteins in *Arabidopsis thaliana.*

| Protein name | bin code | bin name | description |
|---|---|---|---|
| **30S ribosomal protein S5, chloroplastic** | 29.2.1.1.1.1.5 | protein.synthesis.ribosomal protein.prokaryotic.chloroplast.30S subunit.S5 | Binds directly to 16S ribosomal RNA. |
| **3-isopropylmalate dehydratase small subunit 3** | 16.5.1.1.1.4 | secondary metabolism.sulfur-containing.glucosinolates.synthesis.aliphatic.methylthioalkylmalate isomerase small subunit (MAM-IS) | Catalyzes the isomerization between 2-isopropylmalate and 3-isopropylmalate, via the formation of 2-isopropylmaleate. Plays an essential role in leucine biosynthesis and female gametophyte development. |
| **Aminomethyltransferase, mitochondrial** | 1.2.4.2, 13.2.5.2 | PS.photorespiration.glycine cleavage.T subunit, amino acid metabolism.degradation.serine-glycine-cysteine group.glycine | The glycine decarboxylase (GDC) or glycine cleavage system catalyzes the degradation of glycine. |
| **Aspartokinase 2, chloroplastic** | 13.1.3.6.1.1 | amino acid metabolism.synthesis.aspartate family.misc.homoserine.aspartate kinase | Involved in the first step of essential amino acids lysine, threonine, methionine and isoleucine synthesis via the aspartate-family pathway. |
| **ATP synthase subunit beta-1, mitochondrial** | 1.2.4.2, 13.2.5.2 | PS.photorespiration.glycine cleavage.T subunit, amino acid metabolism.degradation.serine-glycine-cysteine group.glycine | Mitochondrial membrane ATP synthase (F1F0 ATP synthase or Complex V) produces ATP from ADP in the presence of a proton gradient across the membrane which is generated by electron transport complexes of the respiratory chain. Subunits alpha and beta form the catalytic core in F1. |
| **ATP-dependent helicase BRM** | 20.1.7 | stress.biotic.PR-proteins | ATPase subunit of a multiprotein complex equivalent of the SWI/SNF complex that acts by remodeling the chromatin by catalyzing an ATP-dependent alteration in the structure of nucleosomal DNA. |
| **ATP-dependent zinc metalloprotease FTSH 2** | 29.5.7, 31.2 | protein.degradation.metalloprotease, cell.division | Part of a complex that function as an ATP-dependent zinc metallopeptidase. Involved in the thylakoid formation and in the removal of damaged D1 in the photosystem II, preventing cell death under high-intensity light conditions, but not involved in thermotolerance. |
| **Auxin-responsive protein IAA9** | 17.2.3 | hormone metabolism.auxin.induced-regulated-responsive-activated | Aux/IAA proteins are short-lived transcriptional factors that function as repressors of early auxin response genes at low auxin concentrations. |
| **Bifunctional enolase 2/transcriptional activator** | 4.1.13 | glycolysis.cytosolic branch.enolase | Multifunctional enzyme that acts as an enolase involved in the metabolism and as a positive regulator of cold-responsive gene transcription. |
| **Catalase-2** | 21.6 | redox.dismutases and catalases | Occurs in almost all aerobically respiring organisms and serves to protect cells from the toxic effects of hydrogen peroxide. |
| **Chaperone protein ClpC2, chloroplastic** | 20.2.1, 29.5.5 | stress.abiotic.heat,protein. degradation.serine protease | Molecular chaperone. Has an ATPase activity, but no ADPase activity. |
| **Chaperonin 60 subunit alpha 1, chloroplastic** | 1.3.13, 29.6 | PS.calvin cycle.rubisco interacting, protein.folding | Binds RuBisCO small and large subunits and is implicated in the assembly of the enzyme oligomer. Involved in protein assisted folding. Required for proper chloroplast development. |

| | | | |
|---|---|---|---|
| **Chaperonin 60 subunit beta 1, chloroplastic** | 1.3.13, 29.6 | PS.calvin cycle.rubisco interacting, protein.folding | Binds RuBisCO small and large subunits and is implicated in the assembly of the enzyme oligomer. Involved in protein assisted folding. Required for proper plastid division. |
| **Chloroplast stem-loop binding protein of 41 kDa a** | 27.3.99, 31.4 | RNA.regulation of transcription.unclassified, cell.vesicle transport | Binds and cleaves RNA, particularly in stem-loops. Associates with pre-ribosomal particles in chloroplasts, and participates in chloroplast ribosomal RNA metabolism. Required for chloroplast integrity. Involved in the regulation of the circadian system. |
| **Cullin-3B** | 29.5.11.4.3.3, 29.5.11.4.5.1 | protein.degradation.ubiquitin.E3.SCF.cullin, protein.degradation.ubiquitin.E3.BTB/POZ Cullin3.Cullin3 | Component of the cullin-RING ubiquitin ligases (CRL). The functional specificity of the CRL complex depends on the BTB domain-containing protein as the susbstrate recognition component. |
| **Elongator complex protein 3** | 27.3.54, 34.22 | RNA.regulation of transcription.histone acetyltransferases transport.cyclic nucleotide or calcium regulated channels | Histone acetyltransferase component of the large multiprotein complex Elongator that is involved in the regulation of transcription initiation and elongation. |
| **Eukaryotic translation initiation factor 5A-2** | 26.8 29.2.3 | misc.nitrilases, nitrile lyases, berberine bridge enzymes, reticuline oxidases, troponine reductases, protein.synthesis.initiation | Bimodular protein capable of binding to both RNA and proteins. Regulates cytokinin-mediated root. Regulates the induction of programmed cell death caused by infection with virulent pathogen. |
| **F-box only protein 7** | 29.5.11.4.3.2 | protein.degradation.ubiquitin.E3.SCF.FBOX | Confers specificity to the E3 ligase through direct physical interactions with the degradation substrate |
| **F-box/kelch-repeat protein At4g19865** | 29.5.11.4.3.2 | protein.degradation.ubiquitin.E3.SCF.FBOX | Confers specificity to the E3 ligase through direct physical interactions with the degradation substrate |
| **F-box/LRR-repeat protein At2g40920** | 29.5.11.4.3.2 | protein.degradation.ubiquitin.E3.SCF.FBOX | Confers specificity to the E3 ligase through direct physical interactions with the degradation substrate |
| **Filament-like plant protein 6** | 27.3.44, 29.5.5, 31.1 | RNA.regulation of transcription.chromatin remodeling factors, protein.degradation.serine protease, cell.organisation | member of the *filament-like plant protein* (*FPP*) family |
| **Folylpolyglutamate synthase** | 19.4, 25.8 | tetrapyrrole synthesis.ALA dehydratase, C1-metabolism.tetrahydrofolate synthase | Catalyzes conversion of folates to polyglutamate. Essential for organellar and whole-plant folate homeostasis. Required for postembryonic root development. Generates polyglutamylated folate cofactors to support C1 metabolism required for meristem maintenance and cell expansion during postembryonic root development |
| **Formate--tetrahydrofolate ligase** | 25.2, 27.3.44 | C1-metabolism.formate-tetrahydrofolate ligase, RNA.regulation of transcription.chromatin remodeling factors | This protein is involved in the pathway tetrahydrofolate interconversion, which is part of One-carbon metabolism.View all proteins of this organism that are known to be involved in the pathway tetrahydrofolate interconversion and in One-carbon metabolism |
| **Fumarate hydratase 1** | 8.1.8 | TCA / organic transformation.TCA.fumarase | This protein is involved in step of the subpathway that synthesizes (S)-malate from fumarate. |
| **Gamma carbonic anhydrase 2** | 9.1.1.5, 21.2.2 | mitochondrial electron transport / ATP synthesis.NADH-DH (type I).complex I.carbonic anhydrase, redox.ascorbate and glutathione.glutathione | Enzyme involved in the catabolism of $H_2CO_3$ but that does not mediates the reversible hydration of carbon dioxide. Mediates complex I assembly in mitochondria and respiration. |

| | | | |
|---|---|---|---|
| **Glutamate--glyoxylate aminotransferase 1** | 1.2.3, 13.1.1.3.1, 13.1.5.2.2, 28.1.1.4 | PS.photorespiration.aminotransferases peroxisomal amino acid metabolism.synthesis.central amino acid metabolism.alanine.alanine aminotransferase, amino acid metabolism.synthesis.serine-glycine-cysteine group.glycine.glycine transaminase, DNA.synthesis/chromatin structure.retrotransposon/transposase.hat-like transposase | Catalyzes the glutamate:glyoxylate (GGT or GGAT), alanine:glyoxylate (AGT), alanine:2-oxoglutarate (AKT) and glutamate:pyruvate (GPT) aminotransferase reactions in peroxisomes. Required for abscisic acid (ABA)- and stress-mediated responses in an $H_2O_2$-dependent manner. Function as a photorespiratory aminotransferase that modulates amino acid content during photorespiration (GGAT activity); promotes serine, glycine and citrulline metabolism in response to light |
| **Glutamine synthetase, chloroplastic/mitochondrial** | 12.2.2, 20.2.99, 27.3.69, 34.12 | N-metabolism.ammonia metabolism.glutamine synthetase stress.abiotic.unspecified, RNA.regulation of transcription.SET-domain transcriptional regulator family, transport.metal | The light-modulated chloroplast/mitochondrial enzyme, encoded by a nuclear gene and expressed primarily in leaves, is responsible for the reassimilation of the ammonia generated by photorespiration. |
| **Glutathione gamma-glutamylcysteinyltransferase 2** | 15.2 | metal handling.binding, chelation and storage | Involved in the synthesis of phytochelatins (PC) and homophytochelatins (hPC), the heavy-metal-binding peptides of plants. |
| **Glutathione S-transferase DHAR3, chloroplastic** | 17.2.3, 21.2.1 | hormone metabolism.auxin.induced-regulated-responsive-activated, redox.ascorbate and glutathione.ascorbate | Exhibits glutathione-dependent thiol transferase and dehydroascorbate (DHA) reductase activities. Key component of the ascorbate recycling system. Involved in the redox homeostasis, especially in scavenging of ROS under oxidative stresses. |
| **Glutathione S-transferase F2** | 26.9 | misc.glutathione S transferases | Binds auxin, endogenous flavonoids and the phytoalexin camalexin and may be involved in regulating the binding and transport of small bioactive natural products and defense-related compounds during plant stress. Acts as glutathione peroxidase on cumene hydroperoxide, linoleic acid-13-hydroperoxide and trans-stilbene oxide. |
| **Glutathione S-transferase F3** | 26.9 | misc.glutathione S transferases | Binds a series of heterocyclic compounds, including lumichrome, harmane, norharmane and indole-3-aldehyde. May be involved in the conjugation of reduced glutathione to a wide number of exogenous and endogenous hydrophobic electrophiles and have a detoxification role against certain herbicides. |
| **Glutathione S-transferase F7** | 26.9 | misc.glutathione S transferases | May be involved in the conjugation of reduced glutathione to a wide number of exogenous and endogenous hydrophobic electrophiles and have a detoxification role against certain herbicides. |
| **Glutathione S-transferase F9** | 26.9 | misc.glutathione S transferases | May be involved in the conjugation of reduced glutathione to a wide number of exogenous and endogenous hydrophobic electrophiles and have a detoxification role against certain herbicides. |
| **Glyceraldehyde-3-phosphate dehydrogenase GAPA1, chloroplastic** | 1.3.4 | PS.calvin cycle.GAP | Involved in the photosynthetic reductive pentose phosphate pathway (Calvin-Benson cycle). Catalyzes the reduction of 1,3-diphosphoglycerate by NADPH |
| **Glyceraldehyde-3-phosphate dehydrogenase GAPA2,chloroplastic** | 1.3.4 | PS.calvin cycle.GAP | Involved in the photosynthetic reductive pentose phosphate pathway (Calvin-Benson cycle). Catalyzes the reduction of 1,3-diphosphoglycerate by NADPH |
| **Glyceraldehyde-3-phosphate dehydrogenase GAPB, chloroplastic** | 1.3.4 | PS.calvin cycle.GAP | Involved in the photosynthetic reductive pentose phosphate pathway (Calvin-Benson cycle). Catalyzes the reduction of 1,3-diphosphoglycerate by NADPH |
| **Glyceraldehyde-3-phosphate dehydrogenase GAPC1, cytosolic** | 4.1.8 | glycolysis.cytosolic branch.glyceraldehyde 3-phosphate dehydrogenase (GAP-DH) | Key enzyme in glycolysis that catalyzes the first step of the pathway by converting D-glyceraldehyde 3-phosphate (G3P) into 3-phospho- |

| | | | |
|---|---|---|---|
| | | | D-glyceroyl phosphate. Essential for the maintenance of cellular ATP levels and carbohydrate metabolism. Involved in response to oxidative stress by mediating plant responses to abscisic acid (ABA) and water deficits May be part of a redox-dependent retrograde signal transduction network for adaptation upon oxidative stress. |
| **Glycine dehydrogenase (decarboxylating) 2** | 1.2.4.1, 13.2.5.2, 25 | PS.photorespiration.glycine cleavage.P subunit, amino acid metabolism.degradation.serine-glycine-cysteine group.glycine, C1-metabolism | The glycine decarboxylase (GDC) catalyzes the degradation of glycine. |
| **Glycine-rich RNA-binding protein 7** | 27.3.75 27.4 | RNA.regulation of transcription.GRP, RNA. RNA binding | Plays a role in RNA transcription or processing during stress. Binds RNAs and DNAs sequence with a preference to single-stranded nucleic acids. |
| **Glycine-rich RNA-binding protein 8** | 17.2.2 27.3.75 27.4 | hormone metabolism.auxin.signal transduction , RNA.regulation of transcription.GRP, RNA.RNA binding | Plays a role in RNA transcription or processing during stress. Binds RNAs and DNAs sequence with a preference to single-stranded nucleic acids. Involved in mRNA alternative splicing of numerous targets by modulating splice site selection. |
| **Heat shock 70 kDa protein 10, mitochondrial** | 20.2.1 | stress.abiotic.heat | In cooperation with other chaperones, Hsp70s stabilize preexistent proteins against aggregation and mediate the folding of newly translated polypeptides in the cytosol as well as within organelles. |
| **Heat shock 70 kDa protein 3** | 10.3, 20.2.1, 26.10, 29.6, 34.99 | cell wall.hemicellulose synthesis, stress.abiotic.heat, misc.cytochrome P450, protein.folding, transport.misc | In cooperation with other chaperones, Hsp70s stabilize preexistent proteins against aggregation and mediate the folding of newly translated polypeptides in the cytosol as well as within organelles. |
| **Histone H1.1** | 11.1.9, 28.1.3, 29.5.11.4.2 | lipid metabolism.FA synthesis and FA elongation.long chain fatty acid CoA ligase, DNA.synthesis/chromatin structure.histone, protein.degradation.ubiquitin.E3.RING | Histones H1 are necessary for the condensation of nucleosome chains into higher-order structures. |
| **Histone H2B.7** | 27.3.12, 28.1.3, 29.4.1.57, 30.2.6 | RNA.regulation of transcription.C3H zinc finger family DNA.synthesis/chromatin structure.histone, protein.postranslational modification.kinase.receptor like, cytoplasmatic kinase VII, signalling.receptor kinases.leucine rich repeat VI | Core component of nucleosome. Nucleosomes wrap and compact DNA into chromatin Histones there by play a central role in transcription regulation, DNA repair, DNA replication and chromosomal stability. |
| **Jacalin-related lectin 33** | 16.5.1.3.1 17.7.3, 26.16 | secondary metabolism.sulfur-containing.glucosinolates.degradation.myrosinase.hormone metabolism.jasmonate.induced-regulated-responsive-activated, misc.myrosinases-lectin-jacalin | Sugar-binding protein showing significant affinity for maltohexaose, isomaltohexaose,. |
| **Kinesin-5** | 31.1 | cell.organisation | ATP binding and microtubule binding |

| | | | |
|---|---|---|---|
| **L-ascorbate peroxidase 1, cytosolic** | 21.2.1, 26.8 | redox.ascorbate and glutathione.ascorbate, misc.nitrilases, nitrile lyases, berberine bridge enzymes, reticuline oxidases, troponine reductases | Plays a key role in hydrogen peroxide removal. Constitutes a central component of the reactive oxygen gene network. |
| **Magnesium-chelatase subunit ChlI-2** | 19.10 29.4 | tetrapyrrole synthesis.magnesium chelatase, protein.postranslational modification | Involved in chlorophyll biosynthesis. Catalyzes the insertion of magnesium ion into protoporphyrin IX to yield Mg-protoporphyrin IX. |
| **Mediator of RNA polymerase II transcription subunit 37a** | 10.3, 20.2.1, 26.10, 29.6, 34.99 | cell wall.hemicellulose synthesis, stress.abiotic.heat, misc.cytochrome P450, protein.folding, transport.misc | Component of the Mediator complex, a coactivator involved in the regulated transcription of nearly all RNA polymerase II-dependent genes. |
| **Mediator of RNA polymerase II transcription subunit 37F** | 10.3, 20.2.1, 26.10, 29.6, 34.99 | cell wall.hemicellulose synthesis, stress.abiotic.heat, misc.cytochrome P450, protein.folding, transport.misc | Component of the Mediator complex, a coactivator involved in the regulated transcription of nearly all RNA polymerase II-dependent genes. |
| **Membrane-associated progesterone-binding protein 4** | 21.2, 27.3.39, 29.4, 34.13 | redox.ascorbate and glutathione, RNA.regulation of transcription.AtSR transcription factor family, protein.postranslational modification, transport.peptides and oligopeptides | heme binding and steroid binding |
| **Methyl-CpG-binding domain-containing protein 13** | 27.3.59 | RNA.regulation of transcription.methyl binding domain proteins | Probable transcriptional regulator. |
| **Molybdenum cofactor sulfurase** | 17.1.1, 30.3 | hormone metabolism.abscisic acid.synthesis-degradation, signalling.calcium | Sulfurates the molybdenum cofactor. Sulfation of molybdenum is essential for xanthine dehydrogenase (XDH) and aldehyde oxidase (ADO) enzymes in which molybdenum cofactor is liganded by 1 oxygen and 1 sulfur atom in active form. Modulates cold stress- and osmotic stress-responsive gene expression by acting as key regulator of abscisic acid (ABA) biosynthesis. |
| **Myosin-16** | 17.3.1.1.1, 26.22, 31.1 | hormone metabolism. brassinosteroid.synthesis-degradation.BRs.DET2, misc.short chain dehydrogenase/reductase (SDR), cell.organisation | Myosin heavy chain that is required for the cell cycle-regulated transport of various organelles and proteins for their segregation. Functions by binding with its tail domain to receptor proteins on organelles and exerting force with its N-terminal motor domain against actin filaments. |
| **Myrosinase 1** | 16.5.1.3.1.1 17.1.2 17.2.1 26.16 | secondary metabolism.sulfur-containing.glucosinolates.degradation.myrosinase.TGG, hormone metabolism.abscisic acid.signal transduction, hormone metabolism.auxin.synthesis-degradation, misc.myrosinases-lectin-jacalin | Degradation of glucosinolates to glucose, sulfate and any of the products: thiocyanates, isothiocyanates, nitriles, epithionitriles or oxazolidine-2-thiones. Seems to function in abscisic acid (ABA) and methyl jasmonate (MeJA) signaling in guard cells. |
| **Oxygen-evolving enhancer protein 1-1, chloroplastic** | 27.3.44, | RNA.regulation of transcription.chromatin remodeling factors | Stabilizes the manganese cluster which is the primary site of water splitting. |
| **Osmotin-like protein OSM34** | 28.99 | DNA.unspecified | defense response to bacterium and fungus. response to salt stress |
| **Patellin-1** | 1.1.1.2 | PS.lightreaction.photosystem II.PSII polypeptide subunits | Carrier protein that may be involved in membrane-trafficking events associated with cell plate formation during cytokinesis. |

| | | | |
|---|---|---|---|
| **Pathogenesis-related protein 5** | 17.3.1.1.1, 26.22, 31.1 | hormone metabolism.brassinosteroid.synthesis-degradation.BRs.DET2, misc.short chain dehydrogenase/reductase (SDR), cell.organisation | Partially responsible for acquired pathogen resistance. |
| **Pentatricopeptide repeat-containing protein At1g09220, mitoc** | 16.2.1.10, 21.5 | secondary metabolism.phenylpropanoids.lignin biosynthesis.CAD, redox.peroxiredoxin | endonuclease activity |
| **Peroxiredoxin-2E, chloroplastic** | 29.3.4.99, 29.5.9, 34.99 | protein.targeting.secretory pathway.unspecified, protein.degradation.AAA type, transport.misc | Plays a role in cell protection against oxidative stress by detoxifying peroxides. May be involved in chloroplast redox homeostasis. |
| **Phosphatidylinositol/phosphatidylcholine transfer protein SFH3** | 1.3.12 | PS.calvin cycle.PRK | Required for transport of secretory proteins from the Golgi complex. |
| **Phosphoribulokinase, chloroplastic** | 1.3.4 | PS.calvin cycle.GAP | protein involved in the pathway Calvin cycle, which is part of Carbohydrate biosynthesis. |
| **Plant intracellular Ras-group-related LRR protein 2** | | | Leucine-rich repeat protein that likely mediates protein interactions, possibly in the context of signal transduction. |
| **Plant UBX domain-containing protein 10** | 29.5 | protein degradation | Biological process, Neutrophil degranulation. |
| **Probable fatty acyl-CoA reductase 4** | 11.9.4.13, 33.99 | lipid metabolism.lipid degradation.beta-oxidation.acyl CoA reductase, development.unspecified | Catalyzes the reduction of fatty acyl-CoA to fatty alcohols. Provides the fatty alcohols required for synthesis of suberin in roots, seed coat and wound-induced leaf tissue. Provides the fatty alcohols required for synthesis of alkyl hydroxycinnamates in root waxes. |
| **Probable fructose-bisphosphate aldolase 2** | 1.3.6, 11.1.30 | PS.calvin cycle.aldolase, lipid metabolism.FA synthesis and FA elongation.pyruvate kinase | Plays a key role in glycolysis and gluconeogenesis. |
| **Probable inactive ATP-dependent zinc metalloprotease FTSHI 1** | 29.5.7 | protein.degradation.metalloprotease | Functions in chloroplast biogenesis and chloroplast division |
| **Probable mediator of RNA polymerase II transcription sub 37c** | 10.3, 20.2.1, 26.10, 29.6, 34.99 | cell wall.hemicellulose synthesis, stress.abiotic.heat, misc.cytochrome P450, protein.folding, transport.misc | Component of the Mediator complex, a coactivator involved in the regulated transcription of nearly all RNA polymerase II-dependent genes. |
| **Probable mediator of RNA polymerase II transcription sub 37e** | 10.3, 20.2.1, 26.10, 29.6, 34.99 | cell wall.hemicellulose synthesis, stress.abiotic.heat, misc.cytochrome P450, protein.folding, transport.misc | Component of the Mediator complex, a coactivator involved in the regulated transcription of nearly all RNA polymerase II-dependent genes. In cooperation with other chaperones, Hsp70s stabilize preexistent proteins against aggregation and mediate the folding of newly translated polypeptides in the cytosol as well as within organelles. |

| | | | |
|---|---|---|---|
| **Probable pectinesterase/pectinesterase inhibitor VGDH2** | 10.8.1, 16.8.3, 26.18, 27.3.99, 28.1 | cell wall.pectinesterases.PME, secondary metabolism.flavonoids.dihydroflavonols, misc.invertase/pectin methylesterase inhibitor family protein, RNA.regulation of transcription.unclassified, DNA.synthesis/chromatin structure | Acts in the modification of cell walls via demethylesterification of cell wall pectin. |
| **Probable protein phosphatase 2C 58** | 26.2, 27.3.28, 28.1, 29.4 | misc.UDP glucosyl and glucoronyl transferases, RNA.regulation of transcription.squamosa promoter binding protein family (SBP), DNA.synthesis/chromatin structure, protein.postranslational modification | serine/threonine phosphate |
| **Probable receptor-like protein kinase At2g47060** | 29.4.4.57, 29.4.1.58 | protein.postranslational modification.kinase.receptor like cytoplasmatic kinase VII, protein.postranslational modification.kinase.receptor like cytoplasmatic kinase VIII | ATP binding and transmembrane receptor protein serine/threonine kinase activity |
| **Prohibitin-3, mitochondrial** | 9.1.1, 31.2 | mitochondrial electron transport / ATP synthesis.NADH-DH (type I).complex I, cell.division | Prohibitin probably acts as a holdase/unfoldase for the stabilization of newly synthesized mitochondrial proteins. Necessary for mitochondrial and cell metabolism and biogenesis. |
| **Protein RETICULATA** | 33.99 | development.unspecified | May play a role in leaf development. |
| **Protein TIFY 8** | | | Repressor of jasmonate responses. |
| **Putative F-box protein At2g19630** | 29.5.11.4.3.2 | protein.degradation.ubiquitin.E3.SCF.FBOX | Confers specificity to the E3 ligase through direct physical interactions with the degradation substrate |
| **Putative F-box/LRR-repeat protein At4g13960** | 20.2.4, 27.3.67, 29.5.11.4.3.2 | stress.abiotic.touch/wounding, RNA.regulation of transcription.putative transcription regulator, protein.degradation.ubiquitin.E3.SCF.FBOX | Confers specificity to the E3 ligase through direct physical interactions with the degradation substrate |
| **Putative RING-H2 finger protein ATL49** | 29.5.11.4.3.2 | protein.degradation.ubiquitin.E3.SCF.FBOX | May be involved in female gametophyte development. |
| **PYK10-binding protein 1** | 16.5.1.3.1, 17.7.3, 26.16 | secondary metabolism.sulfur-containing.glucosinolates.degradation.myrosinase, hormone metabolism.jasmonate.induced-regulated-responsive-activated, misc.myrosinases-lectin-jacalin | Inhibitor-type lectin that may regulate the correct polymerization of BGLU23/PYK10 upon tissue damage. |
| **Pyrophosphate fructose6-phosph1-phosphotransferase sub beta1** | 4.2.5 | glycolysis.plastid branch.pyrophosphate-fructose-6-P phosphotransferase | Catalytic subunit of pyrophosphate--fructose 6-phosphate 1-phosphotransferase. Catalyzes the phosphorylation of D-fructose 6-phosphate, the first committing step of glycolysis. Uses inorganic phosphate (PPi) as phosphoryl donor instead of ATP like common ATP-dependent phosphofructokinases (ATP-PFKs), which renders the reaction reversible, and can thus function both in glycolysis and gluconeogenesis. |
| **Ras-related protein RABF1** | 30.5 | signalling.G-proteins | Endosomal protein probably involved in endocytosis. Probably not involved in vacuolar trafficking. |

| | | | |
|---|---|---|---|
| **Ribulose bisphosphate carboxylase large chain** | 1.3.1, 29.2.1.1.1.15 | PS.calvin cycle.rubisco large subunit, protein.synthesis.ribosomal protein.prokaryotic.chloroplast.30S subunit.S15 | RuBisCO catalyzes two reactions: the carboxylation of D-ribulose 1,5-bisphosphate, the primary event in carbon dioxide fixation, as well as the oxidative fragmentation of the pentose substrate in the photorespiration process. |
| **Ribulose bisphosphate carboxylase/oxygenase activase** | 1.3.13 | PS.calvin cycle.rubisco interacting | Activation of RuBisCO (ribulose-1,5-bisphosphate carboxylase/oxygenase; involves the ATP-dependent carboxylation of the epsilon-amino group of lysine leading to a carbamate structure. |
| **S-adenosylmethionine synthase 1** | 13.1.3.4.11, 15.2 | amino acid metabolism.synthesis.aspartate family.methionine.S-adenosylmethionine synthetase, metal handling.binding, chelation and storage | Catalyzes the formation of S-adenosylmethionine from methionine and ATP. |
| **Serine/arginine-rich SC35-like splicing factor SCL28** | 27.1.1 | RNA.processing.splicing | Involved in intron recognition and spliceosome assembly |
| **Sorbitol dehydrogenase** | 3.3, 5.3, 16.2.1.10, 26.11.1 | minor CHO metabolism.sugar alcohols, fermentation.ADH, secondary metabolism.phenylpropanoids.lignin biosynthesis.CAD, misc.alcohol dehydrogenases.cinnamyl alcohol dehydrogenase | Converts sorbitol to fructose. Mostly active with sorbitol, ribitol and xylitol as substrates. |
| **Sphingosine kinase 1** | 11.8.1, 19.4 | lipid metabolism.exotics (steroids, squalene etc).sphingolipids, tetrapyrrole synthesis.ALA dehydratase | Involved in the production of sphingolipid metabolites. |
| **Terpenoid synthase 25** | 16.1.5, 26.10, 27.3.6, 34.14 | secondary metabolism.isoprenoids.terpenoids, misc.cytochrome P450, RNA.regulation of transcription.basic helix-loop-helix family (bHLH), transport.unspecified cation | This protein is involved in the pathway terpenoid biosynthesis, which is part of Secondary metabolite biosynthesis. |
| **Thylakoid lumenal protein TL20.3** | 21.2.2, 29.5 | redox.ascorbate and glutathione.glutathione, protein.degradation | Pentapeptide repeat protein of unknown function. Subject to degradation when reduced. |
| **Transcription factor TGA4** | 27.3.35, 29.5.11 | RNA.regulation of transcription.bZIP transcription factor family, protein.degradation.ubiquitin | Transcriptional activator that binds specifically to the DNA sequence 5'-TGACG-3'. Recognizes ocs elements like the as-1 motif of the cauliflower mosaic virus 35S promoter. Binding to the as-1-like cis elements mediate auxin- and salicylic acid-inducible transcription. May be involved in the induction of the systemic acquired resistance (SAR) via its interaction with NPR1. Could also bind to the Hex-motif (5'-TGACGTGG-3') another cis-acting element found in plant histone promoters. |
| **Triosephosphate isomerase, cytosolic** | 1.3.5, 4.1.7 | PS.calvin cycle.TPI, glycolysis.cytosolic branch.triosephosphate isomerase (TPI) | This protein is involved in the pathway gluconeogenesis, which is part of Carbohydrate biosynthesis. |
| **tRNA-splicing endonuclease subunit Sen2-1** | 27.1.1, 28.1, 29.2.4, 33.99 | RNA.processing.splicing, DNA.synthesis/chromatin structure, protein.synthesis.elongation, development.unspecified | Constitutes one of the two catalytic subunit of the tRNA-splicing endonuclease complex, a complex responsible for identification and cleavage of the splice sites in pre-tRNA. |
| **UDP-glucuronate 4-epimerase 5** | 10.1.6 | cell wall.precursor synthesis.GAE | Involved in the synthesis of the negatively charged monosaccharide that forms the backbone of pectic cell wall components. |

| | | | |
|---|---|---|---|
| **Vacuolar protein sorting-associated protein 24 homolog 1** | 27.3.71 | RNA.regulation of transcription.SNF7 | Component of the ESCRT-III complex, which is required for multivesicular bodies (MVBs) formation and sorting of endosomal cargo proteins into MVBs. |
| **V-type proton ATPase subunit B1** | 1.1.4, 9.9, 34.1.1.1 | PS.lightreaction.ATP synthase, mitochondrial electron transport / ATP synthesis.F1-ATPase, transport.p- and v-ATPases.H+-transporting two-sector ATPase.subunit B | Non-catalytic subunit of the peripheral V1 complex of vacuolar ATPase. V-ATPase is responsible for acidifying a variety of intracellular compartments in eukaryotic cells. |
| **V-type proton ATPase subunit B2** | 1.1.4, 9.9, 34.1.1.1 | PS.lightreaction.ATP synthase, mitochondrial electron transport / ATP synthesis.F1-ATPase, transport.p- and v-ATPases.H+-transporting two-sector ATPase.subunit B | Non-catalytic subunit of the peripheral V1 complex of vacuolar ATPase. V-ATPase is responsible for acidifying a variety of intracellular compartments in eukaryotic cells. |
| **Zinc finger A20 and AN1 domain-containing stress-assoc prot 1** | 27.3.3 | RNA.regulation of transcription.AP2/EREBP, APETALA2/ethylene-responsive element binding protein family | May be involved in environmental stress response. |

## Table 3. MALDI-TOF/TOF data associated with differentially abundant proteins identified in *Saccharomyces cerevisiae*

| Spot n° | Protein name | Protein code | Gene name | mass | pI | score | expect | match | coverage (%) |
|---|---|---|---|---|---|---|---|---|---|
| 6101 | **1-(5-phosphoribosyl)-5-[(5-phosphoribosylamino)methylideneamino] imidazole-4-carboxamide isomerase** | HIS4_YEAST | HIS6 | 30002 | 5,59 | 23 | 36 | 11 | 41 |
| 3303 | **25S rRNA (uridine(2843)-N(3))-methyltransferase** | BMT6_YEAST | BMT6 | 42414 | 8,03 | 35 | 2,70E+00 | 8 | 29 |
| 2105 | **37S ribosomal protein S18, mitochondrial** | RT18_YEAST | MRPS18 | 24662 | 9,9 | 44 | 3,5 | 7 | 40 |
| 8204 | **37S ribosomal protein S23, mitochondrial** | RT23_YEAST | RSM23 | 50892 | 9,73 | 45 | 0,26 | 14 | 26 |
| 2103 | **40S ribosomal protein S0-B** | RSSA2_YEAS1 | RPS0B | 28002 | 4,69 | 44 | 0,3 | 9 | 28 |
| 3005 | **40S ribosomal protein S1-B** | RS3A2_YEAS2 | RPS1B | 28851 | 10 | 35 | 2,70E+00 | 6 | 34 |
| 2203 | **60S acidic ribosomal protein P0** | RLA0_YEAST | RPP0 | 33696 | 4,75 | 78 | 0,00011 | 14 | 32 |
| 3008 | **60S ribosomal protein L20-A** | RL20A_YEAST | RPL20A | 20424 | 8,5 | 34 | 8,50E+00 | 6 | 34 |
| 2403 | **60S ribosomal protein L20-B** | RL20B_YEAST | RL20B | 20424 | 10,3 | 52 | 0,053 | 7 | 43 |
| 3007 | **Acyl-CoA-binding protein** | ACBP_YEAST | ACB1 | 10055 | 4,85 | 32 | 4,80E+00 | 5 | 58 |
| 4505 | **Asparagine--tRNA ligase, cytoplasmic** | SYNC_YEAST | DED81 | 62690 | 5,6 | 11 | 28 | 17 | 17 |
| 3705 | **ATPase expression protein 2, mitochondrial** | AEP2_YEAS7 | AEP2 | 68220 | 9,58 | 59 | 0,0091 | 77 | 49 |
| 3803 | **ATPase synthesis protein 25, mitochondrial** | ATP25_YEAST | ATP25 | 70796 | 9,29 | 21 | 63 | 8 | 9 |
| 7806 | **ATP-dependent 6-phosphofructokinase subunit beta** | PFKA2_YEAST | PFK2 | 105179 | 6,23 | 58 | 0,14 | 20 | 18 |
| 2805 | **ATP-dependent molecular chaperone HSC82** | HSC82_YEAST | HSC82 | 80850 | 4,78 | 124 | 3,10E-09 | 40 | 47 |
| 7803 | **Cargo-transport protein YPP1** | YPP1_YEAS7 | YPP1 | 95977 | 5,3 | 42 | 0,49 | 25 | 33 |
| 6903 | **Carnitine O-acetyltransferase, mitochondrial** | CACP_YEAST | CAT2 | 77599 | 8,35 | 33 | 4,2 | 25 | 35 |
| 2809 | **Cell division control protein 48** | CDC48_YEAST | CDC48 | 92167 | 4,82 | 120 | 7,90E-09 | 37 | 42 |
| 2502 | **Cystathionine beta-synthase** | CBS_YEAST | CYS4 | 56044 | 6,25 | 55 | 2,4 | 8 | 17 |
| 4601 | **Cysteine--tRNA ligase** | SYC_YEAST | YNL247W | 87824 | 6,4 | 25 | 24 | 44 | 26 |
| 5612 | **Cytochrome c oxidase assembly factor 1** | COA1_YEAST | COA1 | 22031 | 9,55 | 27 | 17 | 19 | 52 |
| 1022 | **Cytochrome c oxidase polypeptide 5A, mitochondrial** | COX5A_YEAST | COX5A | 17130 | 9,82 | 61 | 6,1 | 4 | 24 |
| 2301 | **Diphthine methyltransferase** | DPH7_YEAST | RRT2 | 44078 | 5,2 | 62 | 5,2 | 6 | 12 |
| 4715 | **DNA topoisomerase 3** | TOP3_YEAST | TOP3 | 74962 | 8,71 | 33 | 3,9 | 32 | 14 |
| 7808 | **Double-strand break repair protein MRE11** | MRE11_YEAST | MRE11 | 78001 | 5,57 | 36 | 1,9 | 14 | 21 |
| 4307 | **Dual-specificity protein phosphatase SDP1** | SDP1_YEAST | SDP1 | 24041 | 7,74 | 31 | 5,9 | 7 | 35 |
| 4714 | **Elongation factor 1-alpha** | EF1A_YEAST | TEF1 | 50407 | 9,14 | 26 | 21 | 22 | 20 |

| | | | | | | | | | |
|---|---|---|---|---|---|---|---|---|---|
| 7805 | **Elongation factor 2** | EF2_YEAST | EFT1 | 93686 | 5,92 | 61 | 0,0057 | 29 | 24 |
| 6402 | **Enolase 1** | ENO1_YEAST | ENO1 | 46845 | 6,16 | 70 | 0,00085 | 39 | 64 |
| 6405 | **Enolase 2** | ENO2_YEAST | ENO2 | 46943 | 5,67 | 143 | 4,00E-11 | 54 | 81 |
| 6606 | **Eukaryotic translation initiation factor 3 subunit A** | EIF3A_YEAST | RPG1 | 110334 | 5,97 | 48 | 0,12 | 41 | 44 |
| 1007 | **Factor arrest protein 3** | FAR3_YEAST | FAR3 | 24074 | 7,71 | 36 | 19 | 5 | 22 |
| 2811 | **Folic acid synthesis protein FOL1** | FOL1_YEAST | FOL1 | 93745 | 6,02 | 87 | 1,50E+00 | 18 | 21 |
| 5306 | **Fructose-bisphosphate aldolase** | ALF_YEAST | FBA1 | 39886 | 5,51 | 63 | 0,0041 | 24 | 71 |
| 3706 | **Genetic interactor of prohibitins 3, mitochondrial** | GEP3_YEASZ | GEP3 | 64446 | 9,41 | 56 | 0,02 | 57 | 43 |
| 3009 | **Glucose-6-phosphate 1-epimerase** | YMY9_YEAST | YMR099C | 34048 | 5,75 | 41 | 5,90E+00 | 6 | 19 |
| 8206 | **Glucose-6-phosphate isomerase** | G6PI_YEAST | PGI1 | 61261 | 6 | 37 | 1,6 | 16 | 31 |
| 3015 | **Glutaredoxin-1** | GLRX1_YEAST | GRX1 | 12486 | 4,98 | 47 | 1,50E+01 | 3 | 48 |
| 1406 | **Glutathione S-transferase omega-like 1** | GTO1_YEAST | GTO1 | 41446 | 8,91 | 21 | 85 | 6 | 22 |
| 4602 | **Glutathione S-transferase omega-like 3** | GTO3_YEAST | GTO3 | 42667 | 7,17 | 26 | 19 | 16 | 17 |
| 9304 | **Glyceraldehyde-3-phosphate dehydrogenase 3** | G3P3_YEAST | TDH3 | 35838 | 6,46 | 59 | 0,0093 | 20 | 47 |
| 7802 | **Glycogen [starch] synthase isoform 2** | GYS2_YEAST | GYS2 | 80428 | 5,91 | 40 | 0,77 | 9 | 11 |
| 104 | **GTPase-interacting component 2** | GIC2_YEAST | GIC2 | 42833 | 9,47 | 48 | 1,40E+02 | 5 | 18 |
| 4706 | **GTP-binding protein YPT11** | YPT11_YEAST | YPT11 | 47492 | 6,33 | 32 | 4,5 | 28 | 15 |
| 1005 | **Guanylate kinase** | KGUA_YEAST | GUK1 | 20682 | 6,63 | 59 | 11 | 5 | 43 |
| 2201 | **Histone acetyltransferase GCN5** | GCN5_YEAST | GCN5 | 51208 | 6,23 | 52 | 0,56 | 11 | 25 |
| 7306 | **Homocysteine/cysteine synthase** | CYSD_YEAST | MET17 | 48700 | 5,97 | 50 | 0,089 | 30 | 56 |
| 4604 | **Ingression protein 1** | INN1_YEAST | INN1 | 46478 | 6,81 | 27 | 6,81 | 23 | 24 |
| 5101 | **Inorganic phosphate transporter PHO86** | PHO86_YEAST | PHO86 | 34918 | 9,62 | 24 | 33 | 20 | 28 |
| 5205 | **Iron-sulfur assembly protein 2** | ISA2_YEAST | ISA2 | 21096 | 7,63 | 25 | 23 | 9 | 51 |
| 3105 | **Isocitrate dehydrogenase [NAD] subunit 2, mitochondrial** | IDH2_YEAST | IDH2 | 39886 | 8,83 | 50 | 7,70E+00 | 4 | 14 |
| 8706 | **Kinesin-related protein SMY1** | SMY1_YEAST | SMY1 | 74096 | 6,48 | 30 | 8,3 | 18 | 27 |
| 5405 | **Kinetochore protein NUF2** | NUF2_YEAST | NUF2 | 53172 | 4,53 | 36 | 1,8 | 26 | 28 |
| 1101 | **Mediator of RNA polymerase II transcription subunit 4** | MED4_YEAST | MED4 | 32299 | 4,54 | 63 | 3,80E+02 | 2 | 8 |
| 6005 | **Meiotic sister-chromatid recombination protein 6, mitochondrial** | MSC6_YEAST | MSC6 | 80361 | 8,3 | 38 | 1,4 | 24 | |
| 5512 | **Mitochondrial carrier protein MTM1** | MTM1_YEAST | MTM1 | 41259 | 9,48 | 36 | 1,8 | 18 | 35 |
| 4704 | **Mitochondrial import inner membrane translocase subunit TIM54** | TIM54_YEAST | TIM54 | 54381 | 5,61 | 22 | 51 | 14 | 17 |
| 1502 | **Mitochondrial morphogenesis protein SLD7** | SLD7_YEAST | SLD7 | 29710 | 9,55 | 36 | 2 | 11 | 36 |

| | | | | | | | | | |
|---|---|---|---|---|---|---|---|---|---|
| 5913 | **Multiple RNA-binding domain-containing protein 1** | MRD1_YEAST | MRD1 | 101116 | 6,17 | 34 | 2,8 | 33 | 37 |
| 4603 | **NAD-dependent histone deacetylase SIR2** | SIR2_YEAST | SIR2 | 63860 | 8,7 | 23 | 36 | 17 | 8 |
| 5206 | **NADP-dependent 3-hydroxy acid dehydrogenase** | YM71_YEAST | YMR226C | 29198 | 6,36 | 22 | 49 | 13 | 25 |
| 2007 | **NADP-dependent alcohol dehydrogenase 6** | ADH6_YEAST | ADH6 | 40162 | 6,28 | 66 | 1,9 | 5 | 34 |
| 1210 | **NADP-dependent alcohol dehydrogenase 7** | ADH7_YEAST | ADH7 | 39893 | 6,91 | 100 | 1,50E-05 | 15 | 17 |
| 5103 | **Nicotinamide riboside kinase** | NRK1_YEAST | NRK1 | 27846 | 6,23 | 24 | 31 | 10 | 15 |
| 4503 | **Partitioning protein REP1** | REP1_YEAST | REP1 | 43610 | 2,2 | 36 | 2,2 | 19 | 17 |
| 2113 | **Phosphomannomutase** | PMM_YEAST | SEC53 | 29216 | 5,14 | 87 | 1,50E-05 | 13 | 54 |
| 3503 | **pH-response regulator protein palF/RIM8** | PALF_YEAST | RIM8 | 61169 | 9,24 | 29 | 1,00E+01 | 14 | 23 |
| 8505 | **Pre-mRNA-processing factor 19** | PRP19_YEAST | PRP19 | 57048 | 5,03 | 46 | 0,19 | 20 | 27 |
| 4506 | **Probable alanine aminotransferase, mitochondrial** | ALAM_YEAST | ALT1 | 66728 | 6,55 | 6,55 | 28 | 13 | 13 |
| 3201 | **Protein CBP3, mitochondrial** | CBP3_YEAST | CBP3 | 39173 | 9,36 | 34 | 3,20E+00 | 7 | 34 |
| 4611 | **Protein GAL3** | GAL3_YEAST | GAL3 | 58788 | 6,51 | 25 | 24 | 24 | 20 |
| 2602 | **Protein HBT1** | HBT1_YEAST | HBT1 | 113548 | 5,91 | 54 | 0,03 | 33 | 33 |
| 1504 | **Protein HRB1** | HRB1_YEAST | HRB1 | 52338 | 7,19 | 63 | 0,39 | 15 | 34 |
| 6902 | **Protein SOK1** | SOK1_YEAST | SOK1 | 101542 | 9,19 | 23 | 38 | 39 | 27 |
| 5203 | **Putative carboxymethylenebutenolidase** | DLHH_YEAST | YDL086W | 31124 | 5,91 | 24 | 24 | 9 | 45 |
| 4716 | **Putative protease AXL1** | AXL1_YEAST | AXL1 | 139172 | 8,56 | 37 | 1,5 | 40 | 14 |
| 1002 | **Putative uncharacterized protein YKR012C** | YKZ2_YEAST | YKR12C | 14663 | 8,84 | 42 | 0,51 | 3 | 35 |
| 6501 | **Pyruvate decarboxylase isozyme 1** | PDC1_YEAST | PDC1 | 61689 | 5,8 | 96 | 2,00E-06 | 51 | 63 |
| 6505 | **Pyruvate dehydrogenase complex protein X component, mitochondrial** | ODPX_YEAST | PDX1 | 45450 | 5,55 | 53 | 0,042 | 21 | 43 |
| 1405 | **Rab GDP-dissociation inhibitor** | GDI1_YEAST | GDI1 | 51459 | 5,66 | 66 | 22 | 7 | 14 |
| 5712 | **RNA cytidine acetyltransferase** | NAT10_YEAST | KRE33 | 119621 | 7,63 | 32 | 5,6 | 33 | 30 |
| 3401 | **Serine/threonine-protein phosphatase 2B catalytic subunit A2** | PP2B2_YEAST | CMP2 | 69055 | 5,92 | 31 | 6,10E+00 | 10 | 10 |
| 3606 | **Sigma-like sequence protein 1, mitochondrial** | SLS1_YEAST | SLS1 | 73382 | 9,24 | 25 | 2,40E+01 | 11 | 10 |
| 2004 | **Single-stranded nucleic acid-binding protein** | SSBP1_YEAST | SSBP1 | 33026 | 5,48 | 30 | 8,1 | 9 | 40 |
| 6901 | **Succinate dehydrogenase [ubiquinone] flavoprotein subunit, mitochondrial** | SDHA_YEAST | SDH1 | 70823 | 7,14 | 30 | 8,3 | 26 | 29 |
| 5305 | **Succinate/fumarate mitochondrial transporter** | SFC1_YEAST | SFC3 | 35492 | 9,78 | 45 | 0,26 | 16 | 31 |
| 6004 | **Trafficking protein particle complex II-specific subunit 130** | TR130_YEAST | TR130 | 129035 | 5,73 | 30 | 9,5 | 37 | 20 |
| 5202 | **Transcription initiation factor TFIID subunit 4** | TAF4_YEAST | TAF4 | 42369 | 9,67 | 25 | 24 | 22 | 45 |
| 5004 | **Transcriptional regulator NRG1** | NRG1_YEAST | NRG1 | 27132 | 8,99 | 24 | 28 | 14 | 20 |

| | | | | | | | | | |
|---|---|---|---|---|---|---|---|---|---|
| 5501 | **Translation machinery-associated protein 64** | TMA64_YEAST | TMA64 | 64300 | 9,02 | 27 | 9,02 | 26 | 34 |
| 4001 | **Tricarboxylate transport protein** | TXTP_YEAST | CTP1 | 32381 | 9,6 | 38 | 1,1 | 10 | 22 |
| 4409 | **tRNA (guanine(10)-N2)-methyltransferase** | TRM11_YEAST | TRM11 | 50215 | 7,64 | 41 | 0,59 | 33 | 26 |
| 3104 | **tRNA wybutosine-synthesizing protein 3** | TYW3_YEAST | TYW3 | 31072 | 8,15 | 62 | 5,30E-03 | 14 | 44 |
| 5801 | **tRNA-specific adenosine deaminase subunit TAD2** | TAD2_YEAST | TAD2 | 28640 | 6,71 | 43 | 0,43 | 12 | 14 |
| 5301 | **Tyrosine--tRNA ligase, mitochondrial** | SYYM_YEAST | MSY1 | 55659 | 9,22 | 26 | 21 | 12 | 26 |
| 4103 | **U3 small nucleolar ribonucleoprotein protein LCP5** | LCP5_YEAST | LCP5 | 40826 | 6,45 | 45 | 0,26 | 16 | 36 |
| 4703 | **U3 small nucleolar RNA-associated protein 6** | UTP6_YEAST | UTP6 | 46943 | 5,67 | 36 | 1,9 | 32 | 45 |
| 5003 | **Ubiquitin-conjugating enzyme E2 13** | UBC13_YEAST | UBC13 | 17515 | 5,31 | 33 | 4 | 14 | 28 |
| 5104 | **Uncharacterized isomerase YHR210C** | YH10_YEAST | YHR210C | 38141 | 5,61 | 28 | 13 | 14 | 9 |
| 2605 | **V-type proton ATPase subunit B** | VATB_YEAST | VMA2 | 57770 | 4,95 | 110 | 7,90E-08 | 21 | 45 |

## Table 4. List of unique proteins enriched and their corresponding peptides obtained from iTRAQ proteomics analysis.

| Protein_Name | Protein_Annotation | Protein_Probability | Protein length (AA) | libra-114.0ratio | libra-115.0ratio | libra-116.0ratio | libra-117.0ratio |
|---|---|---|---|---|---|---|---|
| sp\|P40989\|FKS2_YEAST | **1,3-beta-glucan synthase component GSC2** | 1 | 1895 | 0,17 | 0,18 | 0,33 | 0,31 |
| sp\|P22146\|GAS1_YEAST | **1,3-beta-glucanosyltransferase GAS1** | 1 | 559 | 0,29 | 0,29 | 0,2 | 0,21 |
| sp\|P07264\|LEUC_YEAST | **3-isopropylmalate dehydratase** | 1 | 779 | 0,26 | 0,28 | 0,22 | 0,23 |
| sp\|Q12452\|ERG27_YEAST | **3-keto-steroid reductase** | 0,99 | 347 | 0,18 | 0,19 | 0,31 | 0,31 |
| sp\|P48589\|RS12_YEAST | **40S ribosomal protein S12** | 1 | 143 | 0,25 | 0,3 | 0,22 | 0,22 |
| sp\|P0C0V8\|RS21A_YEAST | **40S ribosomal protein S21-A** | 1 | 87 | 0,24 | 0,37 | 0,19 | 0,19 |
| sp\|Q3E754\|RS21B_YEAST | **40S ribosomal protein S21-B** | 1 | 87 | 0,25 | 0,33 | 0,21 | 0,21 |
| sp\|P0C0X0\|RS28B_YEAST | **40S ribosomal protein S28-B** | 1 | 67 | 0,27 | 0,3 | 0,21 | 0,22 |
| sp\|P50861\|RIB4_YEAST | **6,7-dimethyl-8-ribityllumazine synthase** | 1 | 169 | 0,12 | 0,18 | 0,18 | 0,35 |
| sp\|P05318\|RLA1_YEAST | **60S acidic ribosomal protein P1-alpha** | 1 | 106 | 0,19 | 0,19 | 0,18 | 0,38 |
| sp\|P10622\|RLA3_YEAST | **60S acidic ribosomal protein P1-beta** | 0,99 | 106 | 0,25 | 0,29 | 0,23 | 0,23 |
| sp\|P05748\|RL15A_YEAST | **60S ribosomal protein L15-A** | 1 | 204 | 0,27 | 0,28 | 0,21 | 0,23 |
| sp\|P05749\|RL22A_YEAST | **60S ribosomal protein L22-A** | 1 | 121 | 0,27 | 0,27 | 0,23 | 0,23 |
| sp\|P0C2H8\|RL31A_YEAST | **60S ribosomal protein L31-A** | 1 | 113 | 0,28 | 0,28 | 0,21 | 0,22 |
| sp\|P0CX25\|RL43A_YEAST | **60S ribosomal protein L43-A** | 1 | 92 | 0,29 | 0,28 | 0,22 | 0,21 |
| sp\|P16474\|GRP78_YEAST | **78 kDa glucose-regulated protein homolog** | 1 | 682 | 0,18 | 0,18 | 0,32 | 0,3 |
| sp\|Q05911\|PUR8_YEAST | **Adenylosuccinate lyase** | 1 | 482 | 0,32 | 0,28 | 0,2 | 0,19 |
| sp\|A6ZRM0\|PURA_YEAS7 | **Adenylosuccinate synthetase** | 1 | 433 | 0,29 | 0,28 | 0,2 | 0,21 |
| sp\|Q00764\|TPS1_YEAST | **Alpha,alpha-trehalose-phosphate synthase [UDP-forming] 56 kDa subunit** | 1 | 495 | 0,14 | 0,14 | 0,29 | 0,37 |
| sp\|P00812\|ARGI_YEAST | **Arginase** | 1 | 333 | 0,2 | 0,2 | 0,31 | 0,29 |
| sp\|P53379\|MKC7_YEAST | **Aspartic proteinase MKC7** | 1 | 596 | 0,27 | 0,25 | 0,23 | 0,25 |
| sp\|P02829\|HSP82_YEAST | **ATP-dependent molecular chaperone HSP82** | 1 | 709 | 0,17 | 0,15 | 0,35 | 0,31 |
| sp\|A6ZUA1\|DBP3_YEAS7 | **ATP-dependent RNA helicase DBP3** | 1 | 523 | 0,17 | 0,27 | 0,27 | 0,27 |
| sp\|A6ZNQ1\|DBP5_YEAS7 | **ATP-dependent RNA helicase DBP5** | 1 | 482 | 0,19 | 0,19 | 0,29 | 0,29 |
| sp\|A6ZXG9\|DHH1_YEAS7 | **ATP-dependent RNA helicase DHH1** | 1 | 506 | 0,15 | 0,16 | 0,3 | 0,28 |
| sp\|P38009\|PUR92_YEAST | **Bifunctional purine biosynthesis protein ADE17** | 1 | 592 | 0,32 | 0,28 | 0,16 | 0,19 |
| sp\|P38891\|BCA1_YEAST | **Branched-chain-amino-acid aminotransferase, mitochondrial** | 1 | 393 | 0,28 | 0,27 | 0,22 | 0,23 |

| | | | | | | | |
|---|---|---|---|---|---|---|---|
| sp\|A6ZPB3\|CAF20_YEAS7 | **Cap-associated protein CAF20** | 0,987 | 161 | 0,25 | 0,29 | 0,23 | 0,23 |
| sp\|A6ZL22\|ECM33_YEAS7 | **Cell wall protein ECM33** | 1 | 429 | 0,26 | 0,29 | 0,23 | 0,21 |
| sp\|P09232\|PRTB_YEAST | **Cerevisin** | 1 | 635 | 0,19 | 0,2 | 0,31 | 0,3 |
| sp\|P31373\|CYS3_YEAST | **Cystathionine gamma-lyase** | 1 | 394 | 0,18 | 0,2 | 0,28 | 0,32 |
| sp\|A6ZRK4\|BLH1_YEAS7 | **Cysteine proteinase 1, mitochondrial** | 1 | 483 | 0,19 | 0,2 | 0,26 | 0,33 |
| sp\|P25340\|ERG4_YEAST | **Delta(24(24(1)))-sterol reductase** | 1 | 473 | 0,2 | 0,22 | 0,25 | 0,31 |
| sp\|P39976\|DLD3_YEAST | **D-lactate dehydrogenase [cytochrome] 3** | 1 | 496 | 0,2 | 0,21 | 0,28 | 0,29 |
| sp\|P32471\|EF1B_YEAST | **Elongation factor 1-beta** | 1 | 206 | 0,25 | 0,31 | 0,21 | 0,22 |
| sp\|P23301\|IF5A1_YEAST | **Eukaryotic translation initiation factor 5A-1** | 1 | 157 | 0,23 | 0,28 | 0,24 | 0,24 |
| sp\|Q04636\|POB3_YEAST | **FACT complex subunit POB3** | 1 | 552 | 0,2 | 0,23 | 0,28 | 0,29 |
| tr\|C7GP14\|C7GP14_YEAS2 | **Fba1p** | 1 | 359 | 0,27 | 0,33 | 0,18 | 0,22 |
| sp\|P39676\|FHP_YEAST | **Flavohemoprotein** | 1 | 399 | 0,26 | 0,29 | 0,22 | 0,23 |
| sp\|P17709\|HXKG_YEAST | **Glucokinase-1** | 1 | 500 | 0,14 | 0,14 | 0,34 | 0,33 |
| sp\|P14742\|GFA1_YEAST | **Glucosamine--fructose-6-phosphate aminotransferase [isomerizing]** | 1 | 717 | 0,2 | 0,22 | 0,29 | 0,28 |
| sp\|P11412\|G6PD_YEAST | **Glucose-6-phosphate 1-dehydrogenase** | 1 | 505 | 0,19 | 0,19 | 0,29 | 0,31 |
| sp\|Q12680\|GLT1_YEAST | **Glutamate synthase [NADH]** | 1 | 2145 | 0,28 | 0,3 | 0,2 | 0,2 |
| sp\|P32288\|GLNA_YEAST | **Glutamine synthetase** | 1 | 370 | 0,34 | 0,28 | 0,19 | 0,18 |
| sp\|P00360\|G3P1_YEAST | **Glyceraldehyde-3-phosphate dehydrogenase 1** | 1 | 332 | 0,19 | 0,18 | 0,34 | 0,29 |
| sp\|Q00055\|GPD1_YEAST | **Glycerol-3-phosphate dehydrogenase [NAD(+)] 1** | 1 | 391 | 0,15 | 0,21 | 0,32 | 0,29 |
| sp\|P27809\|KRE2_YEAST | **Glycolipid 2-alpha-mannosyltransferase** | 1 | 442 | 0,28 | 0,27 | 0,22 | 0,23 |
| sp\|P15992\|HSP26_YEAST | **Heat shock protein 26** | 1 | 214 | 0,15 | 0,14 | 0,36 | 0,3 |
| sp\|P33416\|HSP78_YEAST | **Heat shock protein 78, mitochondrial** | 1 | 811 | 0,19 | 0,2 | 0,24 | 0,35 |
| sp\|P10591\|HSP71_YEAST | **Heat shock protein SSA1** | 1 | 642 | 0,16 | 0,16 | 0,34 | 0,3 |
| sp\|P15705\|STI1_YEAST | **Heat shock protein STI1** | 1 | 589 | 0,2 | 0,22 | 0,28 | 0,28 |
| sp\|P40495\|LYS12_YEAST | **Homoisocitrate dehydrogenase, mitochondrial** | 1 | 371 | 0,16 | 0,19 | 0,24 | 0,36 |
| sp\|P25297\|PHO84_YEAST | **Inorganic phosphate transporter PHO84** | 0,99 | 587 | 0,25 | 0,32 | 0,19 | 0,24 |
| sp\|P06168\|ILV5_YEAST | **Ketol-acid reductoisomerase, mitochondrial** | 1 | 395 | 0,28 | 0,27 | 0,22 | 0,23 |
| sp\|A7A261\|LSB3_YEAS7 | **LAS seventeen-binding protein 3** | 0,999 | 459 | 0,18 | 0,24 | 0,3 | 0,28 |
| sp\|P34227\|PRX1_YEAST | **Mitochondrial peroxiredoxin PRX1** | 1 | 261 | 0,18 | 0,18 | 0,33 | 0,3 |
| sp\|Q07551\|KAR_YEAST | **NADPH-dependent alpha-keto amide reductase** | 1 | 312 | 0,19 | 0,2 | 0,3 | 0,3 |
| sp\|P07262\|DHE4_YEAST | **NADP-specific glutamate dehydrogenase 1** | 1 | 454 | 0,28 | 0,28 | 0,22 | 0,22 |

| | | | | | | | |
|---|---|---|---|---|---|---|---|
| sp\|P33327\|DHE2_YEAST | **NAD-specific glutamate dehydrogenase** | 1 | 1092 | 0,23 | 0,21 | 0,24 | 0,32 |
| sp\|P35729\|NU120_YEAST | **Nucleoporin NUP120** | 0,997 | 1037 | 0,22 | 0,21 | 0,22 | 0,34 |
| sp\|P35176\|CYPD_YEAST | **Peptidyl-prolyl cis-trans isomerase D** | 1 | 225 | 0,24 | 0,3 | 0,22 | 0,22 |
| sp\|P34760\|TSA1_YEAST | **Peroxiredoxin TSA1** | 1 | 196 | 0,18 | 0,19 | 0,31 | 0,3 |
| sp\|P27616\|PUR7_YEAST | **Phosphoribosylaminoimidazole-succinocarboxamide synthase** | 1 | 306 | 0,31 | 0,29 | 0,19 | 0,2 |
| sp\|P40088\|FTR1_YEAST | **Plasma membrane iron permease** | 1 | 404 | 0,2 | 0,21 | 0,26 | 0,31 |
| sp\|P46367\|ALDH4_YEAST | **Potassium-activated aldehyde dehydrogenase, mitochondrial** | 1 | 519 | 0,16 | 0,2 | 0,31 | 0,31 |
| sp\|P53900\|PFD4_YEAST | **Prefoldin subunit 4** | 0,997 | 129 | 0,25 | 0,28 | 0,23 | 0,23 |
| sp\|P46985\|MNN11_YEAST | **Probable alpha-1,6-mannosyltransferase MNN11** | 1 | 422 | 0,19 | 0,18 | 0,31 | 0,29 |
| sp\|P01095\|IPB2_YEAST | **Protease B inhibitors 2 and 1** | 1 | 75 | 0,2 | 0,21 | 0,3 | 0,3 |
| sp\|P23724\|PSB1_YEAST | **Proteasome component C5** | 1 | 241 | 0,18 | 0,2 | 0,27 | 0,27 |
| sp\|Q06631\|BFR2_YEAST | **Protein BFR2** | 1 | 534 | 0,25 | 0,27 | 0,25 | 0,23 |
| sp\|P06106\|MET17_YEAST | **Protein MET17** | 1 | 444 | 0,16 | 0,15 | 0,33 | 0,32 |
| sp\|P24276\|SSD1_YEAST | **Protein SSD1** | 1 | 1250 | 0,17 | 0,21 | 0,3 | 0,3 |
| sp\|Q12335\|PST2_YEAST | **Protoplast secreted protein 2** | 1 | 198 | 0,19 | 0,21 | 0,3 | 0,28 |
| sp\|Q12044\|RCN2_YEAST | **Regulator of calcineurin 2** | 0,99 | 265 | 0,17 | 0,15 | 0,37 | 0,32 |
| tr\|G2WIM3\|G2WIM3_YEAS K | **Ribosomal protein L15** | 1 | 204 | 0,27 | 0,27 | 0,23 | 0,23 |
| sp\|P25375\|PRTD_YEAST | **Saccharolysin** | 1 | 712 | 0,16 | 0,25 | 0,28 | 0,28 |
| sp\|P07267\|CARP_YEAST | **Saccharopepsin** | 1 | 405 | 0,17 | 0,18 | 0,32 | 0,31 |
| sp\|P19358\|METK2_YEAST | **S-adenosylmethionine synthase 2** | 1 | 384 | 0,16 | 0,23 | 0,29 | 0,28 |
| sp\|P37291\|GLYC_YEAST | **Serine hydroxymethyltransferase, cytosolic** | 1 | 469 | 0,34 | 0,29 | 0,19 | 0,18 |
| sp\|P32476\|ERG1_YEAST | **Squalene monooxygenase** | 1 | 496 | 0,29 | 0,27 | 0,21 | 0,24 |
| sp\|P08536\|MET3_YEAST | **Sulfate adenylyltransferase** | 1 | 511 | 0,1 | 0,1 | 0,36 | 0,38 |
| sp\|P47169\|MET5_YEAST | **Sulfite reductase [NADPH] subunit beta** | 1 | 1442 | 0,18 | 0,2 | 0,29 | 0,31 |
| sp\|P22803\|TRX2_YEAST | **Thioredoxin-2** | 1 | 104 | 0,18 | 0,24 | 0,29 | 0,28 |
| sp\|P07273\|TFS2_YEAST | **Transcription elongation factor S-II** | 0,99 | 309 | 0,26 | 0,26 | 0,22 | 0,26 |
| sp\|P05759\|RS27A_YEAST | **Ubiquitin-40S ribosomal protein S31** | 1 | 152 | 0,31 | 0,28 | 0,21 | 0,2 |
| sp\|P0CH08\|RL401_YEAST | **Ubiquitin-60S ribosomal protein L40** | 1 | 128 | 0,3 | 0,29 | 0,22 | 0,19 |
| sp\|P34223\|UBX1_YEAST | **UBX domain-containing protein 1** | 1 | 423 | 0,2 | 0,22 | 0,29 | 0,29 |
| sp\|Q05016\|YM71_YEAST | **Uncharacterized oxidoreductase YMR226C** | 1 | 267 | 0,2 | 0,24 | 0,28 | 0,27 |

| | | | | | | | |
|---|---|---|---|---|---|---|---|
| sp\|P35719\|MRP8_YEAST | **Uncharacterized protein MRP8** | 1 | 219 | 0,16 | 0,22 | 0,29 | 0,3 |
| sp\|P53912\|YNN4_YEAST | **Uncharacterized protein YNL134C** | 1 | 376 | 0,15 | 0,18 | 0,27 | 0,36 |
| sp\|P18562\|UPP_YEAST | **Uracil phosphoribosyltransferase** | 1 | 216 | 0,28 | 0,27 | 0,23 | 0,22 |
| sp\|P14904\|AMPL_YEAST | **Vacuolar aminopeptidase 1** | 1 | 514 | 0,2 | 0,19 | 0,32 | 0,29 |

**Table 5. KEGG pathway assignation and description of differentially abundant proteins in *Saccharomyces cerevisiae*.**

With "a" are represented the proteins found with 2D-gel, with "b" are represented the proteins found with iTRAQ.

| | Proteins | pathway code | pathway name | description |
|---|---|---|---|---|
| **a** | 1-(5-phosphoribosyl)-5-[(5-phosphoribosylamino)methylideneamino] imidazole-4-carboxamide isomerase | sce00340, sce01100, sce01110, sce01230 | Histidine metabolism, metabolic pathway, biosynthesis of secondary metabolites, biosynthesis of amino acids. | Catalyzes the isomerization of the aminoaldose moiety of ProFAR to the aminoketose of PRFAR. |
| **b** | 1,3-beta-glucan synthase component GSC2 | sce00500, sce04011 | Starch and sucrose metabolism, map kinase | Alternate catalytic subunit of the 1,3-beta-glucan synthase (GS). Synthesizes 1,3-beta-glucan, a major structural component of the yeast cell wall. Required for spore wall assembly. Negative regulation of activity by SMK1 is important for spore wall deposition. Activity is positively regulated by RHO1. |
| **b** | 1,3-beta-glucanosyltransferase GAS1 | | | Involved in cell wall biosynthesis and morphogenesis. |
| **a** | 25S rRNA (uridine(2843)-N(3))-methyltransferase | | | S-adenosyl-L-methionine-dependent methyltransferase that specifically methylates the $N_3$ position of uridine in 25S rRNA. |
| **a** | 37S ribosomal protein S18, mitochondrial | sce03010 | ribosome | Component of the mitochondrial ribosome (mitoribosome), a dedicated translation machinery responsible for the synthesis of mitochondrial genome-encoded proteins, including at least some of the essential transmembrane subunits of the mitochondrial respiratory chain. |
| **a** | 37S ribosomal protein S23, mitochondrial | sce03011, sce03029 | Ribosome Mitochondrial biogenesis | Component of the mitochondrial ribosome (mitoribosome), a dedicated translation machinery responsible for the synthesis of mitochondrial genome-encoded proteins, including at least some of the essential transmembrane subunits of the mitochondrial respiratory chain. |
| **b** | 3-isopropylmalate dehydratase | sce00290, sce01100, sce01110, sce01230 | Valine, leucine and isoleucine biosynthesis, metabolic pathway, biosynthesis of secondary metabolites, biosynthesis of amino acids. | Catalyzes the isomerization between 2-isopropylmalate and 3-isopropylmalate, via the formation of 2-isopropylmaleate. |
| **b** | 3-keto-steroid reductase | sce00100, sce01100, sce01130 | steroid biosynthesis, metabolic pathway, biosynthesis of antibiotics | Responsible for the reduction of the keto group on the C-3 of sterols. Also facilitates the association of ERG7 with lipid particles preventing its digestion in the endoplasmic reticulum and the lipid particles. |
| **a** | 40S ribosomal protein S0-B | sce03010 | ribosome | Required for the assembly and/or stability of the 40S ribosomal subunit. Required for the processing of the 20S rRNA-precursor to mature 18S rRNA in a late step of the maturation of 40S ribosomal subunits. |
| **b** | 40S ribosomal protein S12 | sce03010 | ribosome | Component of the ribosome, a large ribonucleoprotein complex responsible for the synthesis of proteins in the cell. |
| **a** | 40S ribosomal protein S1-B | sce03010 | ribosome | structural constituent of ribosome, traslation |
| **b** | 40S ribosomal protein S21-A | sce03010 | ribosome | Component of the ribosome, a large ribonucleoprotein complex responsible for the synthesis of proteins in the cell. |
| **b** | 40S ribosomal protein S21-B | sce03010 | ribosome | Component of the ribosome, a large ribonucleoprotein complex responsible for the synthesis of proteins in the cell. |

| | | | | |
|---|---|---|---|---|
| **b** | 40S ribosomal protein S28-B | sce03010 | ribosome | Component of the ribosome, a large ribonucleoprotein complex responsible for the synthesis of proteins in the cell. |
| **b** | 6,7-dimethyl-8-ribityllumazine synthase | sce00740, sce01100, sce01110 | metabolism secondary, metabolic pathway, biosynthesis of secondary metabolites | Catalyzes the formation of 6,7-dimethyl-8-ribityllumazine by condensation of 5-amino-6-(D-ribitylamino) uracil with 3,4-dihydroxy-2-butanone 4-phosphate. |
| **a** | 60S acidic ribosomal protein P0 | sce03010 | ribosome | Component of the ribosome, a large ribonucleoprotein complex responsible for the synthesis of proteins in the cell. |
| **b** | 60S acidic ribosomal protein P1-alpha | sce03010 | ribosome | Component of the ribosome, a large ribonucleoprotein complex responsible for the synthesis of proteins in the cell. |
| **b** | 60S acidic ribosomal protein P1-beta | sce03013 | RNA transport | Component of the ribosome, a large ribonucleoprotein complex responsible for the synthesis of proteins in the cell. |
| **b** | 60S ribosomal protein L15-A | sce03013 | RNA transport | Component of the ribosome, a large ribonucleoprotein complex responsible for the synthesis of proteins in the cell. |
| **a** | 60S ribosomal protein L20-A | sce03010 | ribosome | Component of the ribosome, a large ribonucleoprotein complex responsible for the synthesis of proteins in the cell. |
| **a** | 60S ribosomal protein L20-B | sce03010 | ribosome | Component of the ribosome, a large ribonucleoprotein complex responsible for the synthesis of proteins in the cell. |
| **b** | 60S ribosomal protein L22-A | sce03013 | RNA transport | Component of the ribosome, a large ribonucleoprotein complex responsible for the synthesis of proteins in the cell. |
| **b** | 60S ribosomal protein L31-A | sce03013 | RNA transport | Component of the ribosome, a large ribonucleoprotein complex responsible for the synthesis of proteins in the cell. |
| **b** | 60S ribosomal protein L43-A | sce03013 | RNA transport | Component of the ribosome, a large ribonucleoprotein complex responsible for the synthesis of proteins in the cell. |
| **b** | 78 kDa glucose-regulated protein homolog | sce03060, sce04141 | protein export, protein processing in RE | Probably plays a role in facilitating the assembly of multimeric protein complexes inside the ER. Is required for secretory polypeptide translocation. |
| **a** | Acyl-CoA-binding protein | | | Binds medium- and long-chain acyl-CoA esters with very high affinity and may function as an intracellular carrier of acyl-CoA esters. |
| **b** | Adenylosuccinate lyase | sce00230, sce00250, sce01100, sce01110, sce01130 | Purine metabolism, ala asp glu metabolism, metabolism secondary, biosynthesis of secondary metabolites, biosynthesis of antibiotics | This protein is involved in the subpathway that synthesizes AMP from IMP. |
| **b** | Adenylosuccinate synthetase | sce00230, sce00250, sce01100 | Purine metabolism, ala asp glu metabolism, metabolism secondary, biosynthesis of secondary metabolites, biosynthesis of antibiotics | Plays an important role in the de novo pathway and in the salvage pathway of purine nucleotide biosynthesis. Catalyzes the first committed step in the biosynthesis of AMP from IMP. |
| **b** | Alpha,alpha-trehalose-phosphate synthase [UDP-forming] 56 kDa subunit | sce00500, sce01100 | Starch and sucrose metabolism, biosynthesis of secondary metabolites | Synthase catalytic subunit of the trehalose synthase complex that catalyzes the production of trehalose from glucose-6-phosphate and UDP-glucose in a two steps process. |
| **b** | Arginase | sce00220, sce00330, sce01100, sce01110, sce01130 | arginine biosynthesis, arginine and proline biosynthesis, metabolic pathway,secondary metabolites, biosynthesis of antibiotics | This protein is involved in the subpathway that synthesizes L-ornithine and urea from L-arginine. |
| **a** | Asparagine--tRNA ligase, cytoplasmic | sce00970 | Aminoacyl-tRNA biosynthesis | Asparagine-tRNA ligase activity and ATP binding |
| **b** | Aspartic proteinase MKC7 | sce04011 | mapk kinase | Cleaves proteins C-terminally to the most C-terminal basic residue. |

| | | | | |
|---|---|---|---|---|
| **a** | ATPase expression protein 2, mitochondrial | sce03029 | mitochondrial biogenesis | Required for translation of the mitochondrial OLI1 transcript coding for the mitochondrial ATP synthase subunit 9. |
| **a** | ATPase synthesis protein 25, mitochondrial | | | mRNA stabilization factor specific for the OLI1 mRNA. Also involved in OLI1 ring formation. |
| **aa** | ATP-dependent 6-phosphofructokinase subunit beta | sce00010, sce00030, sce00051, sce00680, sce01100, sce01110, sce01130, sce01200, sce01230, sce03018 | Glycolysis, pentose phosphate pathway, fructose and mannose metabolism, methane metabolism, metabolic pathway, biosynthesis of secondary metabolites biosynthesis of antibiotics, carbon metabolism, biosynthesis of amino acid, RNA degradation | Catalyzes the phosphorylation of D-fructose 6-phosphate to fructose 1,6-bisphosphate by ATP, the first committing step of glycolysis. |
| a<br>b | **ATP-dependent molecular chaperone HSC82** | **sce04141** | **Protein processing in ER** | **Molecular chaperone that promotes the maturation, structural maintenance and proper regulation of specific target proteins involved in cell cycle control and signal transduction. Undergoes a functional cycle that is linked to its ATPase activity. Interacts dynamically with various co-chaperones that modulate its substrate recognition, ATPase cycle and chaperone function.** |
| **b** | ATP-dependent RNA helicase DBP3 | | | ATP-dependent RNA helicase required for 60S ribosomal subunit synthesis. |
| **b** | ATP-dependent RNA helicase DBP5 | | | ATP-dependent RNA helicase associated with the nuclear pore complex and essential for mRNA export from the nucleus. |
| **b** | ATP-dependent RNA helicase DHH1 | sce03018 | RNA degradation | ATP-dependent RNA helicase involved in mRNA turnover, and more specifically in mRNA decapping by activating the decapping enzyme DCP1. |
| **b** | Bifunctional purine biosynthesis protein ADE17 | sce00230, sce00670, sce01110, sce01130 | purine metabolism, One carbon pool by folate, secondary metabolites, biosynthesis of antibiotics | This protein is involved in the subpathway that synthesizes 5-formamido-1-(5-phospho-D-ribosyl)imidazole-4-carboxamide from 5-amino-1-(5-phospho-D-ribosyl)imidazole-4-carboxamide (10-formyl THF route). |
| **b** | Branched-chain-amino-acid aminotransferase, mitochondrial | sce00270, sce00280, sce00290, sce00770, sce01100, sce01110, sce01130, sce01210, sce01230 | Cysteine and methionine metabolism, Valine leucina isoleucine degradation, Valine leucine isoleucine biosynthesis, Pantothenate and CoA biosynthesis, metabolic pathway,secondary metabolites, biosynthesis of antibiotics | Involved in the biosynthesis of the branched chain amino acids leucine, isoleucine, and valine. |
| **b** | Cap-associated protein CAF20 | | | Acts as an inhibitor of cap-dependent translation. |
| **a** | Cargo-transport protein YPP1 | sce04131 | endocytosis | Involved in endocytosis. |
| **a** | Carnitine O-acetyltransferase, mitochondrial | sce04146 | peroxisome | Carnitine acetylase is specific for short chain fatty acids. It seems to affect the flux through the pyruvate dehydrogenase complex. It may be involved as well in the transport of acetyl-CoA into mitochondria. |
| **a** | Cell division control protein 48 | sce04141 | Protein processing in ER | Involved in spindle disassembly, degradation of ubiquitinated proteins and protein export from the endoplasmic reticulum to the cytoplasm. |
| **b** | Cell wall protein ECM33 | | | Required for proper cell wall integrity and for the correct assembly of the mannoprotein outer layer of the cell wall. Important for apical bud growth (By similarity). |

| | | | | |
|---|---|---|---|---|
| **b** | Cerevisin | sce04138 | autophagy | Vacuolar proteinase B involved in protein degradation in the vacuole. Required for meiosis and spore formation, and for optimal survival in stationary phase. |
| **a** | Cystathionine beta-synthase | sce00260, sce00270, sce01100, sce01130, sce01230, | Glycine sereine and threonine metabolism, Cysteine and methionine metabolism, metabolic pathway, biosynthesis of amino acid | This protein is involved in the subpathway that synthesizes L-cysteine from L-homocysteine and L-serine. |
| **b** | Cystathionine gamma-lyase | sce00260, sce00270, sce00450, sce01100, sce01130, sce01230 | Glycine sereine and threonine metabolism, Cysteine and methionine metabolism, selenocompound metabolism, metabolic pathway, biosynthesis of antibiotics, biosynthesis of amino acid | This protein is involved in the subpathway that synthesizes L-cysteine from L-homocysteine and L-serine. |
| **b** | Cysteine proteinase 1, mitochondrial | | | The normal physiological role of the enzyme is unknown, but it is not essential for the viability of yeast cells. |
| **a** | Cysteine--tRNA ligase | sce00970 | Aminoacyl-tRNA biosynthesis | ATP binding and cysteine-tRNA ligase activity |
| **a** | Cytochrome c oxidase assembly factor 1 | | | Required for efficient assembly of cytochrome c oxidase in the mitochondrial inner membrane. |
| **a** | Cytochrome c oxidase polypeptide 5A, mitochondrial | sce00190, sce01100 | Oxidative phosphorylation, Metabolic pathways | cytochrome-c oxidase activity |
| **b** | Delta(24(24(1)))-sterol reductase | sce00100, sce01100, sce01130 | steroid biosynthesis, metabolic pathway, biosynthesis of antibiotics | This protein is involved in the subpathway that synthesizes ergosterol from zymosterol. |
| **a** | Diphthine methyltransferase | | | Catalyzes the demethylation of diphthine methyl ester to form diphthine, an intermediate in diphthamide biosynthesis, a post-translational modification of histidine which occurs in translation elongation factor 2 (EFT1 and EFT2). |
| **b** | D-lactate dehydrogenase [cytochrome] 3 | sce00620 | Pyruvate metabolism | Catalyzes the reversible oxidation of (R)-2-hydroxyglutarate to 2-oxoglutarate coupled to reduction of pyruvate to (R)-lactate. Can also use oxaloacetate as electron acceptor instead of pyruvate producing (R)-malate. |
| **a** | DNA topoisomerase 3 | sce03440 | Homologous recombination | Releases the supercoiling and torsional tension of DNA introduced during the DNA replication and transcription by transiently cleaving and rejoining one strand of the DNA duplex. |
| **a** | Double-strand break repair protein MRE11 | sce03440, sce03450 | homolugus recombination | Involved in DNA double-strand break repair (DSBR). Possesses single-strand endonuclease activity and double-strand-specific 3'-5' exonuclease activity. |
| **a** | Dual-specificity protein phosphatase SDP1 | | | Mediates dephosphorylation of MAPK substrates such as SLT2, acquiring enhanced catalytic activity under oxidative conditions. |
| **a** | Elongation factor 1-alpha | sce03013 | RNA transport | GTP-binding component of the eukaryotic elongation factor 1 complex (eEF1). In its active GTP-bound form, binds to and delivers aminoacyl-tRNA to the A-site of ribosomes during protein biosynthesis. |
| **b** | Elongation factor 1-beta | | | Catalytic subunit of the guanine nucleotide exchange factor (GEF) (eEF1B subcomplex) of the eukaryotic elongation factor 1 complex (eEF1). |
| **a** | Elongation factor 2 | sce03012 | trascription factor | Catalyzes the GTP-dependent ribosomal translocation step during translation elongation. |
| **a** | Enolase 1 | sce00010, sce00680, sce01100, sce01110, | Glycolysis, methane metabolism, metabolic pathway, biosynthesis of secondary metabolites, biosynthesis of antibiotics, | This protein is involved in the subpathway that synthesizes pyruvate from D-glyceraldehyde 3-phosphate. |

| | | | | |
|---|---|---|---|---|
| | | sce01130, sce01200, sce01230, sce03018 | carbon metabolism, biosynthesis of amino acid, RNA degradation | |
| **a** | Enolase 2 | sce00010, sce00680, sce01100, sce01110, sce01130, sce01200, sce01230, sce03019 | Glycolysis, methane metabolism, metabolic pathway, biosynthesis of secondary metabolites, biosynthesis of antibiotics, carbon metabolism, biosynthesis of amino acid, RNA degradation | This protein is involved in the subpathway that synthesizes pyruvate from D-glyceraldehyde 3-phosphate. |
| **a** | Eukaryotic translation initiation factor 3 subunit A | sce03013 | RNA transport | RNA-binding component of the eukaryotic translation initiation factor 3 (eIF-3) complex, which is involved in protein synthesis of a specialized repertoire of mRNAs and, together with other initiation factors, stimulates binding of mRNA and methionyl-tRNAi to the 40S ribosome. |
| **b** | Eukaryotic translation initiation factor 5A-1 | | | mRNA-binding protein involved in translation elongation. |
| **b** | FACT complex subunit POB3 | | | Component of the FACT complex, a general chromatin factor that acts to reorganize nucleosomes. |
| **a** | Factor arrest protein 3 | | | Participates in the control of the reentry into the cell cycle following pheromone treatment. |
| **b** | Flavohemoprotein | | | Is involved in NO detoxification in an aerobic process. |
| **a** | Folic acid synthesis protein FOL1 | sce00790, sce01100 | folate biosynthesis | Catalyzes three sequential steps of tetrahydrofolate biosynthesis. |
| a<br>b | **Fructose-bisphosphate aldolase** | **sce00010, sce00030, sce00051, sce00680, sce01100, sce01110, sce01130, sce01200, sce01230** | **Glycolysis, pentose phosphate pathway, fructose and mannose metabolism, methane metabolism, metabolic pathway, biosynthesis of secondary metabolites biosynthesis of antibiotics, carbon metabolism, biosynthesis of amino acid** | **Catalyzes the aldol condensation of dihydroxyacetone phosphate (DHAP or glycerone-phosphate) with glyceraldehyde 3-phosphate (G3P) to form fructose 1,6-bisphosphate (FBP) in gluconeogenesis and the reverse reaction in glycolysis.** |
| **a** | Genetic interactor of prohibitins 3, mitochondrial | sce03009 | ribosome biogenesis | Interacts genetically with prohibitins and thus may be involved in the mitochondrial lipid metabolism. |
| **b** | Glucokinase-1 | sce00010, sce00051, sce00052, sce00500, sce00520, sce01100, sce01110, sce01130, sce01200 | Glycolysis, fructose and mannose metabolism, galactose metabolism, Starch and sucrose metabolism, amino sugar and nucleotide sugar metabolism, metabolic pathway,secondary metabolites, biosynthesis of antibiotics, carbon metabolism | Two isoenzymes, hexokinase-1 and hexokinase-2, can phosphorylate keto- and aldohexoses in yeast, whereas a third isoenzyme, GLK, is specific for aldohexoses. |
| **b** | Glucosamine--fructose-6-phosphate aminotransferase [isomerizing] | sce00250, sce00520, sce01100, sce01130 | Alanine aspartate gutamate metabolism, amino sugar and nucleotide sugar metabolism, metabolic pathway, biosynthesis of antibiotics | Involved in amino sugar synthesis (formation of chitin, supplies the amino sugars of asparagine-linked oligosaccharides of glycoproteins). |
| **b** | Glucose-6-phosphate 1-dehydrogenase | sce00030, sce04800, sce01100, sce01110, sce01130, sce01200 | pentose phosphate pathway, glutatione metabolism, metabolic pathway,secondary metabolites, biosynthesis of antibiotics, carbon metabolism | Catalyzes the rate-limiting step of the oxidative pentose-phosphate pathway. The main function of this enzyme is to provide reducing power (NADPH) and pentose phosphates for fatty acid and nucleic acid synthesis. |
| **a** | Glucose-6-phosphate 1-epimerase | | | Catalyzes the interconversion between the alpha and beta anomers from at least three hexose 6-phosphate sugars (Glc6P, Gal6P, and Man6P). |
| **a** | Glucose-6-phosphate isomerase | sce00010, sce00030, sce00500, sce00520, | Glycolysis, pentose phosphate pathway, fructose and mannose metabolism, methane metabolism, metabolic pathway, biosynthesis | This protein is involved in the subpathway that synthesizes D-glyceraldehyde 3-phosphate and glycerone phosphate from D-glucose. |

| | | | | |
|---|---|---|---|---|
| | | sce01100, sce01110, sce01130, sce01200 | of secondary metabolites, biosynthesis of antibiotics, carbon metabolism | |
| **b** | Glutamate synthase [NADH] | sce00250, sce00910, sce01100, sce01110, sce01130, sce01230 | Alanine aspartate gutamate metabolism, nitrogen metabolism, metabolic pathway, secondary metabolites, biosynthesis of antibiotics, biosynthesis of amino acid | Forms L-glutamate from L-glutamine and 2-oxoglutarate |
| **b** | Glutamine synthetase | sce00250, sce00220, sce00630, sce00910, sce01100, sce01230 | Alanine aspartate gutamate metabolism, arginine biosynthesis, glyoxylate and dicarboxylate metabolism, nitrogen pathway, metabolic pathway, biosynthesis of amino acid | ATP binding and glutamate-ammonia ligase activity |
| **a** | Glutaredoxin-1 | sce03110 | chaperone and folding | Component of the glutathione system which performs several activities such as glutathione-dependent oxidoreductase, glutathione peroxidase and glutathione S-transferase (GST) activity. |
| **a** | Glutathione S-transferase omega-like 1 | | | Active as '1-Cys' thiol transferase against beta-hydroxyethyl disulfide (HED), as dehydroascorbate reductase and as dimethylarsinic acid reductase. |
| **a** | Glutathione S-transferase omega-like 3 | | | Active as '1-Cys' thiol transferase against beta-hydroxyethyl disulfide (HED), as dehydroascorbate reductase and as dimethylarsinic acid reductase. |
| **b** | Glyceraldehyde-3-phosphate dehydrogenase 1 | sce00010, sce01100, sce01110, sce01130, sce01200, sce01230 | Glycolysis, metabolic pathway,secondary metabolites, biosynthesis of antibiotics, carbon metabolism, biosynthesis of amino acid | This protein is involved in the subpathway that synthesizes pyruvate from D-glyceraldehyde 3-phosphate. |
| **a** | Glyceraldehyde-3-phosphate dehydrogenase 3 | sce00010, sce01100, sce01110, sce01200, sce01230 | Glycolysis, , metabolic pathway, biosynthesis of secondary metabolites , carbon metabolism, biosynthesis of amino acid | This protein is involved in the subpathway that synthesizes pyruvate from D-glyceraldehyde 3-phosphate. |
| **b** | Glycerol-3-phosphate dehydrogenase [NAD(+)] 1 | sce04011, sce01110 | Mapk kinase, metabolic pathway | Catalyzes the production and accumulation of glycerol during hyperosmotic stress conditions. |
| **a** | Glycogen [starch] synthase isoform 2 | | | Transfers the glycosyl residue from UDP-Glc to the non-reducing end of alpha-1,4-glucan. Is believed to regulate the synthesis of glycogen. |
| **b** | Glycolipid 2-alpha-mannosyltransferase | sce00514 | N-glycan biosynthesis | Mannosyltransferase that transfers an alpha-D-mannosyl residue from GDP-mannose into lipid-linked oligosaccharide, forming an alpha-(1->2)-D-mannosyl-D-mannose linkage. Required for the attachment of the third mannose residue of O-linked saccharides. |
| **a** | GTPase-interacting component 2 | | | Required for cell size and shape control, bud site selection, bud emergence, actin cytoskeletal organization, mitotic spindle orientation/positioning, and mating projection formation in response to mating pheromone. |
| **a** | GTP-binding protein YPT11 | sce03029 | Mithochondrial biogenesis | Involved in the positive control of both endoplasmic reticulum (ER) and mitochondrion inheritance during cell divison. |
| **a** | Guanylate kinase | sce00230, sce01100 | Purine metabolism | Essential for recycling GMP and indirectly, cGMP. |
| **b** | Heat shock protein 26 | sce04141 | prot processing in RE | One of the major polypeptides produced on heat shock. |
| **b** | Heat shock protein 78, mitochondrial | | | Required for the dissociation, resolubilization and refolding of aggregates of damaged proteins in the mitochondrial matrix after heat stress. |

| | | | | |
|---|---|---|---|---|
| **b** | Heat shock protein SSA1 | | | May play a role in the transport of polypeptides both across the mitochondrial membranes and into the endoplasmic reticulum. |
| **b** | Heat shock protein STI1 | | | May play a role in mediating the heat shock response of some HSP70 genes. It is required for optimal growth of yeast cells at both low and high temperature. |
| **a** | Histone acetyltransferase GCN5 | | | Acetylates histone H2B |
| a<br>b | **Homocysteine/cysteine synthase** | **sce00270, sce00920, sce01100, sce01110, sce01130, sce01200, sce01230** | **Cysteine and methionine metabolism, sulphur metabolism, metabolic pathway, biosynthesis of secondary metabolites , biosynthesis of antibiotics, carbon metabolism, biosynthesis of amino acid** | **Catalyzes the conversion of O-acetyl-L-homoserine (OAH) into homocysteine in the methionine biosynthesis pathway.** |
| **b** | Homoisocitrate dehydrogenase, mitochondrial | sce00300, sce01100, sce01130, sce1230 | lysine biosynthesis, secondary metabolites, biosynthesis of antibiotics, biosynthesis of amino acid | Catalyzes the $NAD^+$-dependent conversion of homoisocitrate to alpha-ketoadipate. |
| **a** | Ingression protein 1 | | | Required for the ingression of the plasma membrane into the bud neck at the end of cytokinesis, leading to the separation of the mother and daughter cells. Stimulates the synthesis of the primary septum (PS) by CHS2. |
| **b** | Inorganic phosphate transporter PHO84 | | | High-affinity transporter for external inorganic phosphate. |
| **a** | Inorganic phosphate transporter PHO86 | | | Involved in the uptake of inorganic phosphate. |
| **a** | Iron-sulfur assembly protein 2 | sce03029 | mithocondial biogenesis | Involved in the assembly of mitochondrial and cytoplasmic iron-sulfur proteins. |
| **a** | Isocitrate dehydrogenase [NAD] subunit 2, mitochondrial | sce00020, sce01100, sce01110, sce01130, sce01200, sce01230 | Citrate cycle, metabolic pathway, biosynthesis of secondary metabolites , biosynthesis of antibiotics, carbon metabolism, biosynthesis of amino acid | Performs an essential role in the oxidative function of the citric acid cycle. Also binds RNA. |
| **b** | Ketol-acid reductoisomerase, mitochondrial | sce00290, sce00770, sce01100, sce01110, sce01130, sce1210, sce01230 | Valine leucine isoleucine biosynthesis, Pantothenate and CoA biosynthesis, metabolic pathway, secondary metabolites, biosynthesis of antibiotics | This protein is involved in the subpathway that synthesizes L-isoleucine from 2-oxobutanoate. |
| **a** | Kinesin-related protein SMY1 | sce04144 | endocytosis | Possible microtubule-based motor that can interact or substitute with myosin 2 (MYO2). |
| **a** | Kinetochore protein NUF2 | sce03036 | chromosome | Acts as component of the essential kinetochore-associated NDC80 complex, which is involved in chromosome segregation and spindle checkpoint activity. |
| **a** | Mediator of RNA polymerase II transcription subunit 4 | sce03021 | transcription machinery | Component of the Mediator complex, a coactivator involved in the regulated transcription of nearly all RNA polymerase II-dependent genes. |
| **a** | Meiotic sister-chromatid recombination protein 6, mitochondrial | | | May be involved in the control of meiotic sister-chromatid recombination. |
| **a** | Mitochondrial carrier protein MTM1 | | | Involved in the mitochondrial activation of SOD2 by specifically facilitating insertion of the essential manganese cofactor. |
| **a** | Mitochondrial import inner membrane translocase subunit TIM54 | sce03029 | mithocondrial biogenesis | Essential component of the TIM22 complex, a complex that mediates the import and insertion of multi-pass transmembrane proteins into the mitochondrial inner membrane. |
| **a** | Mitochondrial morphogenesis protein SLD7 | | | Required for the proper function of SLD3 at the initiation of DNA replication. Binds to SLD3 and reduces its affinity for CDC45, a |

| | | | | |
|---|---|---|---|---|
| | | | | component of the replication fork. Required for mitochondrial morphology. |
| **b** | Mitochondrial peroxiredoxin PRX1 | | | Involved in mitochondrial protection of cadmium-induced oxidative stress. |
| **a** | Multiple RNA-binding domain-containing protein 1 | sce03009 | ribosome biogenesis | Involved in pre-rRNA processing. Required for maintaining steady-state levels of 40S ribosomal subunit. |
| **a** | NAD-dependent histone deacetylase SIR2 | sce00760, sce01100, sce04213 | Niconitate and nicotinamide metabolism, metabolic pathway, peroxisome | NAD-dependent deacetylase, which participates in a wide range of cellular events including chromosome silencing, chromosome segregation, DNA recombination and the determination of life span. |
| **a** | NADP-dependent 3-hydroxy acid dehydrogenase | sce00240, sce00260, sce01100 | Pyrimidine metabolism, glycine serene threonine metabolism, metabolic pathway | NADP-dependent dehydrogenase with broad substrate specificity acting on 3-hydroxy acids. |
| **a** | NADP-dependent alcohol dehydrogenase 6 | sce00010, sce00040, sce00561, sce01100, sce01110, sce 01130 | Glycolysis, pentose and glucoronate interconversion, glycerolipid metabolism, metabolic pathway, biosynthesis of secondary metabolites, biosynthesis of antibiotics | NADP-dependent alcohol dehydrogenase with a broad substrate specificity. |
| **a** | NADP-dependent alcohol dehydrogenase 7 | sce00010, sce00040, sce00561, sce01100, sce01110, sce01130 | Glycolysis, pentose and glucoronate interconversion, glycerolipid metabolism, metabolic pathway, biosynthesis of secondary metabolites, biosynthesis of antibiotics | NADP-dependent alcohol dehydrogenase with a broad substrate specificity. |
| **b** | NADPH-dependent alpha-keto amide reductase | | | Involved in mitochondrial protection of cadmium-induced oxidative stress. |
| **b** | NADP-specific glutamate dehydrogenase 1 | sce00220, sce00250, sce00910, sce01100 | arginine biosynthesis, arginine alanine glutamine biosynthesis, nitrogen metabolism, metabolic pathway | ammonia assimilation cycle and glutamate biosynthetic process |
| **b** | NAD-specific glutamate dehydrogenase | sce00220, sce00250, sce00910, sce01100 | arginine biosynthesis, arginine alanine glutamine biosynthesis, nitrogen metabolism, metabolic pathway | $NAD^+$-dependent glutamate dehydrogenase which degrades glutamate to ammonia and alpha-ketoglutarate. |
| **a** | Nicotinamide riboside kinase | | | Catalyzes the phosphorylation of nicotinamide riboside (NR) and nicotinic acid riboside (NaR) |
| **b** | Nucleoporin NUP120 | sce03013 | RNA transport | Functions as a component of the nuclear pore complex (NPC). |
| **a** | Partitioning protein REP1 | sce02000 | trasporter | Part of the plasmid partitioning system, which ensures the equal distribution of replicated plasmid molecules to daugther cells. |
| **b** | Peptidyl-prolyl cis-trans isomerase D | | | PIases accelerate the folding of proteins. It catalyzes the cis-trans isomerization of proline imidic peptide bonds in oligopeptides. |
| **b** | Peroxiredoxin TSA1 | | | Thiol-specific peroxidase that catalyzes the reduction of hydrogen peroxide and organic hydroperoxides to water and alcohols, respectively. |
| **a** | Phosphomannomutase | sce00051, sce00520, sce01100, sce01110, sce01130 | Fructose and mannose metabolism, amino sugar and nucleotide sugar metabolism, metabolic pathway, biosynthesis of secondary metabolites, biosynthesis of antibiotics | Involved in the synthesis of the GDP-mannose and dolichol-phosphate-mannose required for a number of critical mannosyl transfer reactions. |

| | | | | |
|---|---|---|---|---|
| **b** | Phosphoribosylaminoimidazole-succinocarboxamide synthase | sce00230, sce01100, sce01110, sce01130 | purine metabolism, metabolic pathway, secondary metabolites, biosynthesis of antibiotics | This protein is involved in step **1** of the subpathway that synthesizes 5-amino-1-(5-phospho-D-ribosyl)imidazole-4-carboxamide from 5-amino-1-(5-phospho-D-ribosyl)imidazole-4-carboxylate. |
| **a** | pH-response regulator protein palF/RIM8 | | | Required for the proteolytic cleavage of the transcriptional repressor RIM101 in response to alkaline ambient pH, which is necessary for sporulation and invasive growth. |
| **b** | Plasma membrane iron permease | | | Permease for high affinity iron uptake. |
| **b** | Potassium-activated aldehyde dehydrogenase, mitochondrial | sce00010, sce00071, sce00280, sce00310, sce00620, sce01110 | Glycolysis, fatty acid degradation, valine lucine isoleucine degradation, lysine degradation, pyruvate metabolism, metabolic pathway, | Potassium-activated aldehyde dehydrogenase involved in acetate formation during anaerobic growth on glucose. |
| **b** | Prefoldin subunit 4 | | | Binds specifically to cytosolic chaperonin (c-CPN) and transfers target proteins to it. Binds to nascent polypeptide chain and promotes folding in an environment in which there are many competing pathways for nonnative proteins. |
| **a** | Pre-mRNA-processing factor 19 | sce03040, sce04120 | Spliceosome, ubiquintin mediated proteolysis | Probable ubiquitin-protein ligase involved in pre-mRNA splicing. |
| | Probable alanine aminotransferase, mitochondrial | sce00220, sce00250, sce01100, sce01200, sce01210, sce01230 | Arginine biosynthesis, alanine aspartate glutamate metabolism, metabolic pathway, carbon metabolism, 2-oxocarboxylic acid metabolism, biosynthesis of amino acid | This protein is involved in the subpathway that synthesizes pyruvate from L-alanine. |
| **b** | Probable alpha-1,6-mannosyltransferase MNN11 | sce00513, sce01100 | N- glycan biosynthesis, secondary metabolites | Required for synthesis of full-length mannan chains. |
| **b** | Protease B inhibitors 2 and 1 | | | Cytosolic inhibitor of vacuolar proteinase B (yscB), probably regulating protease B activity during limited proteolysis. |
| **b** | Proteasome component C5 | sce03050 | proteasome | The proteasome degrades poly-ubiquitinated proteins in the cytoplasm and in the nucleus. |
| **b** | Protein BFR2 | | | Involved in endoplasmic reticulum to Golgi transport. |
| **a** | Protein CBP3, mitochondrial | sce03029 | mithocondrial biogenesis | Chaperone required for the assembly of ubiquinol-cytochrome c reductase of the mitochondrial respiratory chain. |
| **a** | Protein GAL3 | sce00052, sce00520, sce01100 | Galactose metabolism, amino sugar and nucleotide sugar metabolism, metabolic pathway | The GAL3 regulatory function is required for rapid induction of the galactose system. |
| **a** | Protein HBT1 | | | Polarity-determining protein which forms a conjugate with the ubiquitin-like modifier HUB1. Involved in bud site selection and cellular morphogenesis during conjugation. |
| **a** | Protein HRB1 | | | RNA binding |
| **a** | Protein SOK1 | | | High copy suppressor of a cyclic AMP-dependent protein kinase mutant. |
| **b** | Protein SSD1 | | | Can suppress the lethality due to deletion of SIT4, and partially the defects due to BCY1 disruption. Is implicated in the control of the cell cycle G1 phase. |
| **b** | Protoplast secreted protein 2 | | | FMN binding. NAD(P)H dehydrogenase (quinone) activity |
| **a** | Putative carboxymethylenebutenolidase | | | carboxymethylenebutenolidase activity |
| **a** | Putative protease AXL1 | | | Probable protease. Involved in axial budding. |

| | | | | |
|---|---|---|---|---|
| **a** | Putative uncharacterized protein YKR012C | | | Partially overlaps PRY2. |
| **a** | Pyruvate decarboxylase isozyme 1 | sce00010, sce01100, sce01110, sce01130 | Glycolysis, , metabolic pathway, biosynthesis of secondary metabolites, biosynthesis of antibiotics | Major of three pyruvate decarboxylases (PDC1, PDC5, PDC6) implicated in the nonoxidative conversion of pyruvate to acetaldehyde and carbon dioxide during alcoholic fermentation. |
| **a** | Pyruvate dehydrogenase complex protein X component, mitochondrial | sce00010, sce01100, sce01110, sce01130 | Glycolysis, , metabolic pathway, biosynthesis of secondary metabolites, biosynthesis of antibiotics | Required for anchoring dihydrolipoamide dehydrogenase (E3) to the dihydrolipoamide transacetylase (E2) core of the pyruvate dehydrogenase complexes of eukaryotes. |
| **a** | Rab GDP-dissociation inhibitor | sce04147 | exosome | Regulates the GDP/GTP exchange reaction of SEC4 by inhibiting the dissociation of GDP from it, and the subsequent binding of GTP to SEC4. Plays an essential role in the yeast secretory pathway. |
| **b** | Regulator of calcineurin 2 | | | Present with 967 molecules/cell in log phase SD medium. |
| **b** | Ribosomal protein L15 | | | structural constituent of ribosome |
| **a** | RNA cytidine acetyltransferase | sce03008 | Ribosome biogenesis in eukaryotes | NA cytidine acetyltransferase with specificity toward both 18S rRNA and tRNAs. |
| **b** | Saccharolysin | | | Could be involved in late stage of protein degradation. |
| **b** | Saccharopepsin | sce04138 | autophagy pathway | Aspartyl protease implicated in the post-translational regulation of S.cerevisiae vacuolar proteinases. Acts on YSCB, on YSCY and on itself. |
| **b** | S-adenosylmethionine synthase 2 | sce00270, sce01100, sce01110, sce01230 | Cysteine and methionine metabolism, metabolic pathway, secondary metabolites, amino acid biosynthesys | Catalyzes the formation of S-adenosylmethionine from methionine and ATP. |
| **b** | Serine hydroxymethyltransferase, cytosolic | sce00260, sce01230 | | Interconversion of serine and glycine. |
| **a** | Serine/threonine-protein phosphatase 2B catalytic subunit A2 | | | Calcium-dependent, calmodulin-stimulated protein phosphatase. This subunit may have a role in the calmodulin activation of calcineurin. |
| **a** | Sigma-like sequence protein 1, mitochondrial | sce04141 | Protein processing in ER | Involved in aerobic respiration where it is required for assembly of respiratory chain enzyme complexes III and IV. Also has a role in mitochondrial gene expression. |
| **a** | Single-stranded nucleic acid-binding protein | | | Functions in the transition of mRNAs from translation to an mRNP complex destined for decapping. |
| **b** | Squalene monooxygenase | sce00100 | Steroid biosynthesis | Catalyzes the first oxygenation step in sterol biosynthesis and is suggested to be one of the rate-limiting enzymes in this pathway. |
| **a** | Succinate dehydrogenase [ubiquinone] flavoprotein subunit, mitochondrial | sce00020, sce00190, sce01100, sce01110, sce01130, sce01200 | Citrate cycle, oxidative phosphorylation, metabolic pathway, biosynthesis of secondary metabolites , biosynthesis of antibiotics, carbon metabolism, | Catalytic subunit of succinate dehydrogenase (SDH) that is involved in complex II of the mitochondrial electron transport chain and is responsible for transferring electrons from succinate to ubiquinone (coenzyme Q). |
| **a** | Succinate/fumarate mitochondrial transporter | | | Transports cytoplasmic succinate, derived from isocitrate by the action of isocitrate lyase in the cytosol, into the mitochondrial matrix in exchange for fumarate. |
| **b** | Sulfate adenylyltransferase | sce00230 | Purine metabolism | Catalyzes the first intracellular reaction of sulfate assimilation, forming adenosine-5'-phosphosulfate (APS) from inorganic sulfate and ATP. |
| **b** | Sulfite reductase [NADPH] subunit beta | sce00920 | sulfur metabolism | Catalyzes the reduction of sulfite to sulfide, one of several activities required for the biosynthesis of L-cysteine from sulfate. |
| **b** | Thioredoxin-2 | | | Participates as a hydrogen donor in redox reactions through the reversible oxidation of its active center dithiol to a disulfide. |

| | | | | |
|---|---|---|---|---|
| **a** | Trafficking protein particle complex II-specific subunit 130 | | | Specific subunit of the TRAPP II complex, a highly conserved vesicle tethering complex that functions in the late Golgi as a guanine nucleotide exchange factor (GEF) for the Golgi YPT1 GTPase. |
| **b** | Transcription elongation factor S-II | | | Necessary for efficient RNA polymerase II transcription elongation past template-encoded arresting sites. |
| **a** | Transcription initiation factor TFIID subunit 4 | | | Functions as a component of the DNA-binding general transcription factor complex TFIID. Binding of TFIID to a promoter is the initial step in pre-initiation complex (PIC) formation. |
| **a** | Transcriptional regulator NRG1 | | | Transcriptional repressor involved in regulation of glucose repression. Binds to UAS-1 in the STA1 promoter. |
| **a** | Translation machinery-associated protein 64 | | | -RNA binding and translation initiation factor activity |
| **a** | Tricarboxylate transport protein | sce02000 | transporters | Transport of citrate across inner mitochondrial membrane. |
| **a** | tRNA (guanine(10)-N2)-methyltransferase | | | Catalytic subunit of an S-adenosyl-L-methionine-dependent tRNA methyltransferase complex that mediates the methylation of the guanosine nucleotide at position 10 (m2G10) in tRNAs. |
| **a** | tRNA wybutosine-synthesizing protein 3 | | | S-adenosyl-L-methionine-dependent methyltransferase that acts as a component of the wybutosine biosynthesis pathway. |
| **a** | tRNA-specific adenosine deaminase subunit TAD2 | | | Deaminates adenosine-34 to inosine in many tRNAs. |
| **a** | Tyrosine--tRNA ligase, mitochondrial | sce00970 | Aminoacyl-tRNA biosynthesis | Catalyzes the attachment of tyrosine to tRNA(Tyr) in a two-step reaction: tyrosine is first activated by ATP to form Tyr-AMP and then transferred to the acceptor end of tRNA(Tyr). |
| **a** | U3 small nucleolar ribonucleoprotein protein LCP5 | sce03009 | ribosome biogenesis | Component of the U3 small nucleolar ribonucleoprotein. Required for the early cleavages at sites A0, A1 and A2 of the pre-ribosomal RNA. Participates in ribosome biogenesis. |
| **a** | U3 small nucleolar RNA-associated protein 6 | sce03008 | Ribosome biogenesis in eukaryotes | Component of the SSU processome, a pre-ribosomal particle required for the maturation of the 18S rRNA from the 35S pre-rRNA precursor. |
| **b** | Ubiquitin-40S ribosomal protein S31 | sce03010 | ribosome | Component of the ribosome, a large ribonucleoprotein complex responsible for the synthesis of proteins in the cell. |
| **b** | Ubiquitin-60S ribosomal protein L40 | sce03010 | ribosome | Exists either covalently attached to another protein, or free (unanchored). |
| **a** | Ubiquitin-conjugating enzyme E2 13 | sce04120 | Ubiquitin mediated proteolysis | Has a role in the DNA error-free postreplication repair (PRR) pathway. |
| **b** | UBX domain-containing protein 1 | sce041012 | Protein processing in RE | Involved in CDC48-dependent protein degradation through the ubiquitin/proteasome pathway. |
| **a** | Uncharacterized isomerase YHR210C | | | carbohydrate binding (galactose catabolic process via UDP-galactose and glucose metabolic process) |
| a<br>b | **Uncharacterized oxidoreductase YMR226C** | **sce00240, sce00260, sce01100** | **Pyrimidine metabolism, glycine serine threonine biosynthesis, metabolic pathway** | **NADP-dependent dehydrogenase with broad substrate specificity acting on 3-hydroxy acids.** |
| **b** | Uncharacterized protein MRP8 | | | Present with 1550 molecules/cell in log phase SD medium. |
| **b** | Uncharacterized protein YNL134C | | | aldehyde dehydrogenase (NAD) activity |
| **b** | Uracil phosphoribosyltransferase | sce00240, sce01100 | Pyrimidine metabolism, metabolic pathway | Catalyzes the conversion of uracil and 5-phospho-alpha-D-ribose 1-diphosphate (PRPP) to UMP and diphosphate. |
| **b** | Vacuolar aminopeptidase 1 | | | Resident vacuolar enzyme that catalyzes the removal of amino acids from the N-terminus of peptides and proteins. |

| | | |
|---|---|---|
| **a** | V-type proton ATPase subunit B | Non-catalytic subunit of the peripheral V1 complex of vacuolar ATPase. V-ATPase is responsible for acidifying a variety of intracellular compartments in eukaryotic cells. |